



Politecnico di Torino

Department of Production System and Industrial Design

Ph.D- XXVII cycle

INNOVATIVE CERAMIC MATERIALS AND PROCESSES FOR AERONAUTIC APPLICATIONS

PhD Student

Azhar Hussain

Supervisors

Prof. Luca Settineri (DIGEP)

Prof. Paolo Fino (DISAT)

Tutors

Matteo Pavese

Sara Biamino

Coordinator:

Prof. Luca Settineri

**Dedicated to my Parents, my Guide, Sheikh Zulfiqar Ali
Naqashbandi Mujadadi and my Family.**

1 Acknowledgement

With the name of Almighty, Allah, His mercy on Prophet Muhammad (PBUH) and countless blessings on us, I have great respect for the HEC (Higher Education Commission, Pakistan) for giving me the wonderful opportunity to study at Politecnico di Torino, Italy. I am humbly grateful to peer saab, Shekh Zulfiqar Ali Naqashbandi Mujadadi sahib who encouraged me to pursue for PhD from Italy.

I would like to express my sincere gratitude to my supervisors, Prof. Luca Settineri and Prof. Paolo Fino for their special guidance and assistance in conducting this research based study. They made my stay at Politecnico very happy by involving me in laboratory work.

Special thanks to my tutor, Prof. Matteo Pavese for helping me in analyzing the results and performing the experiments.

I am grateful to Prof. Sara Biamino with whom I initiated my research on Sialon ceramics and learned tape casting.

Not to name the individuals I appreciate the coordination of all the group mates, researchers and PhD fellows. These people gave their valuable time to teach the use of equipment and facilitated experimentation.

I would like to extend my thanks to the PhD coordinator, Prof. Luca Settineri, staff of DIGEP and DISAT and other university persons who helped me in research and made my time comfortable in Torino.

I would like to express my appreciations to a lot of friends, roommates, friends in OPS and non OPS. especially, Muhammad Ramzan Abdul Karim who facilitated on arrival to Torino and Engineer Muhammad Talha and Ahmed Afify who conducted experiments and did the proof reading of my thesis.

Azhar Hussain

January, 2015, Torino

2 Contents

1. Summary.....	1
1. Introduction	3
1.1 Aim of the Study	3
1.2 Aircrafts and Materials.....	3
1.3 Aircraft Engine Types	3
1.3.1 Ramjet Engine.....	3
1.3.2 Pulsejet.....	4
1.3.3 Scramjet	4
1.3.4 Turbo ramjet.....	5
1.3.5 Turborocket.....	5
1.4 Classification of Gas Turbine Engines.....	5
1.4.1 Turbojet Engine	6
1.4.2 Turboprop Engine	6
1.4.3 Turboshaft Engine.....	7
1.4.4 Turbofan Engines.....	7
1.4.5 Engines Role and Performance.....	7
1.5 Engine Hardware and Materials.....	10
1.5.1 Compressor	10
1.5.2 Combustor/Combustion Chamber	12
1.5.3 Turbine.....	12
1.6 Efficiency of Engines	13
1.6.1 Propulsive Efficiency (Thrust).....	13
1.6.2 Thermal Efficiency	14

1.6.3	Propeller Efficiency	14
1.6.4	Overall efficiency.....	14
1.6.5	Take Off Thrust.....	14
1.6.6	Specific Fuel Consumption.....	14
1.7	Material and Manufacturing Process Evolution.....	15
2	Silicon Nitride and Sialons	21
2.1	Processing.....	22
2.1.1	Sintered Silicon Nitride (SSN).....	22
2.1.2	Two stage Reactive Gas Pressure Sintering.....	22
2.1.3	Cladd HIP'ing/Glass Encapsulated Sintering:	23
2.1.4	Hot isostatic pressing (HIP).....	23
2.1.5	RBSN	23
2.2	Dissociation of Si_3N_4	23
2.3	Sialons	24
2.3.1	β -Sialon.....	26
2.3.2	α -Sialon.....	29
2.4	Phases in α - β -Sialon Systems.	33
2.5	α - β Phase Relation	34
2.6	Multication-Sialon.....	34
2.6.1	Sialon-Graphene Interaction	35
2.6.2	$\text{Si}_3\text{N}_4/\text{SiC}$ Composites.....	35
2.6.3	Sialon-Carbon Interaction.....	35
3	Processing of Ceramics-Sialons.	37
3.1	Raw Materials and Powders.....	37
3.1.1	Nature of Powder	37

3.1.2	Particle Size	38
3.1.3	Shape of the Particles	38
3.2	Melting	39
3.3	Dry Powder Processing	39
3.3.1	Agglomerates and Heterogeneities	39
3.3.2	Inclusions	39
3.3.3	Density Gradient:	40
3.3.4	Defects Remedy	40
3.4	Colloidal Processing	40
3.4.1	Consolidation from the Slurry State	42
3.5	Slip Casting:	43
3.6	Tape Casting	44
3.6.1	Powder Preparation	45
3.6.2	Dispersion Milling	46
3.6.3	Slip De-Gassing	47
3.6.4	Slip Characterization	47
3.6.5	Tape Casting and Drying	47
3.6.6	Static Charge Elimination	48
3.6.7	Slitters, Cutoffs, and Take-Up Systems	48
3.6.8	UV Curable Tapes	49
3.6.9	Tape Calendering	50
3.6.10	Lamination	50
3.6.11	Isostatic Lamination	51
3.6.12	Shaping	51
3.7	Calendering	51

3.8	Pressure Casting	51
3.9	Extrusion-injection Molding	53
3.10	Extrusion-Shaping	54
3.11	Injection Molding	55
3.12	Rapid Prototyping (RP)	57
3.13	Pressing.....	58
3.13.1	Uniaxial Pressing.....	60
3.14	Iso-static Pressing.....	61
3.15	Spark Plasma Sintering (SPS)	61
4	Experimental.....	64
4.1	Colloidal Processing By Controlled Rheology (Compatibility of Colloidal Processing) 64	
4.1.1	Tape Casting	64
4.1.2	Centrifugal/slip Casting	65
4.1.3	Pressing (Quasi colloidal processing).....	65
4.1.4	Debinding.....	65
4.2	Production of $\alpha\beta$ -Sialon (Quasi- Colloidal Processing).....	67
4.2.1	Sialon Composition with Aluminosilicates	68
4.2.2	Colloidal Processing	68
4.3	Characterization	70
4.3.1	X-ray diffraction	70
4.3.2	Bulk Density Measurement.....	70
4.3.3	Relative Density.....	71
4.3.4	Vicker's Hardness.....	71
4.3.5	Fracture Toughness.....	72

4.3.6	Bending Strength (Flexural Strength).....	73
5	Results	74
5.1	Production of S215 (Composite Sialon) with Kaolinite	76
5.2	Production of S215 (Composite Sialon) modified with Muscovite	82
5.3	Production of S1212 (Composite Sialon) with Kaolinite.	84
5.4	Production of S1212 (Composite Sialon) with Muscovite.....	85
5.5	Production of Pless (Pressureless sinterable) Sialon.....	88
5.6	Production of S215 (Composite Sialon) with Free Alumina	91
5.7	Production of S1212 (Composite Sialon) with Free Alumina	97
5.8	MgO-Y ₂ O ₃ and Spinel-Y ₂ O ₃ based Sialons (S215)	101
5.9	Effect of Free Alumina and Kaolinite on Sialon (S215).....	102
5.10	Effect of MgO on S215K.....	102
5.11	Effect of Ce ₂ O ₃ on S215K.....	102
5.12	Graphene-S215K	103
5.13	Colloidal Processing of Si ₃ N ₄ /SiC.....	104
5.14	Thermal Analysis.....	105
5.14.1	Hot Chamber XRD of Colloidal Processed β-Sialon	105
5.14.2	Hot Chamber XRD of αβ-Sialon.....	107
5.15	Thermal Gravimetry	109
5.16	Results Comparison.....	111
5.17	Comparison between colloidal processed pressureless sintered and other systems.	112
6	Conclusions.	113
7	Future Works.....	113

1. Summary

In the field of aerospace, aircrafts are the most dominant element with other spacecrafts and research satellites finding a limited usage. All the space vehicles are run by the highly efficient engines to make them escape the gravity in case of spacecraft or enable them to carry heavy loads and move quickly to the long destination as achieved by the civil and military planes. To achieve the excellence in transportation in the space, air vehicles are fitted with the engines (rocket or jet engines), these are termed as the power houses and are operated at extremely high temperature and pressure. Such a high temperature achievement and sustainment over the passage of time has put the challenges to the manufacturers and material producers. Spacecrafts and other research crafts which are specifically designed to achieve supersonic flights use special type of non-air breathing engines (rocket engine or scramjet/ramjet) and materials and comprise only up to 10% of the aeronautical industry. All other planes used by the airliners or being used as military planes rely on the air-breathing engines (jet engines).

Depending upon the function and role of a plane these jet engines have different modifications but the operating unit and principle of all these engines remain same and is a variant of gas generator. Common goal of achieving the maximum fuel efficiency (thermal efficiency) in all the planes still remain same.

Achievement of high thermal efficiency led to the development of materials and new methods to extract the maximum possible effectiveness of the materials. Simultaneously, new techniques also emerged to boost the overall operation. One such milestone was the development of superalloys and evolve of the process to fabricate superalloyed blades from equiaxed to single crystal. And introduction of cooling channels and thermal barrier coatings has carried this to limits of the current systems.

With the metals and existing technology reaching the limit, focus is placed on the development of ceramic materials. Most of the technical (high temperature) ceramics are brittle and difficult to fabricate, Si_3N_4 one among this class is overlapping with metals in terms of toughness but production of this material into useful components is challenging. There are some derivatives of Si_3N_4 which are easy to produce (develop) into components but their development is limited to few special ceramic processing techniques. These derivatives are α -Sialon and β -Sialon later is

easy to fabricate and develop into the components but is very soft, the former is hard and strong and impossible to be synthesized without the use of hot isostatic pressing (HIP), hot pressing and spark plasma sintering (SPS). All of these methods limit the size and geometry of the object to be produced. Machining of these hard materials at cost of diamond to make useful shapes is another restriction; additionally highly machined components may get notches and other fabrication defects which limit the mechanical properties.

Production of Si_3N_4 based materials, Sialons, using the colloidal processing and pressure less consolidation (sintering) technique has been the challenge. Composition of the pure α -Sialon material was modified with another material, aluminosilicate (β -Sialon former) and this system could be sintered without applying pressure. Modification of this system (material-method) as influenced by the other useful additives like MgO, Spinel and Ce_2O_3 was also observed.

Hence a new material system capable to be processed by shaping and forming methods linked to colloidal processing was designed.

1. Introduction

2.1 Aim of the Study

Objective of this research has been to process Sialon precursor materials by colloidal processing and develop a composite Sialon, $\alpha\beta$ -Sialon, similar to the one developed by shape limiting and expensive processing techniques, spark plasma sintering (SPS) and hot isostatic pressing (HIP)

It was anticipated that success of this processing technique can boost the research of technical ceramics for turbine applications.

2.2 Aircrafts and Materials

Aircrafts and space vehicles make together the entities filling the space. Space shuttle and rockets are still applicable only at research scale and economic considerations is beyond the scope of this study whereas aircrafts in the civil and military use are in abundance for the transportation and other peace keeping purposes and there economic and sustainable operation has kept open the research in the sector of materials and manufacturing for the turbine (jet engine) applications. Ever since the discovery of jet engines there has been a great race to develop the new materials and invent novel processing techniques to make the flight operation successful and economic.

In this study we have discussed various types of jet engines to understand how crucial the research and development has been or could be in the field of ceramic materials and what are the challenges encountered by the development of these ceramic materials

2.3 Aircraft Engine Types

There are two main types of jet engines, air breathing and non-air breathing engines, non-air breathing engines has limited use in the aviation industry and few subclasses, whereas air breathing engines have several subclasses as shown in the figure 1.1. Few engine systems are explained in the next sections.

2.3.1 Ramjet Engine

Ramjet is a simple duct as shown in figure 1.2. It has no rotating parts major elements are: inlet, a divergent duct, combustion zone and convergent-divergent exit. Its function is based on the forward motion provide by an auxiliary source. Ingested air is forced into the nozzle at high

speed where this high speed air creates a pressure in the combustion zone and when lit ignites and creates hot gasses which are accelerate to atmosphere through the outlet duct.

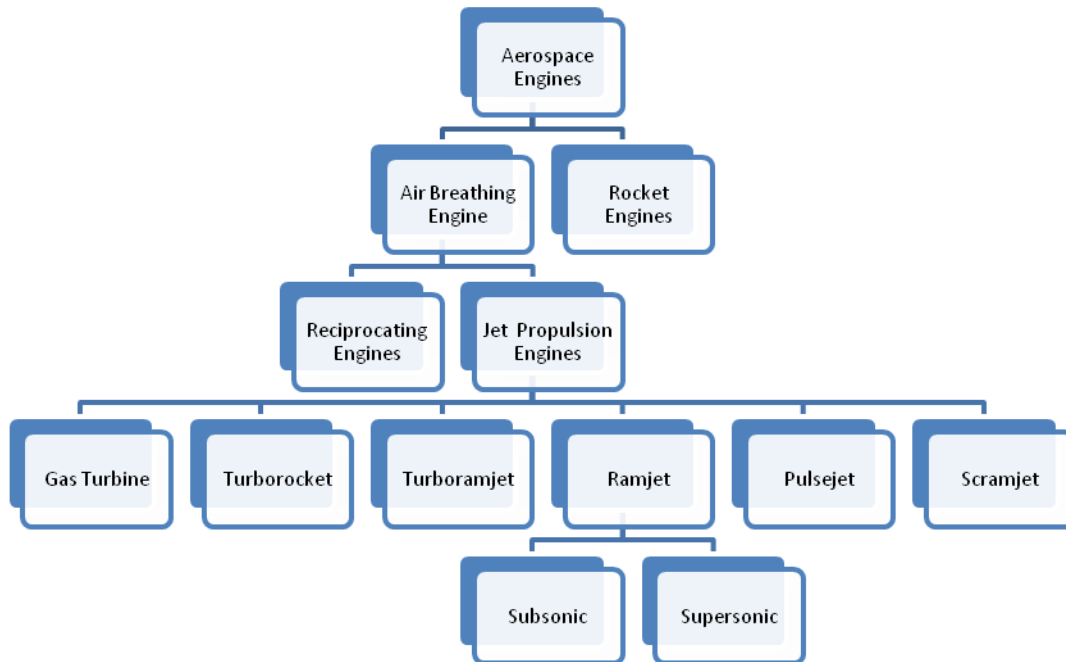


Figure 1-1 Classification of aerial vehicles

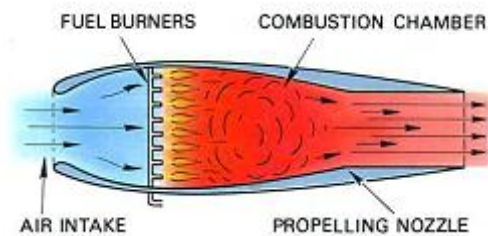


Figure 1-2 Ramjet engine schematic. [1]

2.3.2 Pulsejet

This is an intermittent type of engine where the inlet has valves which slam shut during the combustion and reopens when the first fired gas has been ejected out. This type of engine finds application in helicopters and are unfit for the aircrafts because of high consumption of the fuel

2.3.3 Scramjet

It is a supersonic ramjet engine which only works at high speeds.

2.3.4 Turbo ramjet

This is a combination of turbo jet engine with the ramjet engine where a turbojet is functional at takeoff and low mach conditions whereas the ramjet becomes functional when high mach cruising function is necessary[2].

2.3.5 Turborocket

This is another modification of turboramjet engine where engine carries oxygen as a fuel and after combustion product is mixed with air/fuel mixture for cooling. Afterburning produces more thrust this type of engine is short in size but consumption of fuel is very high[2].

2.4 Classification of Gas Turbine Engines

Gas turbines are the hub for all type of flying aircrafts/helicopters and are named as aero engines.

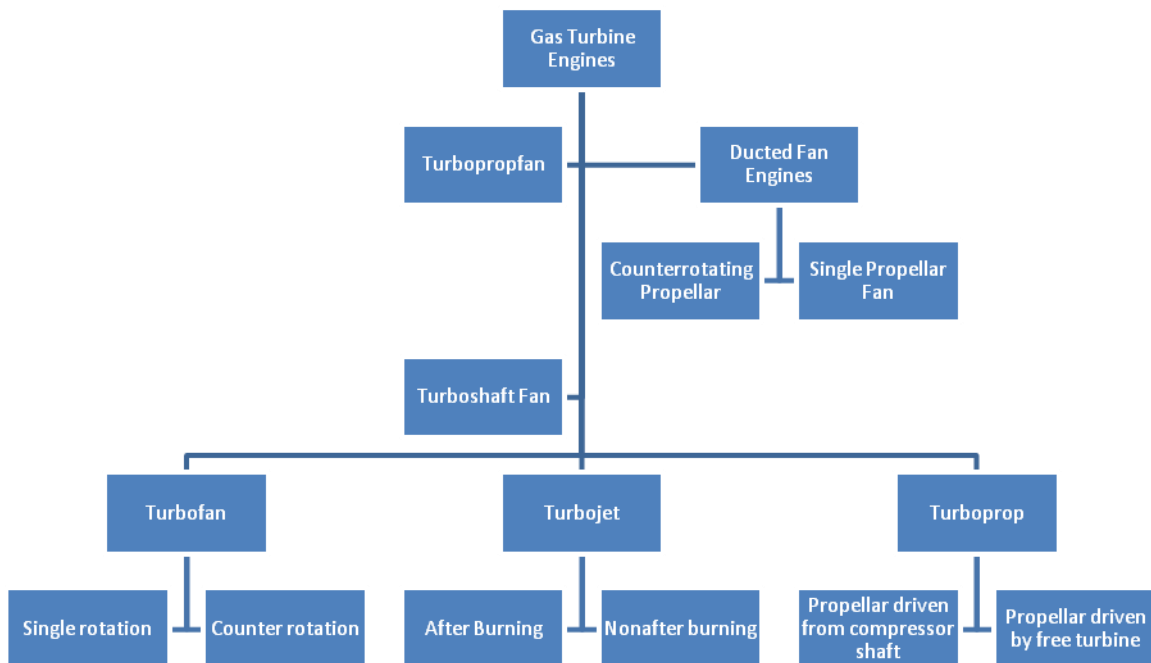


Figure 1-3 Classification of Gas Turbine Engine

2.4.1 Turbojet Engine

Turbojet engine can be a single spool or double spool, each may be further subdivided into centrifugal and compressor types. Turbojet may have centrifugal and axial compressors both in single spool, other variations may be with afterburner and without burner, various types are shown in figure 1.4.

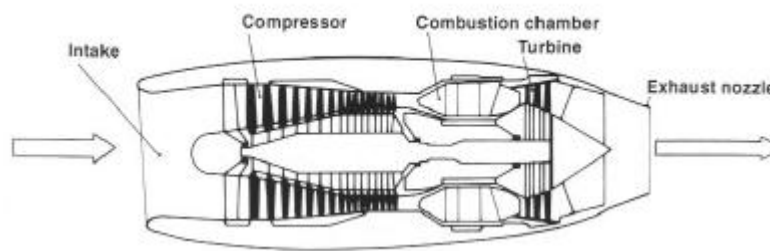


Figure 1-4 Turbo jet engine [3]

2.4.2 Turboprop Engine

This type of engine combines the best features of piston and turbojet engines its main features are economic plane at low speed and low altitude a plane driven by a propeller fan with reduced noise. Such engine with the types is shown in the figure 1.5.

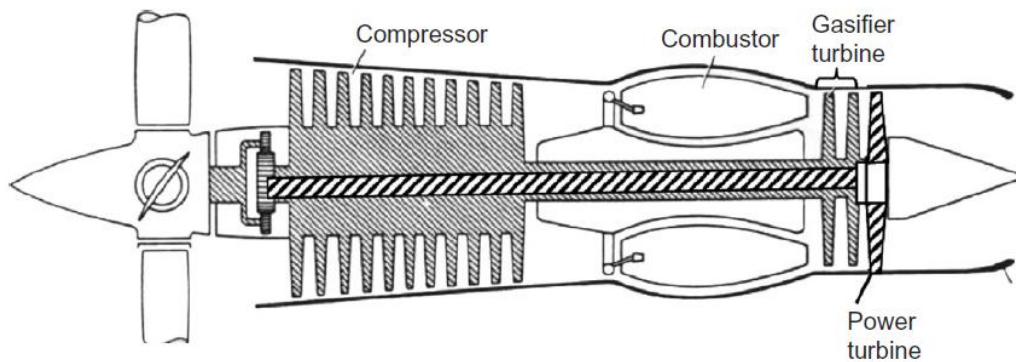


Figure 1-5 A turboprop engine is shown schematically[4]

2.4.3 Turboshaft Engine

This is a variation of turboprop and is mainly used for the helicopters, figure 1.6 shows the turboshaft engine

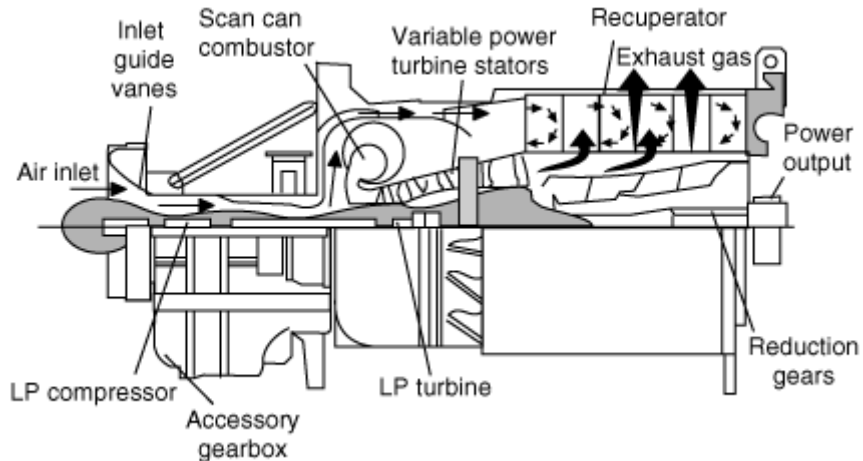


Figure 1-6 Turboshaft engine [5]

2.4.4 Turbofan Engines

These engines are designed as the hybrid of turbojet and turbofan engines. It consists of a large internal propeller and two streams of air flowing through the engine. One stream of the air goes through turbine and secondary may be either used as cooling air or mixed with hot gasses in the rear of engine to enhance the thrust.

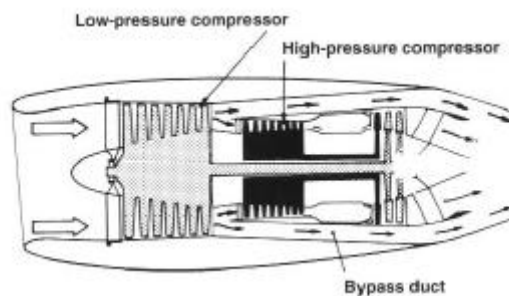


Figure 1-7 Turbofan Engine[3]

2.4.5 Engines Role and Performance

Different engines has different role depending upon the requirement as shown in the figure1.8[6]

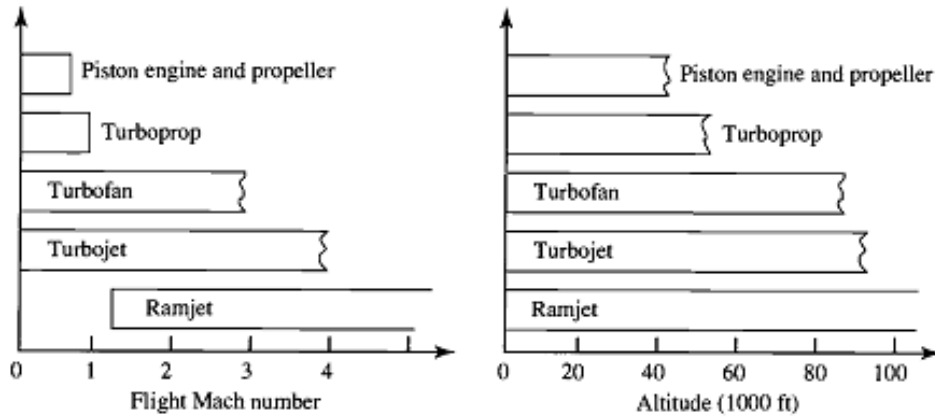


Figure 1-8 Efficiency of various engines in terms of mach number and altitude [6].

All the air breathing engines work on the same basic principle of gas generators (shown in the figure 1.9). Major components of a gas turbine engine are compressor, combustor, and turbine. These components are basic to all the major types of air breathing engines common to the turbojet, turbofan, turboprop, and turbo shaft engines. The purpose of a gas generator is to supply high-temperature and high-pressure gas

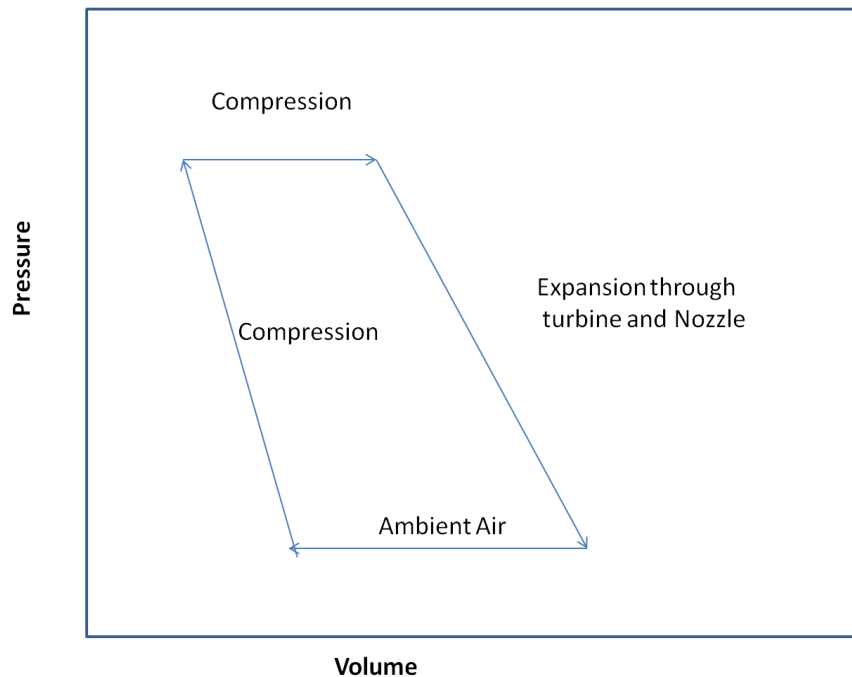


Figure 1-9 Principle of an air breathing engine (Gas generator)

A gas generator is shown in the figure 1.10

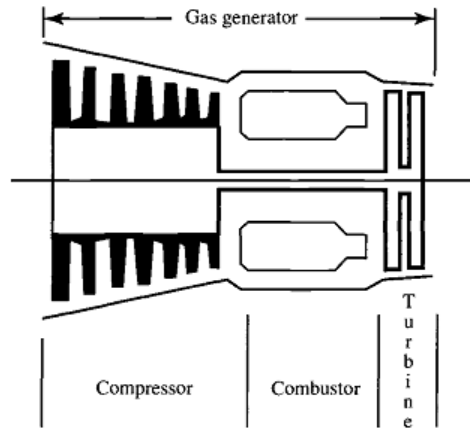


Figure 1-10 Schematic of Gas Generator [6]

The thrust of a turbojet is developed by compressing air in the inlet and compressor, mixing the air with fuel and burning in the combustor, and expanding the gas stream through the turbine and nozzle. The expansion of gas through the turbine supplies the power to turn the compressor. The net thrust delivered by the engine is the force acting on the different parts of the engine as a result of the gas movement in the direction of the exit.

Different engines are the extensions of the gas generator as discussed above and one such example is shown in the figure 1.11, also the regimes of engine are shown with respect to the high pressure and temperature cycle during the operation.

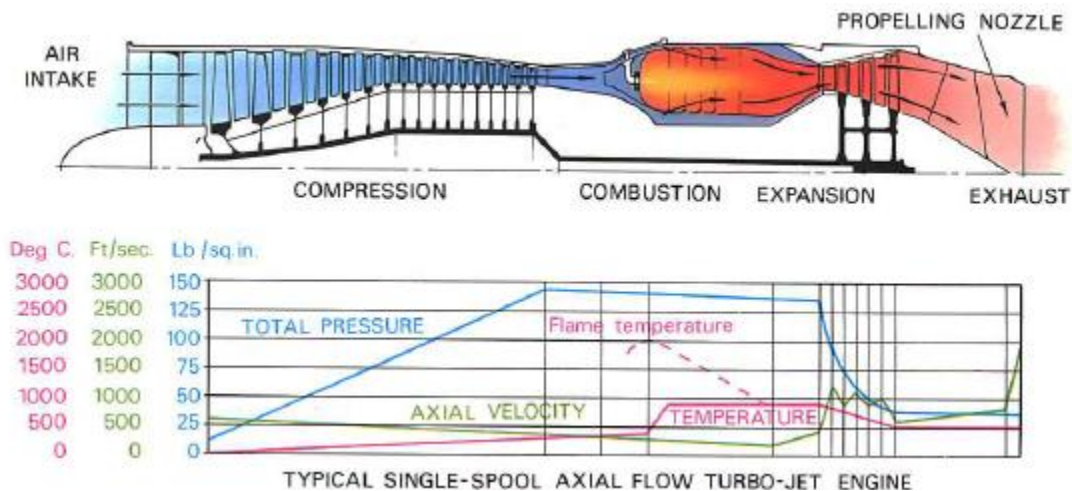


Figure 1-11 Zones of an engine and illustration of pressure and temperature distribution over the length [1].

2.5 Engine Hardware and Materials

The basic and most significant components of all the jet engines are; compressor, combustion zone and turbine each is fitted with several components to ensure the stable functioning of the engine

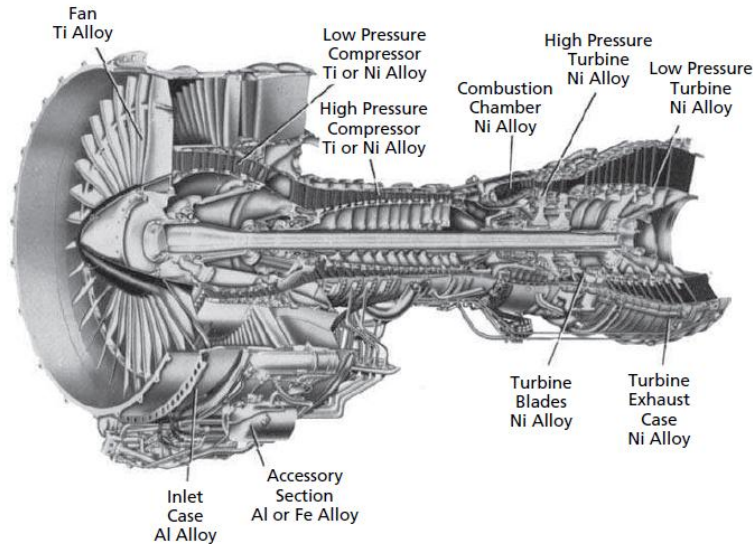


Figure 1-12 Major Components and Manufacturing Materials [7]

2.5.1 Compressor

This unit of engine takes the air from exterior and compresses it to 30 times which increases the initial temperature of air. Compressors are either of the axial type or of the centrifugal type.

Axial type compressors may be having up to 19 stages whereas the centrifugal type of compressors may have one or two impellers. Compressors unit consist of beam and cantilever style stator vanes and rotor blades, pressure increase and distribution in the compressor zone is shown in the figure 1.13. Improvement in the materials and manufacturing processes has enabled the achievement of more than 35% thermal efficiency-as the new compressors has attained compressing ratio up to 30:01, such high compressions help attaining very high temperature in the

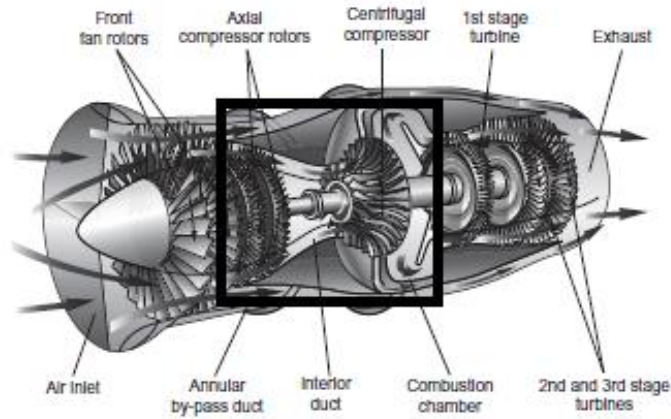


Figure 1-13 Schematic of axial and centrifugal compressor[4]

Different materials applicable to the compressor unit are shown in the table 1.1.

Table 1-1 Compressor parts and Materials [8]

S.No.	Component Name	Material
1	Air Inlet Housings	Aluminum
2	Forward Bearings	Aluminum
		Iron
3	Stator Vanes	Aluminum
		Titanium
		SS
4	Rotor Blade	Aluminum
		Titanium
		SS
5	Rear Bearing support	Aluminum, iron

2.5.2 Combustor/Combustion Chamber

This is the critical part of the engine as it controls the burning of the fuel. Its main purpose is to supply uniformly burnt gasses to the turbine section. There are three basic configurations of the combustors annular, can and can-annular. It is made of superalloys and titanium.

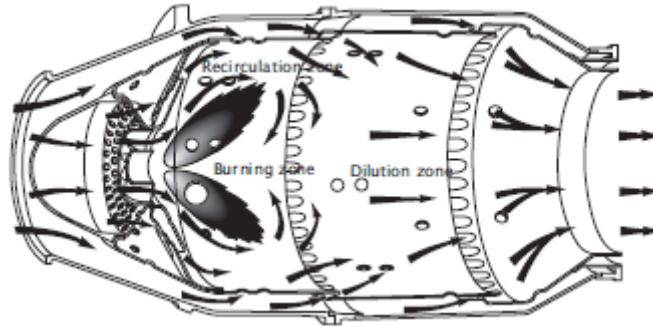


Figure 1-14 Schematic of diffusion combustor can with straight flow [4].

2.5.3 Turbine

This is a machine which extracts energy from the fluid and converts it into the mechanical energy. The components of the turbine are the limiting factor to run the compressor and combustion chamber at high pressure and temperature to increase the efficiency of the engine.

Downstream the combustion chamber turbine blades are the component at highest temperature 800-1700°C[2]. As these blades are rotated at very high speed by the moving exhaust gasses, such high rotation puts the mounting disc (base of blades) under high stresses too.

There has been much design and metallurgical modifications to make these components sustainable under the severe conditions, as explained in the next section. Materials of the few components of the turbine are mentioned in the table 1.2.

Table 1-2 Components in the turbine section and materials[8].

No.	Component	Material
1	Casing	Iron, Steel, Stainless Steel
2	Nozzle Vanes	Stainless Steel, Precipitation hardening Super Alloys

3	Rotor blades	Precipitation Hardening Super Alloys
4	Discs, Wheels, Drums	Steel

2.6 Efficiency of Engines

This high temperature operating machine has several performance parameters and different planes use one or the other depending upon the main requirement in the field, e.g. military planes have different requirement than commercial airliners. The basic performance parameters of this heat and energy machine are:

1. Propulsive Efficiency(Thrust)
2. Thermal Efficiency
3. Propeller Efficiency
4. Overall Efficiency
5. Takeoff Thrust
6. Specific fuel consumption
7. Aircraft range

2.6.1 Propulsive Efficiency (Thrust)

It is the first parameter available for the sustainable flight, it is conversion of air's kinetic energy as it passes through engine to propulsive power it is denoted by η_p

$\eta_p = \text{Thrust power} / \text{power imparted to engine flow}$, this term is closely related to the exhaust speed thermoprop engines have higher exhaust speed and higher propulsive efficiency

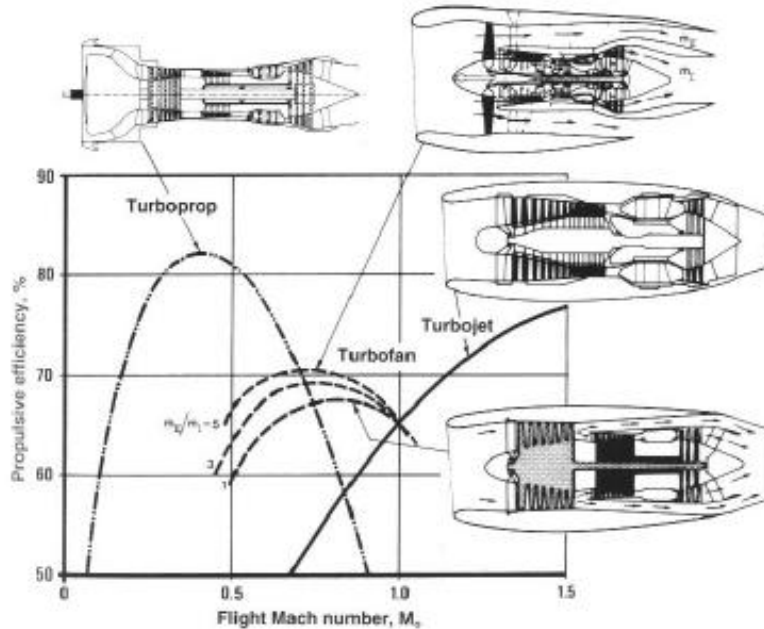


Figure 1-15 Specific thrust characteristics of typical aircraft engines [6]

2.6.2 Thermal Efficiency

It is the internal efficiency which is related to the power imparted to the engine airflow and rate of energy supplied in the fuel

$$\eta_{th} = \text{Power imparted to the engine airflow} / \text{Rate of energy supplied in the fuel}$$

2.6.3 Propeller Efficiency

This parameter is related with conversion of shaft power into thrust $\eta_{pr} = TP/SP$, TP=turbine power and SP=shaft power

2.6.4 Overall efficiency

It is the product of the propulsive and thermal efficiencies

2.6.5 Take Off Thrust

This parameter determines the ability of the airplane to take off utilizing its own power

2.6.6 Specific Fuel Consumption

It is the fuel consumption either per unit thrust force or the horsepower it is most vital component in considering the developments necessary in all type of jet engines

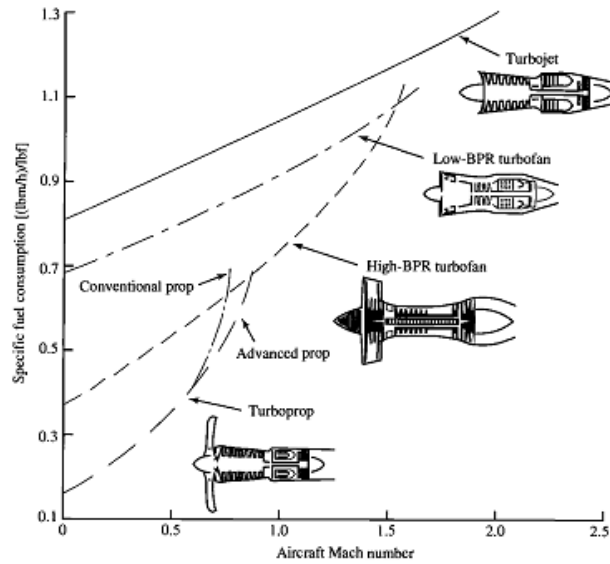


Figure 1-16 Thrust-specific fuel consumption characteristics of typical aircraft

Engines. (Courtesy of Pratt & Whitney.)[6]

2.7 Material and Manufacturing Process Evolution

As discussed previously all types of efficiencies are somehow connected with the better fuel economy (high temperature and high pressure), as shown in the figure 1.17&1.18. Achievement of better fuel economy, high thrust and low manufacturing and operational cost are the motives for the material and process development in this field. Fuel economy requires high temperature combustion from fuel[9].

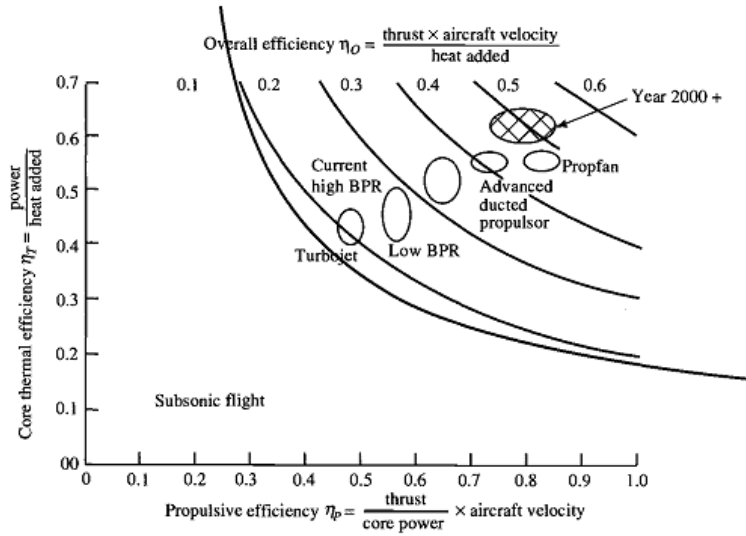


Figure 1-17 Efficiency characteristics of typical aircraft engines [6].

High thrust and low operational costs are related to the weight and fuel's efficient consumption, low cost of materials and manufacturing process is also vital in the development of commercial airplanes. This increased thermal efficiency makes it possible to reduce cost as well, whereas, high temperature is directly related to the increase in pressure[1]

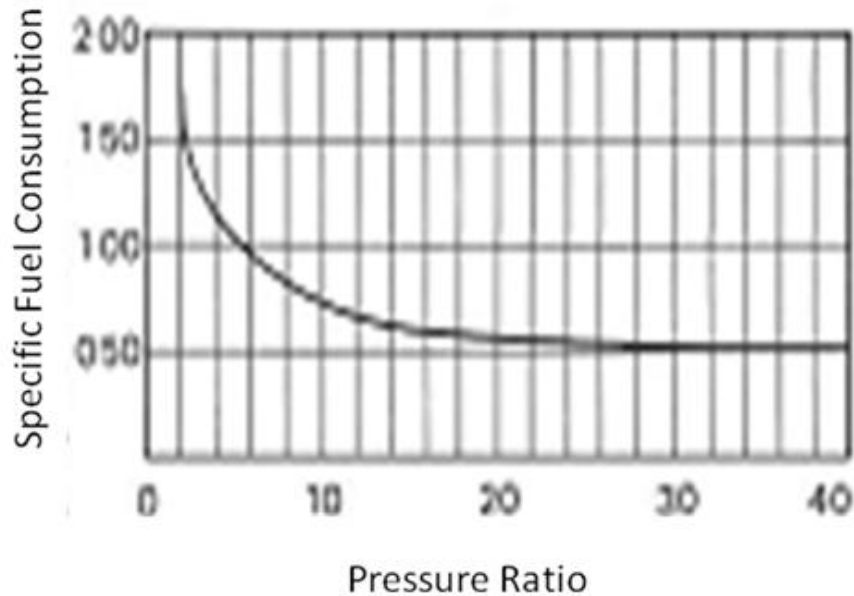


Figure 1-18 Relationship between specific fuel consumption and pressure ratio[1].

Thermal efficiency of the operation depends upon the high temperature combustion of the fuel. The goals of achieving high temperature were achieved with concomitant increase in the pressure, this is depicted in the performance graph, figure 1.19

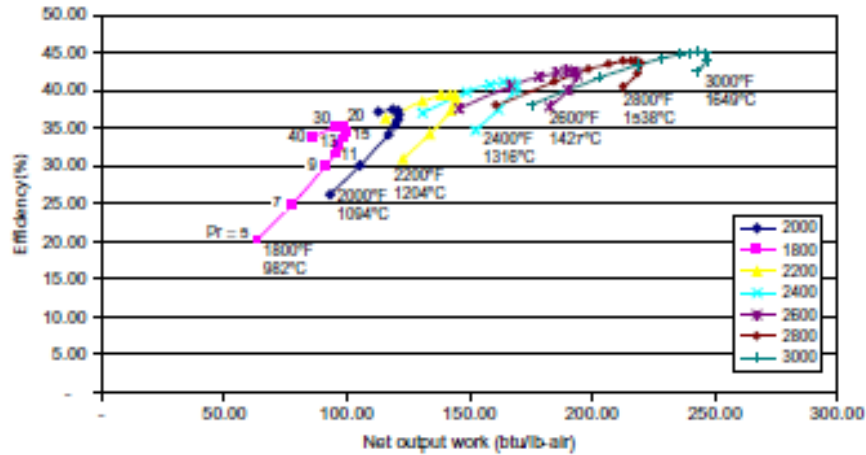


Figure 1-19 The performance map of a simple-cycle gas turbine[4].

With increase in temperature new materials to be functional in the turbine and high temperature end of the compressor are being sought. It is not possible to have all the blades in the compressor and turbine made of superalloys, as the weight of super alloys is three times higher than the ceramics[10]. It adds to the cost and limits the thrust factor which is greatly dependent on the weight of the engine.

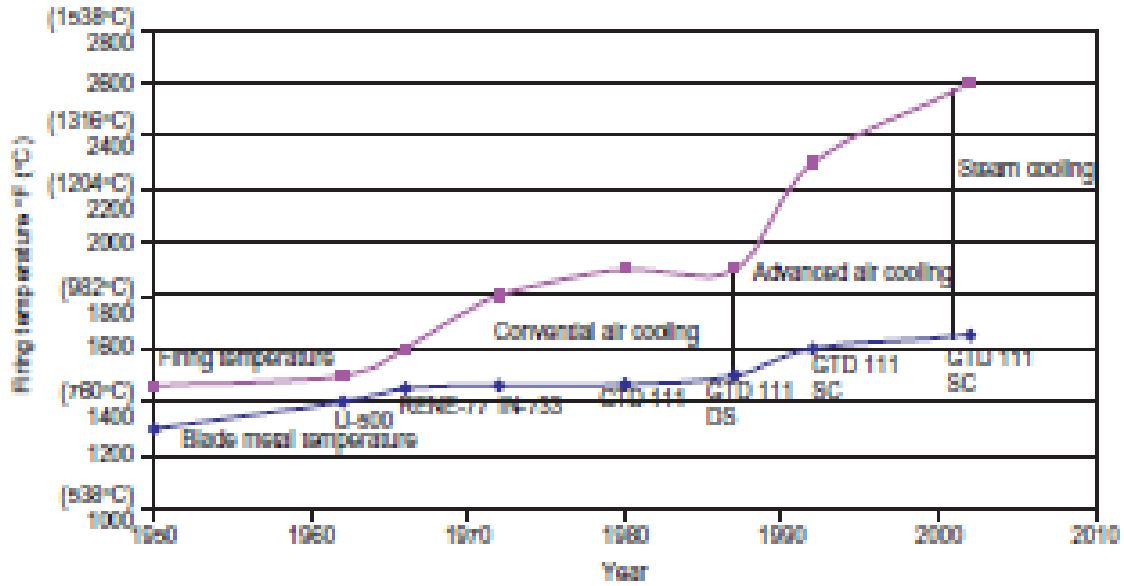


Figure 1-20 Turbine temperature improvement over the years with the process modification[4].

Materials and manufacturing methods are under study as these are to cut not only the manufacturing cost but also to make the process efficient. Ceramics and other lightweight materials with high temperature properties are replacing the parts made of heavy and expensive metals, as shown in figure 1.21.

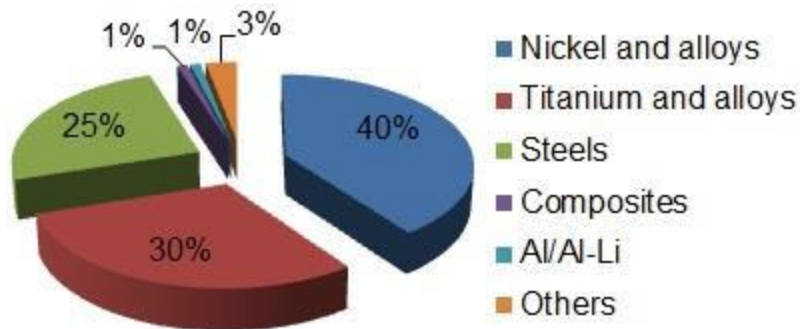


Figure 1-21 Replacement of Nickel based alloys with other materials [11].

Many of the challenges (high temperature combustion, corrosion, low hot temperature strength and high weight and low thrust) associated with the current metal component based engines can be resolved by application of ceramics[12]. Most significant challenges in advancement linked to the current material and advantages of ceramic system are:

1. Cooling system with superalloys-economical up to 1275°C but this system makes the superalloys unfit for the aircraft applications.
2. Possible future trend in increasing temperature per year-is difficult to be achieved with the current material system[4].
3. Ceramics are more resistant to Na and other elements present in the fuel
4. Cost of the ceramics is around 5% of the superalloys.
5. Ceramics are capable of attaining high temperature

Turbines operating at higher temperatures; yielding higher power; having longer life; economical in terms of production and operation with smaller engine sizes can be pragmatic if the material replacements are successful. Ceramic materials are capable of withstanding higher temperatures and they are also tolerant to oxidation/wear and hot corrosion caused by the elements (sodium, sulphur and vanadium ions) present in the low priced fuel. To gain better thrust in terms of weight ceramics up to 40% lighter than the comparable high temperature alloys. Additionally, their cost much less – their cost is about 5% of the cost of superalloys[13].

There are some compounds like molybdenum disilicide, carbides (SiC) and nitrides (Si₃N₄) that are expected next generation ceramic materials. SiC and its derivatives are brittle as compared to the Si₃N₄. But SiC/Si₃N₄ composites can perform better than individual SiC and Si₃N₄[14]. Si₃N₄ when processed without additive is very difficult to shape but with suitable additive can be processed into the useful components, but still the application of Si₃N₄ is limited to the simpler designs, and also the second phase is an amorphous glass which reduces the hot strength of the Si₃N₄ composites[15].

Processing of these composite nitrides is an issue as only α -Sialon is possible to be manufactured by Spark Plasma Sintering (SPS) or Hot Isostatic Pressing (HIP), whereas, β -Sialon can be shaped into different components as post processing sintering is possible[16]. SPS and HIP are only limited to the simple and flat shapes. Such flat shapes can give components only if welding or other ceramic fabrication technology could have emerged to connect the small slabs into a component. Other possibility is to make a large block using SPS or HIP and then machine these prefabs to desired shapes but the sialons are very hard materials and this can be achieved at the expense of diamond making the processing extremely uneconomical. Contrary to these methods, Lange[17] has highlighted the import of colloidal processing of ceramics and manufacturing, this

is economical and leads to defect free products as explained in the article, 'Colloidal Processing'. Whereas, fast, nearnet shape forming methods to any of the designed components give a control in global economy[18]. In the current study manufacturing of silicon nitride based ceramics which were being processed through spark plasma (SPS) and hot isostatic pressing (HIP) is carried through colloidal processing, economically.

3 Silicon Nitride and Sialons

In this section we discuss both, silicon nitride and Sialon, a material with similar properties. Silicon nitride, Si_3N_4 , exhibits very high resistance to heat and corrosion, and is exceptionally strong [19]. Sialon, a family of silicon aluminum-silica oxynitrides, has properties comparable to those of silicon nitride, and is much easier to manufacture and form into complex shapes.

Because pure Si_3N_4 powders are difficult to sinter, several methods are used to achieve finished parts of desired size and shape, and the processing technology used has a significant effect on the physical properties of the finished part as shown in the table 2.1. These processing technologies are (1) reaction bonding, (2) hot pressing, and isostatically hot pressing, and (3) sintering and gas-pressure-assisted sintering.

Table 3-1 Most commonly used Si_3N_4 production processes and physical properties[19]

Property	Units	Hot Pressed (HPSN)*	Sintered (SSN)	Reaction bonded (RBSN)
Density	g/cm^3	3.10 (3.07–3.37)	3.13 (2.8–3.4)	2.4 (2.0–2.8)
Hardness	Knoop 100 g	2200 (k100)		900 (VHN, 0.5 kg)
Coef. thermal expansion, 20–1000°C	$10^{-6}/\text{K}$	3.3 (3.0–3.9)	3.5	2.9 (2.5–3.1)
Young's modulus, 20°C	GPa	300 (250–325)	245 (195–315)	175 (100–220)
Young's modulus, 1400 °C	GPa	175 (175–250)		155 (120–200)
Flexure strength, 20°C	MPa	750 (450–1100)	415 (275–840)	200 (50–300)
Flexure strength, 1400°C	MPa	300 (0–600)	70 (0–700)	250 (0–400)
Fracture toughness	$\text{MPa} \cdot \text{m}^{1/2}$	4.8 (2.8–6.6)	4.3 (3.0–5.6)	3.6
Coefficient of thermal expansion, 20–1000°C	$10^{-6}/^\circ\text{C}$	3.3 (3.0–3.9)	3.5	2.9 (2.5–3.1)
Thermal conductivity, 25°C	$\text{W}/(\text{m} \cdot \text{K})$	32		8–12
Maximum service temp.	°C	1300		1300

Table 3-2 Properties of Sialon compared with HP Si₃N₄[20]

Property	Units	Sialon	Si ₃ N ₄
Density	g/cm ³	3.25	3.2
Hardness	Knoop, k100	1800	2200
Melting point	°C		
Modulus of elasticity	GPa	0.28	0.31
Compressive strength	MPa	>3500	>3500
Toughness	MPa · m ^{1/2}	7.7	5
Weibull modulus		11–15	10–15
Poisson's ratio		0.23	0.27
Thermal conductivity at 25°C	W/(m · K)	21.3	25
Specific heat at 25°C	Cal/g · K	0.15	0.17
TCE (0 to 1000°C)	10 ⁻⁶ /K	3.04	3.2

3.1 Processing

Si₃N₄ is very difficult to sinter as the sintering temperature is raised beyond the dissociation of Si₃N₄. Good sinterability is achieved only in the pressurized sintering conditions. Densification of Si₃N₄ and resulting densities are mentioned in the table 2.1.

3.1.1 Sintered Silicon Nitride (SSN)

The need for a fully dense silicon nitride, which can be readily formed to near net shape by mass production processes, has long conventional sintering could give only 90% of theoretical density. The major problem was dissociation of Si₃N₄ at the temperature where atomic diffusion was required for sintering. This problem of dissociation was solved by Mitomo et al. [21-23]. They proposed few points to sinter, it should have:

- 1 Fine particle size < .5um.
2. Sintering under gas pressure
3. Preventing SiO₂ loss from the sintering system by enclosed system as in the case of HIP etc.
4. Keeping some oxygen in the system.

3.1.2 Two stage Reactive Gas Pressure Sintering

Close pore stage, reaching to the level where porosity becomes less than .1MPa and then increasing the pressure up to 6~8MPa densification above 99% can be achieved advantage of this process over the HIP'ing is no external devices are needed to hold the sample.[24]

3.1.3 Cladd HIP'ing/Glass Encapsulated Sintering:

In this process a preform of can or glass is used to shape the powder. This process was used successfully to get 95% of the theoretical density. In certain aspects, isotropy and achieving high Weibull modulus as compared to the HPSN, the process of glass encapsulated sintering was considered better. Than HPSN [25] applied during experiments by Thomy et al[26, 27]

3.1.4 Hot isostatic pressing (HIP)

Hot isostatic pressing is carried out in the hot conditions where uniaxial load up to 200MPa is applied on the material and density values 100% of the theoretical density are achievable. Hot isostatic pressing resulted better products with improved hot MOR and fatigue resistance as compared to the products developed previously. High pressure use and its application to the complex designs is the major challenge.[28]

HIP would be a choice, if we want a high toughness material with coarse microstructure, otherwise the GPS would be a choice[29].

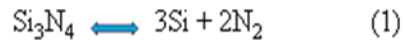
3.1.5 RBSN

Sintered RBSN Sinterable powder was bedded in the similar powder and preform up to 95% density with higher shrinkage was obtained. Additionally this preform has the ability to be resintered up to theoretical density with increased strength and oxidation resistance. First stage of a preform making bears the high shrinkage to be appeared during the normal sintering process and the component during final sintering undergoes only 7~8% shrinkage

3.2 Dissociation of Si_3N_4 .

In the absence of controlled atmosphere and high temperature Si_3N_4 decomposes and the evaporation is increased when Si_3N_4 partial pressure reaches equilibrium partial pressure of reaction (1)

Decomposition of Si_3N_4 affects the sample and limits the sintering temperature. Additionally, it alters the vaporisation of SiO_2 formed by the reaction of additives and silica present on the sample[30]. It also affects the composition of sample, it can be prevented by high nitrogen pressure achieved by powder bed and encapsulation.



Without controlled atmosphere evaporation becomes more pronounced. The change in colour of sample is caused by such dissociations.

Dissociation can cause a change in the amount and composition of additive during interaction with atmosphere i.e. Al_2O_3 can be reduced to AlN, which will be dissolved in Si_3N_4 .

Al_2O_3 acts as a buffer, the dissolution of Al in Si_3N_4 is proportional to evaporation of SiO_2 . The amount of Al in Si_3N_4 depends upon sintering parameters and on ratio of Al_2O_3 to other additives. The reduction of Al_2O_3 and SiO_2 depends upon strong reducing atmosphere and high weight losses.

Rare earth oxides and Y_2O_3 are more stable additives, it has been proved experimentally.

Alkaline and their earth oxides are unstable and evaporates. For instance, MgO behaves as



3.3 Sialons

As through the previous section we have come to know that problem of dissociation of sintering and the complications of high temperature pressing methods in producing the desired shapes. Comparison of Sialon and Si_3N_4 characteristics is given in the table 2.2.

Sialon is solid solution (a derived material) of Si_3N_4 . Sialons are produced at commercial level and there are two main phases, namely, α -Sialon and β -Sialon whereas δ -Sialon is less commonly studied phase. The phases which are of structural importance, i.e. α -Sialon and β -

Sialon are the solid solutions based on the structural modifications and has the close relevance to the parent α -Si₃N₄ and β -Si₃N₄ as shown in the figures 2.1 and 2.2.

Table 3-3 Structural parameters dependence upon the chemical composition, for α and β -Sialon[20]

Phase	a, nm	c, nm
β ss	$0.7601 + 0.00304z$	$0.2906 + 0.002554z$
$\text{Si}_{6-z}\text{Al}_z\text{N}_{8-z}\text{O}_z$	$0.7603 + 0.002967z$	$0.2907 + 0.002554z$
	$0.76069 + 0.00279z$	$0.29068 + 0.00263z$
α ss		
$\text{MSi}_{12-n-m}\text{Al}_{m+n}\text{N}_{16-n}\text{O}_n$	$0.7752 + 0.0036m + 0.002n$	$0.5620 + 0.0031m + 0.004n$
M = Y	$0.7752 + 0.0045m + 0.0009n$	$0.5620 + 0.0048m + 0.0009n$
α ss		
$\text{MSi}_{12-n-m}\text{Al}_{m+n}\text{N}_{16-n}\text{O}_n$	$0.7749 + 0.00673m + 0.00023n$	$0.5632 + 0.0055m + 0.00054n$
M = Ca		

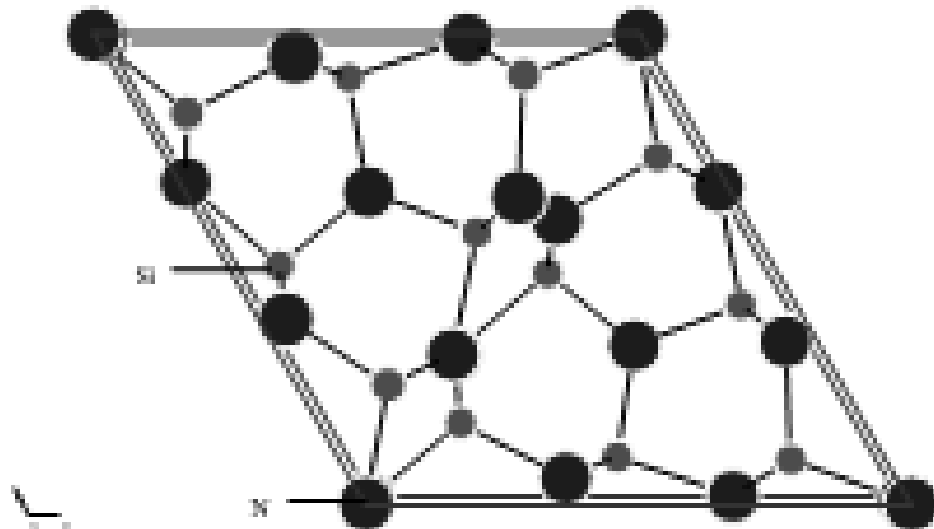


Figure 3-1 A view of atom arrangements in the α -Si₃N₄[31]

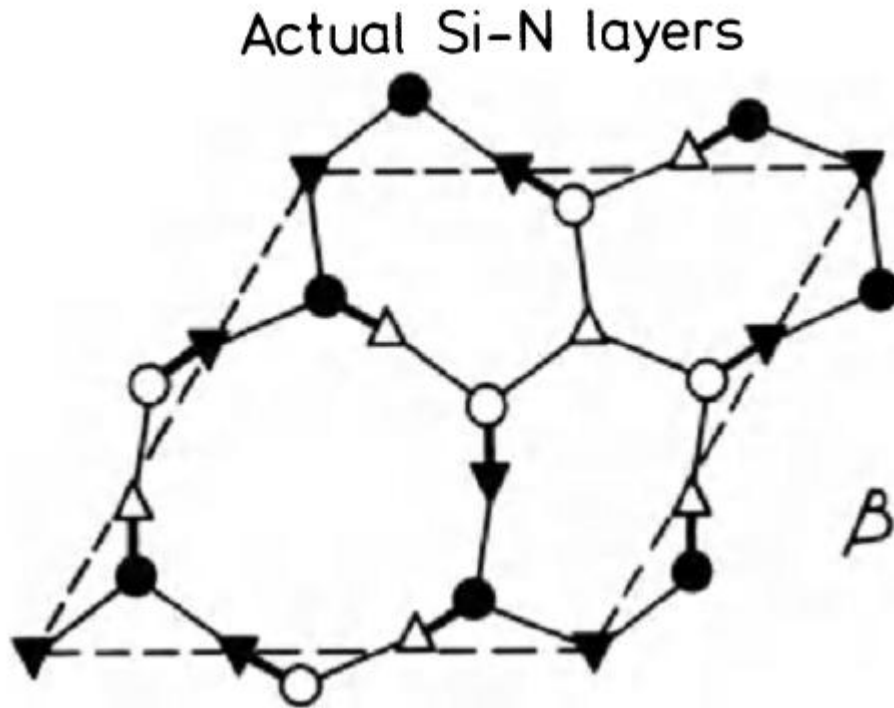


Figure 3-2 A view of atom arrangements in the β - Si_3N_4 [31]

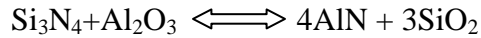
3.3.1 β -Sialon.

Si_3N_4 has the capability of accepting Al_2O_3 and BeO_2 in high amounts. This type of transformation can happen for both α and β - Si_3N_4 starting materials, transformation does not highly depend on the initial phase of starting powder. Additionally, at high temperature α - Si_3N_4 is unstable and starts transformation to β -Sialon.

This type of Sialon is formed by the substitution of Al-O for the Si-N units in the original β - Si_3N_4 structure. Actually, β -Sialon has a range of composition as shown on the diagram, Janeck prism, figure 2.2[16] and it has the general formula $\text{Si}_{6-z}\text{Al}_z\text{O}_z\text{N}_{8-z}$, where $z=0\sim 4.2$. During the beta sialon formation loss of SiO_2 takes place. Along with β -Sialon the other compound formed is X-Sialon as show in Figure with increase in temperature X-Sialon decreases. High variations in the hardness values can be found for the β - Si_3N_4 and same might be true for the β -Sialon[20].

3.3.1.1 Kinetics of β -Sialon.

Additives added are more than one and their effect can be explained in terms of phase diagrams. In β -Sialon formation all the starting materials can be represented by the regular tetrahedron, as shown in the figure 2.3, and any point in the diagram can be explained by a planar rectangle, shown in the figure 2.4. This type of rectangle can represent the system as a reciprocal salt system. Phases in this system



are best explained by quasy ternary system[32] rather than the ternary systems, Si_3N_4 -AlN- Al_2O_3 and Si_3N_4 - SiO_2 - Al_2O_3 , one such diagram's isothermal section at

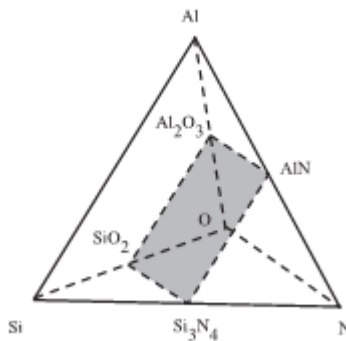


Figure 3-3 Si_3N_4 -AlN- Al_2O_3 - SiO_2 , quasi-ternary subsystem for the components, Al-Si-O-N[20].

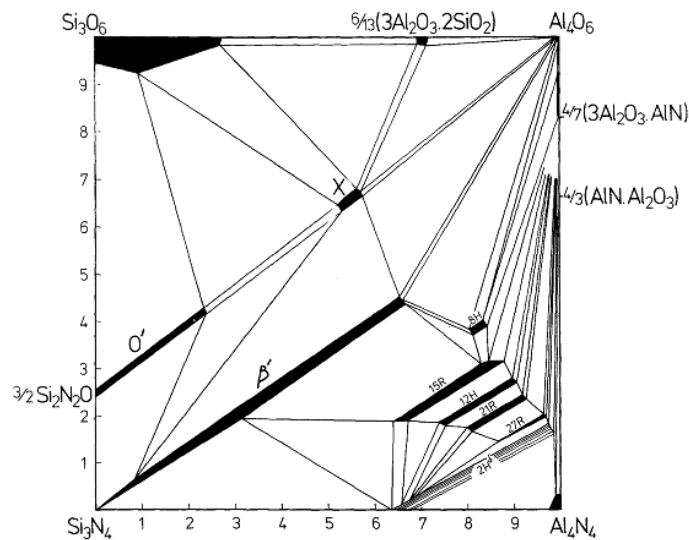


Figure 3-4 The Si_3N_4 -AlN- Al_2O_3 - SiO_2 system based on research at Newcastle [15]

In separate work two different starting materials reached the same chosen composition

3.3.1.2 Yttria as an Additive:

In most of the sialons yttria is used as the additive to improve the sintering behavior of the sialon. In the Si-N-O-Y system a quasi-ternary system, $\text{Si}_3\text{N}_4\text{-}4(\text{YN})\text{-}2(\text{Y}_2\text{O}_3)\text{-}3(\text{SiO}_2)$ exists and phases in SiYON system similar to the mellilite, wollastonite, woehlerite exists. In the practical compositions on the tie line, $\text{Si}_3\text{N}_4\text{-Y}_2\text{Si}_2\text{O}_7$ a binary eutectic forms at 1550°C and crystallizes at 1500°C . With increasing the contents of Yttria composition shifts to the compatibility diagrams with lower eutectic temperature, composition shift with increasing Yttria content towards left is shown with arrow on the diagram in figure 2.5.

When Y_2O_3 is considered with Al_2O_3 quasy-quaternary systems as shown in figure 2.4, explains the relationship.

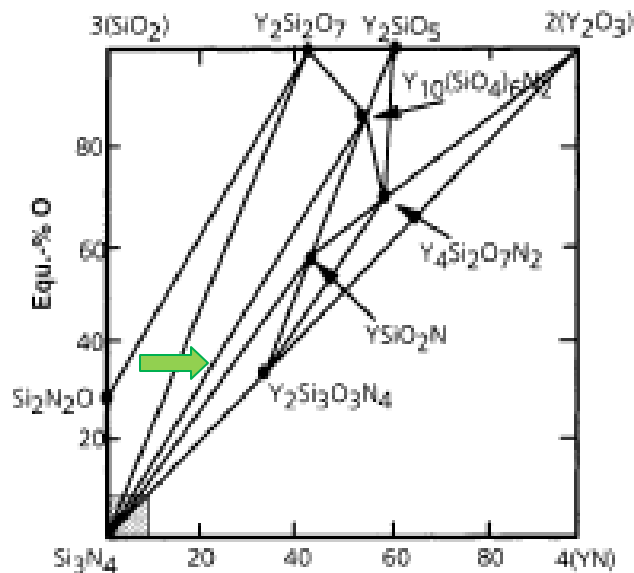


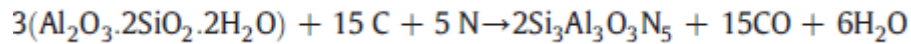
Figure 3-5 The subsystem $\text{Si}_3\text{N}_4\text{-}4\text{YN}\text{-}2(\text{Y}_2\text{O}_3)\text{-}3(\text{SiO}_2)$. Isothermal section at 1770K

3.3.1.3 Synthesis of β -Sialon

β -Sialon production has as many ways as the Si_3N_4 synthesis but the high purity β -Sialon production needs to be synthesized from the original materials

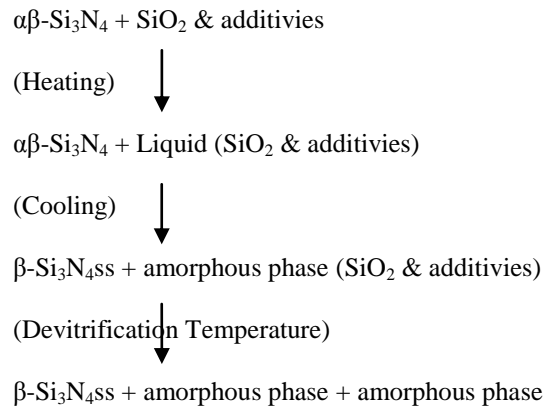
3.3.1.3.1 From Aluminosilicate (Kaolinite)

There are two dominant methods of producing β -Sialon from aluminosilicate, nitridation of the aluminosilicates and carbothermal nitridation reduction of aluminosilicates where kaolinite has the tendency of capturing the N_2 and be converted to β -Sialon according to the general reaction[33, 34].



3.3.1.3.2 From Si_3N_4

Technological ceramics are derived by adding more than 3 elements to the base materials[20]. Theologically, obtaining pure β -Sialon is possible if additives are mixed with the Si-Al-O-N and S-O-N-Be and system is heated to 1500°C . β -Sialon ($\alpha\beta\text{-Si}_3\text{N}_4\text{ss}$) can be produced according to the following reaction.



In such reaction sequence we get the final product (β -Sialon) through liquid reprecipitation of the reactants where the final product contains a main phase, secondary crystallized phase (an oxynitride) and a glassy phases that is vital in holding the crystallites together.

3.3.2 α -Sialon.

This type of Sialon is a solid solution of $\alpha\text{-Si}_3\text{N}_4$, it resemble closely $\alpha\text{-Si}_3\text{N}_4$ as shown in figure 2.6 and it is represented by the general formula $\text{Me}_x\text{Si}_{12-(m+n)}\text{O}_n\text{N}_{16-n}$, where $x=m/3$, $m=\text{Al-N}$

units replacing Si-N units and $n=Al-O$ units substituting Si-N units. In this type of transformation at 1st place $n(Al-O)$ units replace $n(Si-N)$ units and secondly, further replacement of Si^{4+} by Al^{3+} is stabilized by Me^+ into the phase structure.

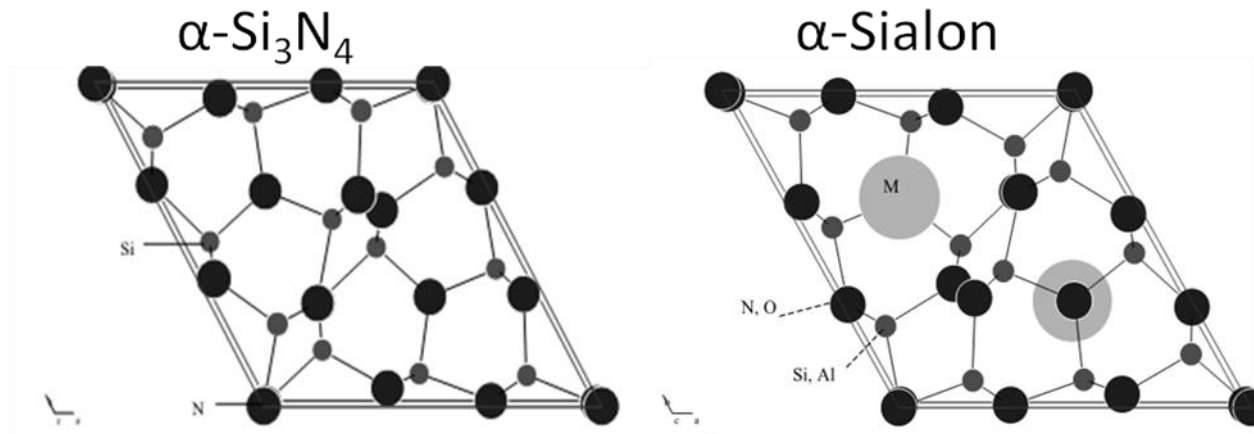


Figure 3-6 Structure of $\alpha-Si_3N_4$ (Left) and of the $\alpha-SiAlON$ (right).[31]

On two dimensional phase diagrams it is shown in the region bounded by subsystem, Si_3N_4-ReN , $3AlN-4/3(AlN-Al_2O_3)$, and is shown on the diagram for Ytria containing system as a shaded region as shown in the figure 2.7.

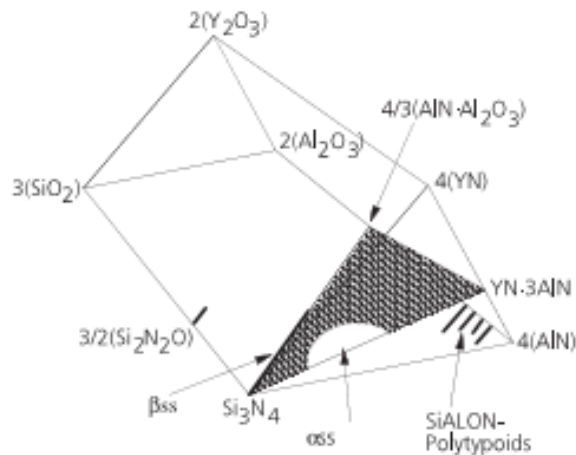


Figure 3-7 α -Sialon region on the Janeck prism

Extension of the phase field is represented by the $Y_xSi_{3-(3x+n)}O_nN_{4-n}$, where $.08 < x < .17$ and $0.13 < n < .31$. Solubility limits are governed by the cation sizes. i.e. $x = .08 \sim .20$ for the cations

additions in the Sialon by Menon et al[39]. Wetting characteristics of the eutectics melts based on the RE-SiO₂-Al₂O₃ are different for the Si₃N₄ and AlN as shown in the figure 2.9.

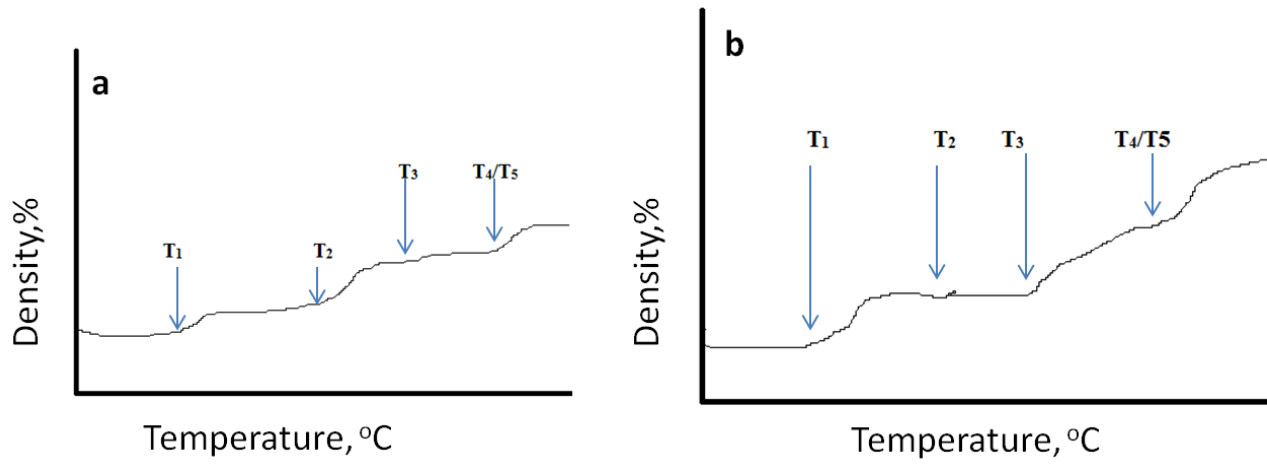


Figure 3-9 Wetting behavior for Si₃N₄ first (a), and for AlN first type (b).

Wetting behavior has been explained in terms of acid base interactions by Pearson et al. [40]. He has shown that strong acid (Si₃N₄) has greater tendency to react with the strong base of oxide systems giving melts of lithium, calcium, magnesium and lighter earth metals up to Gd. Contrary to this soft acid AlN reacts with the soft bases of heavy RE melts up to Dy. This data matched with the observed eutectic and dissolution temperature to that of the calculated based on the assumptions. Overall temperatures at which reactions take place during this wetting of the material are:

- T₁, it is temperature at which the eutectic formation takes place.
- At T₂ as the nitride powder wets intermediate precipitation takes place
- T₃ is the temperature at which wetting of the second nitride phase takes place
- T₄ is the onset of secondary phase dissolution.
- T₅ is marked by precipitation of the final phase.

Wetting of AlN gives no or very little effect on immediate shrinkage in the powder compact as the quantity of AlN present in the Sialon is not significant, but a significant immediate shrinkage indicates the wetting of Si₃N₄. Change in the curves is not unusual as T₂ can be lower than the

full wetting. Sometimes T_4 can precede the T_3 as in the case of lithium and calcium where partial formation of Sialon has taken place before the final dissolution of the AlN.

Final densification temperature becomes crucial if the secondary reprecipitation takes place it consumes the liquid and process of densification gets retarded.

3.4 Phases in α - β -Sialon Systems.

Sialons production, mechanical properties and end use relies greatly on the kind of additives[20]. These additives are often the oxides of various alkali and rare earth metals, these give the practicability to engineer not only the structure of Sialons but also to get rid of glass by tailoring the composition. Various authors have given phases formed in the Re, Si, Al, O, N systems, like, Dy, compatibility phase relationship by Sun, et al. Y, Si, Al, O, N compatibility phase relationship by[41, 42]

Excerpts from the phase relationship for the system Y, Si, Al, O, N are given in detail here.

Table 3-4 Compatibility tetrahedra and possible phases close to the region of Sialon on Janeck Prism

S.No	System/Region	No. Of Compatible Tetrahedra	Phases
1	Si_3N_4 -AlN- Al_2O_3 - Y_2O_3	39	J_{ss} , 15R, 15R', YAG, 12H', 12H, 21R, J, M, α' , 27R, 27R', 2H, 2H', β , β_2 , β_{10} , β_8 , β_{60} , β_{25} , β_{30} , $J_{ss}M$, $2H^\delta$
2	Si_3N_4 -AlN- Y_2O_3	23	J_{ss} , 15R, YAG, 12H', 12H, 21R, J, AlN, M, α' , 27R, β , β_{60} , β_{25} , β_{30} , $J_{ss}M$, $2H^\delta$
3	Si_3N_4 -AlN-YN – Y_2O_3	7	Al_2O_3 , J_{ss} , 15R, 15R', YAG, 12H', 12H, 21R, J, M, α' , 27R, 27R', $2H^\delta$, YAG, 2H', β , β_2 , β_5 , β_8 , β_{60} , β_{25} , β_{30} , β_{111} , AlN, $2H^\delta$

3.5 α - β Phase Relation

β -Sialon does not absorb most of the rare earth additives, and even most of them are α -Sialon formers. In Sialon formation some amount of additives remains as a residual M-Si-Al-O-N, inter granular glassy phase, which degrades the mechanical and chemical properties of the material above the glass-softening temperature, which normally is about 900–1100°C.

Heat treatment is performed to eliminate or minimize the glassy grain boundary phase. Slow cooling or holding at glass transition temperature can convert this glass phase into the crystalline material[43]. During the study with multiple cations (Yb_2O_3 , Dy_2O_3 , Sm_2O_3 cations of these oxides) in Sialon in place of Y_2O_3 either singly or in combination with Y_2O_3 Mandal et al[44] reported that the transformation from α -Sialon to β -Sialon occurred in some RE containing (α + β) composite materials when heat treated between 1000°C and 1600°C. Transformation was exaggerated by increasing temperature.

Although, both the phases are basically built up of corner sharing (Si, Al) (O, N) tetrahedrally, But there is a distinct difference in the atomic arrangement. Change from one form to other requires lot of energy and time for the atoms to break one bond, diffuse and then form another type of configuration

3.6 Multication-Sialon

In the production of Sialon RE elements are vital to stabilize the α -Sialon structure and currently, whereas β -Sialon cannot take any of these cations in the structure because of the small spaces available. Currently, yttria is the highly used material to provide this cation (stabilizer) for the α -Sialon, it is expensive material and not much stable at high temperature (during heat treatment). To replace the yttria in order to reduce cost and include structural stress (enhance high temperature stability) various metallic oxides, i.e. CaO, MgO, CeO etc., are tried.

3.6.1 Sialon-Graphene Interaction

Production of carbon nanotube (CNT), SWNT, based composites has demonstrated 100% increase in the fracture toughness of ceramics. Graphene imparts similar characteristics to the ceramics but it is easy to disperse in the materials during processing[45]

3.6.2 Si₃N₄/SiC Composites

The concept of nanocomposite development, In 1990s, to manufacture hard, strong and wear resistant composites is appreciated by the many scientists in this field[46, 47]. Composites with SiC distribution, intergranular and intergranular, were achieved. The improved powder manufacturing and handling technology enabled the development of materials with high strength at ambient and high temperatures.

Now a days development of Si₃N₄/SiC composites is based on: mixture of Si₃N₄ and SiC powders, in-situ synthesis of SiC during sintering, etc.

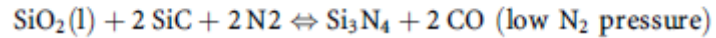
Most of the Si₃N₄/SiC composites are produced by hot pressing to overcome the difficulties during densification, as encountered in the consolidation of Si₃N₄[48]. SiC particles can be surrounded by the Si₃N₄ grains SiC or glass. Pinning introduced by the inclusion of nano SiC up to 50% of the composite volume in Si₃N₄/SiC can introduce superplasticity[49].

Improvement in the high temperature strength is achieved as the SiC interaction with glassy phase in the Si₃N₄/SiC composite around the Si₃N₄ particles alters the composition and turns this glassy phase into crystalline[50]. SiC presence also improves creep resistance, as SiC particles form a hard skeleton.

In Si₃N₄/SiC composites higher oxidation resistance at high temperature is achievable as the oxidation mechanism is changed by the SiC.

3.6.3 Sialon-Carbon Interaction

SiO₂ can be reduced by the presence of carbon and SiC as the later can react with SiO₂ as shown in the equations.



N₂ pressure controls the kinetics of the reactions, along with the temperature. At 1800°C the SiC is converted to C and Si₃N₄, in the presence of nitrogen at 6 MPa[51]. At high pressure more SiO₂ can be consumed by the reaction of C and N as mentioned in the reaction. Contrary to this in usual sintering conditions a reduced weight loss with increasing nitrogen pressure is observed[30,52].

A strategy to avoid this loss (decomposition) of materials with C interaction is sintering under CO partial pressure. By keeping the CO partial pressure in equilibrium shown in equations, CO formation can be reduced and so does the concurrent weight loss is reduced. Additionally, achieving the condition of over pressure SiO₂ and C (up to 0.6% C) can be incorporated into the system.

4 Processing of Ceramics-Sialons.

There are two types of production processes for Sialon

1. Sialon synthesis-Processing –Consolidation (mostly applicable to β -Sialon)
2. Starting from raw materials processing-Shaping/ Forming –consolidation(mostly applicable to β -Sialon)
3. Processing (colloidal or powder mixing) Forming and shaping combined with consolidation production processes i.e., HIP'ing, SPS etc.

All the processes enlisted involve mixing of the powders with binders and additives; shaping and consolidation(in conventional ceramics) but the production of α -Sialon $\alpha\beta$ -Sialon combines the step of shaping and consolidation because of the dissociating nature of the Si_3N_4 (explained in the article)

Forming and production processes separately give the advantage of economization of the overall process. As this type of processing gives the shapes with good tolerance and almost any intricate shape can be manufactured eliminating the need of machining.[53].

Since, the Sialon production involves the production route similar to many other ceramics at some stage so the count about ceramic processing starting from the raw materials is given in the next sections.

4.1 Raw Materials and Powders

Powder are manufactured by various techniques, typically most of the oxides are prepared by using the chemical methods and then undergo milling to produce the desired sized particles

Each step introduces a detrimental inhomogeneity, which serves as a strength reducer source in the final part as shown in the figure 3.1.

4.1.1 Nature of Powder

Manufacturing mode imparts certain level of impurities or service oxides which impact the shaping processes and densification[54]

4.1.2 Particle Size

Powders carefully controlled in size and having a size range are good in green packing, results in high green density (density of the shape before firing). Green state density influence drastically final densification behavior and changes the mechanical character of material. Nanosized particles are easy to sinter as compared to the large sized particles and shape[55]. As the particle size is reduced less energy is required to reach the theoretical density value. Additionally, fine particle size results in final fine grained particles[56]. There are several methods to measure the particle size of the particles as mentioned in the table 3.1.

Table 4-1 Particle size ranges and Method of Measuring the particle size.

Method	Medium	Size (μm)	wt (g)	t
Light microscopy	Liquid/gas	400-0.2	<1	S-L
Electron microscopy	Vacuum	20-0.002	<1	S-L
Sieving	Air	8000-37	50	M
	Air	5000-37	5-20	M
	Liquid	5000-5	5	L
	Inert gas	5000-20	5	M
Gravity sedimentation	Liquid	100-0.2	<5	M-L
Centrifuge sedimentation	Liquid	100-0.02	<1	M
Electrical sensing zone (Coulter counter)	Liquid	400-0.3	<1	S-M
Fraunhofer scattering	Liquid/gas	1800-1	<5	S
Me scattering	Liquid	1-0.1	<5	S
Intensity fluctuation	Liquid	5-0.005	<1	S
X-ray line broadening	Air	<0.1	<1	S-M

4.1.3 Shape of the Particles

Flat and irregular shapes are considered as the source of defects, round shaped particles are considered best for as the shape irregularities. Considering the strength limited in terms of flaws, this type of defects are primary limiting factors. In the materials like SiC flakes or agglomeration causes the voids because of this type of defects[57]. Particle shape information may be either desirable or critical depending on the degree to which shape affects product performance. Particle shape also influences bulk properties of powders including flow and compaction behavior and the viscosity of suspensions

4.2 Melting

Melting is only suitable for eutectic ceramics[58] or glass ceramics, where no long range order exists and the residual stresses developed can be removed by annealing[59]. Ceramics with crystalline phases are very difficult to be processed by melting as solidification progresses thermodynamics of solidification is very difficult to control, hence uncontrolled grain size is the outcome of such processing.

4.3 Dry Powder Processing

Mixing of powders manually or using mixing mills in the dry condition and pressing with or without binder. This is the quickest production method but most vulnerable for the ceramics. This technique incorporates various inclusions and introduces the factors to reduce the mechanical strength of the component as mentioned below

4.3.1 Agglomerates and Heterogeneities

Ceramic powders which are produced by the reaction of a precursor at moderate temperatures. In such powders nano sized crystallites are formed which sinter together to a continuous low-density network of crystallites. Again to break the network of particles material is ground to; the resulting particles can be partially dense crystallites in the form of strong agglomerates. Whereas conventional pressing technology is based on dry pressing and requires flowable powders to uniformly fill a die cavity. Particles within dry powders are held together by van der Waals forces. The attractive interparticle forces combined with moisture condensed at particle contacts are responsible for cementing particles together, whereas, previously, present impurities having salt contents get dissolved with the water and act as cements. Not only the shape forming process is inefficient, but also the reposition of particles during the drying and consolidation is difficult[60]. This behavior of particles results in the formation of drying cracks and voids. Whereas the agglomerates produced by spray drying may not uniformly deform to fill inter particle void spaces during consolidation

4.3.2 Inclusions

Inorganic inclusions are added to facilitate densification or during the processing of powders. Densification of ceramics containing inclusions results in microcracks. Such cracks are a potential strength limiting factor as shown on the figure 3.1 These cracks are caused by

inclusions during either cooling from the densification temperature or subsequent stressing. Such inclusions are impossible to be removed even the clean rooms are ineffective because the manufacturer supplies powders mixed with the inclusions-remedy for these inclusions is the washing carried out through colloidal processing.

4.3.3 Density Gradient:

Different materials have difference in their density, this difference can result in differential density based segregation during the flow while pressing or in storage bins and compositional gradients can be caused.

4.3.4 Defects Remedy

Hot-gas isopressing is carried out to eliminate some voids that remain after pressureless densification. Voids are closed by deformation and crack like voids are the first to be closed by this treatment but cracks that intersect the surface and other heterogeneities, e.g., inclusions are difficult to be mitigated. Additionally, post densification treatment can exaggerate the size of voids just beneath the surface.

4.4 Colloidal Processing

Colloidal processing gives better control of interparticle forces, attractive or repulsive forces can be controlled to the desired level and problems of agglomerations and segregation can be avoided[61]. Additionally, solid loading in a slurry can be handled, to manipulate the loading of solid contents in the slurry there are a number of factors that can be modified to alter the rheology of slip.

1. Attractive van der Waals forces,
2. Repulsive electrostatic forces
3. Steric forces (Attractive or repulsive)
4. Attractive Capillary Forces.

Except attractive forces all other forces are set by the incorporation of the external surface active (surface modifying) agents. The colloidal approach conforms to the requirements of breaking

agglomerates and avoiding many of the defects incorporated during powder processing as shown in figure 3.1.

- Defects in ceramics Start from Processing(Structural Inhomogenities)

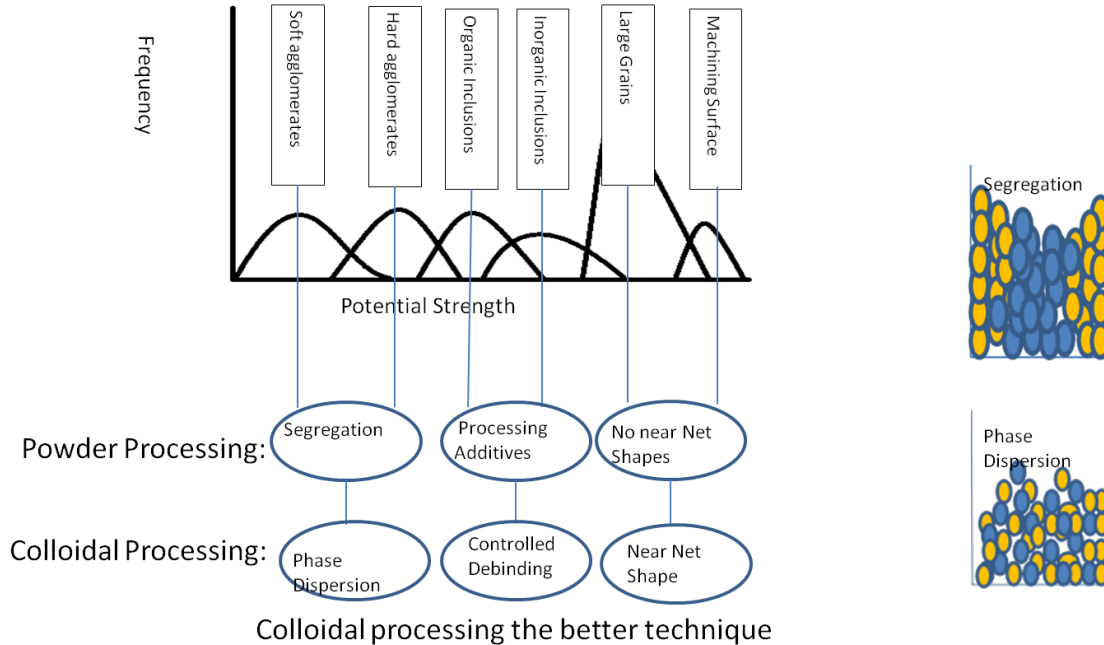


Figure 4-1 Potential strength limiting factors and possible remedies suggested by the colloidal processing.

By controlling the rheology, i.e., interparticle forces, many of the heterogeneities discussed in the earlier sections can be eliminated. Powders floc together to form a low-density network of touching particles if the attractive forces are higher, otherwise, particles are dispersed to form a system of separated particles when repulsive forces are the dominant factor. In case of the strong repulsive forces interparticle forces are used to set apart weak agglomerates. In the colloidal processing initially high repulsive forces are intentionally developed in the system to break the agglomerates and once the agglomerates are fractionated into the desired size then rheology of the system is changed. Attractive forces are applied to form a low-density, deformable network that prevents mass segregation and inclusions.

Mixing of multiple phases homogeneously is attainable via colloidal processing. Powders with differential density can be flocculated first and then breaking this flocculated network mechanically by applying high shear rate sets apart the particles but they have tendency to interact with other type of particles at this stage such mixture is introduced with another type of particles they are easily

made the part of earlier network and hence homogeneous solution with multiple phases having density difference is achieved. Such systems are considered better in the flocced state as compared to the unflocced. One such a system, containing materials with different density, was cast into a shape in the flocced and dispersed state to compare the effect and it was noticed that system with flocced particles did not show a compositional variance after densification. Contrary to this other system showed severe differences in the composition [61].

Wide area EDX with low magnification can be a valuable parameter to analyze the phase dispersion in the slip/slurry such a test performed on the green body can help controlling the quality of slip.

Slurry rheology is strongly governed by interparticle forces and particle volume fraction.[62]. In the dilute systems slurries exhibit Newtonian rheology, whereas, for high volume fractions, the slurries viscosity increases with shear rate.

The slurries under the influence of attractive forces exhibit pseudo plastic, thixotropic rheology, viscosity decreases with increasing shear rate, as the applied forces separating attractive particles depends on shear rate. Refloccing of the particles into the network requires some time.

Slurries with repulsive forces dominating in the system allows to develop slips with high powder contents, such slurries can contain up to 60 vol% solids. Whereas, the capacity of the flocced slurries in castable condition is just up to 20 vol%

4.4.1 Consolidation from the Slurry State

In colloidal processing the colloiddally treated powders should not be dried directly from the slurry/slip. As slurries contain soluble salts produced by the reaction of solvent with the powder, such salts can cement the particles at different places and form agglomerates again which are removed during mixing. Inclusions can also come from the environment during drying process or the remnants of drying/combustion can act as inclusions.

Colloiddally treated slurries could be shaped/consolidated by the following shaping/forming methods

- *Slip Casting*
- *Consolidation Machine*
- *Spray dried Powder*
- *Tape Casting*
- *Filter Pressing*
- *Injection Molding*
- *Extrusion*

4.5 Slip Casting:

Direct shape is formed from the colloids in the porous mold of ceramics, process is shown in the flow diagram, figure 3.3

Slip is poured in the mold and after a certain time mold is inverted a thin layer of solid is formed along the walls of the mold as the liquid adjacent to the mold is seeped quickly by the porous mold leaving behind particulate mass which forms a uniform thickness along the surface. It can be slip casting to give thin walls or a solid casting as shown in the figure.3.2. Additionally, slip casting can be combined with a centrifugal casting unit where pressure/centrifugal force can enhance the densification process

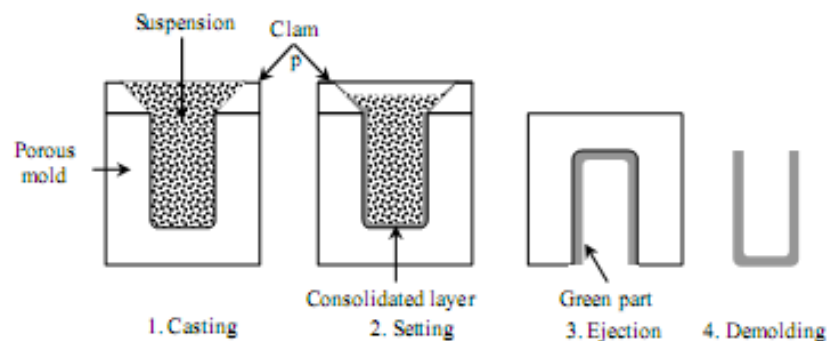


Figure 4-2 Schematic of slip casting steps[63]

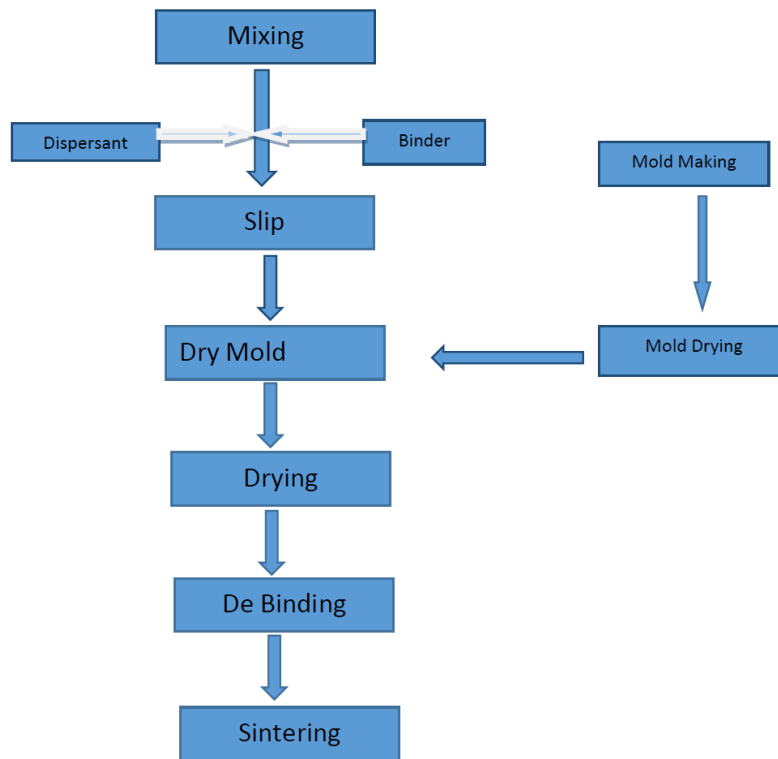


Figure 4-3 Flow chart of the slip casting process

The problem with conventional slip casting is low green density as the volume of solid particles loaded in the slurry is limited up to 60%, and other aspect limiting the slip casting is that components with adequate thickness can be made by this technique.

4.6 Tape Casting

In tape making colloidal solution is heavily loaded with organic binders. Slip is cast in the form of thin tapes on a Mylar (carrier) using doctor blade process, as shown in the figure 3.4.

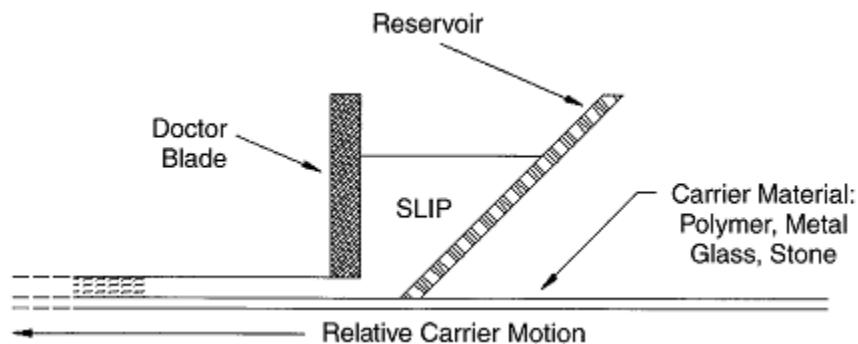


Figure 4-4 Tape Casting Process, Doctor Blade Process[64]

In a tape casting process, the slip is poured into a reservoir behind the doctor blade, and the carrier to be cast upon is set in motion[64]. Gap between the blade and the carrier, speed of the carrier, shape of the doctor blade and viscosity of the slip defines the wet thickness of the tape being cast. Immediately, cast tape is passed through a drying chamber of, solvents are evaporated and a thin flexible film is retained on the carrier surface. Formed tapes are delaminated from the mylar and bound together and can be cut into any final shape required. This stack needs removal of organic binders in controlled atmosphere the process of debinding reduces the density greatly

Tape casting technology from casting to densification consists of the several steps as mentioned in the flow chart

Powder Preparation-----Dispersion Milling-----Plasticizer and Binder Mixing-----Slip De-Airing-----Tape Casting-----Drying-----Shaping-----Calendaring and Lamination.

4.6.1 Powder Preparation.

This step is critical to remove the impurities imparted during the process of manufacturing, handling, storage and transportation of the powders, it includes the following procedures.

4.6.1.1 Powder Washing:

Dry ball milled powders contain the binder that prevent the balling up for slip making. To remove this additive sticking on the surface powders may need a hot water (95°C) wash and then oven drying to evaporate the water[65].

4.6.1.2 Drying of the Powder

Hygroscopic materials and materials containing free water (moisture) need to be dried before mixing with organic solvent as it can create troubles in controlling viscosity and hydroxyl content of hygroscopic powders etc.[66]

4.6.1.3 Surface Hydration

Some powders perform much better in the presence of a uniformly distributed moisture contents on the surface and such materials are given a heat treatment at ~90°C in the humid environment[64]

4.6.1.4 Chemical Surface Treatment

To improve the contact between the inorganic surface and the organic solvent sometimes coupling agents, organometallic compounds like silanes, are used. This type of modifications help achieve lowering of viscosity and higher solid loading in the slip [67]. Additionally, similar treatment can be applied to process the hygroscopic particles in aqueous solutions by applying a suitable coating(steric acid/octadecanoic acid) on the surface[68].

4.6.2 Dispersion Milling

Dispersion milling is the primary stage in the colloidal processing (Tape Casting) and material is milled in the presence of a dispersant/deflocculant in the solvent(s). The primary purpose of milling is; to break agglomerates; to coat particles with organic solvent which are freshly set apart Milling equipment consist of vibratory, short filled paint mills and ball mills, ball mills are designed for mixing in the range of .3liter to 3000 liters[64].

Milling parameters are designed based on the batch size and the degree of comminution to be attained. The ball mill size is chosen according to the size of the batch to be processed.

Media Selection in the ball mill is critical for purity of powders to be maintained and particle dispersions achievable, commonly used grinding media in tape casting is:

1. High Purity Alumina(High Density)- Alumina contents>85%
2. Polyethylene jar- To avoid inorganic contamination in the powder.
3. Rubber linings or polyurethane linings-dispersion energy is reduced.
4. Steel mills and grinding media-limited to ferrite slips mostly

Other than contamination the factor to be considered in selection of grinding media is the hardness of the media and target powder, media should have greater hardness than the target powder to be milled.

Filling of mill with grinding media is from one-third to one-half of the mill volume. After the loading with milling media mill is charged with the powder and other additives in the following sequence

Solvent-----Dispersant-----Wetting agent(s) -----Powders----- plasticizer and binder mixing

4.6.2.1 Plasticizer and Binder Mixing

Plasticizers are added when adequate mixing and deagglomeration of the powders is attained these are basically added to the slip to make it castable and be handled in the later stages[69, 70]. Plasticizer is added before the binder so that plasticizer makes the mixing and attachment of binder to the particles easy.

4.6.3 Slip De-Gassing

During the milling and mixing processes slips can entrap air from the powder or the reaction of organic additives, also the air present inside the jar may get dissolved in the slurry. It is necessary to remove any air that may have been entrained. Air entrapped can cause defects like, pinholes, elongated streaks or thin spots in the tape casting direction. The slip containing all the ingredients in an intimate mixture just before casting needs to be de-aired to get rid of mentioned probable defects. Degassing is carried out by applying low vacuum and leaving the system for several minutes in that state. Most common systems used for de-gassing a slip are, Lab. vacuum desiccators and a venturi pump etc. are used for de-gassing and best practice is the simultaneous agitation supporting the degassing process, performance of degasser is enhanced in the later setup as the less viscous solution makes the degassing take place easily. Problem associated with high vacuum degassing is vaporization of the solvent. By applying low vacuum for constant time will result in consistent slip with uniform viscosity from batch to batch

4.6.4 Slip Characterization

Slip is characterized for viscosity, specific gravity and particle size distribution are determined to characterize the slip. First two parameters are determined on every batch of slip brought to the casting line. Particle size distribution, on the other hand, is usually only checked if there has been a change in the batch materials.

4.6.5 Tape Casting and Drying

Prepared slip is fed into the doctor blade and cast in the form of thin tapes as shown in the figure 3.4.

Tapes are cast in different designs and shapes, but all the designs and shapes require few components in common, i.e. A flat surface for casting, a drying chamber facilitated with air blowing equipment.

Flat surface can be granite (polished surface) or a moving carrier which in stretched condition appears as a flat surface.

Drying of the tapes is carried out to remove solvents as quickly as possible but the care is exercised to avoid the skin formation (at earliest stages of the drying) and remove the solvent(s) without case hardening taking place. Usually, ideal condition in drying is to have a high concentration of solvent vapors at the entrance end of the machine and this decrease in the concentration should be gradual. This drying system contains fans to blow air avoiding the counter current

Air Blowing is dictated by the type of solvent, solid loading, temperature of air, type and quantity of binders and thickness of the tape to be dried.

Temperature in the drying unit is maintained at a gradient hot end is kept in the direction opposite to the casting head; this is achieved by applying in line heating arrangement.

4.6.6 Static Charge Elimination

Winding and unwinding movement of the insulator (organic polymers) on the tapes surface produce static charge. This charge may attract dust particles to the surface, and also static discharges can cause explosion, in the presence of flammable solvents. Static discharging can be done by applying a kind of grounded stainless steel brushes on the dry end of tape casting unit or in the driers.

4.6.7 Slitters, Cutoffs, and Take-Up Systems

Tapes from the edges are cut using a device that is called slitter. Slitter removes the thin section (feathered edge) from the edges, thin section which is cut is about 6 to 12 mm. If the product is being stripped from the carrier, the take-up system is a bit more complex.

If the tape is being gathered altogether with carrier it can be collected by take up roll without considering the stress development in the tape as carrier provides the mechanical strength. Whereas the systems where tape is detached from the system and only tape has to be spooled on the take up rolls in this case take-up rolls speed is carefully controlled to avoid stress development in the tape

4.6.8 UV Curable Tapes

In this type of tapes drying stage is modified by the UV treatment of binder system. Tape is formed using identical process for forming the thin films on a carrier as mentioned previously. Only the drying, or in this case curing, step is modified to produce the flexible tapes that are ready for further processing at the end of the casting machine. All of these UV-curable systems contain a dispersant, a plasticizer (if needed), a photopolymerizable binder, and an initiator to activate the UV curing. Mostly, a typical polyester acrylate is used as a binder and 2-hydroxy-2-methyl-1-phenyl-propan-1-one is used as an initiator. UV-curable systems contain an acrylate monomer as they have relatively low viscosities. Systems with low viscosity allow the preparation of ceramic slurries with relatively high solids loads. This type of mechanically strong tapes are passed under UV lamps, where the range of spectra between 200nm to 450nm

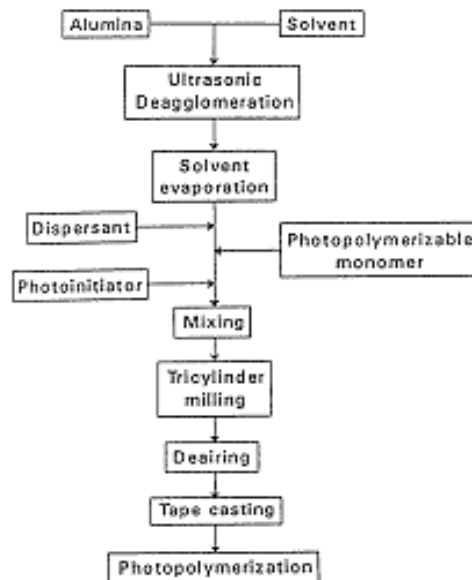


Figure 4-5 Flow chart of the tape casting process.

Major advantage associated with it is the short length of UV tape casting machine and less burnout of solvent.

Contrary to this main disadvantage of this process is the short depth of cure due to limited UV penetration. This limit of UV allows only casting thin tapes and can create a problem with thick tapes. Most of the work reported to date has been up to about 0.014 inch in thickness. There are also some materials that limit the depth of cure. Some of the heavy metal compounds based

4.6.9 Tape Calendering

This process is applied to prepare tapes by passing the tapes through the pair of rolls. This action is performed to achieve certain advantages like.

To reduce the sintering shrinkage and increasing the green density. Additionally, differential shrinkage can be minimized; surface smoothness achievement is possible; reduction in warping caused by one-side drying and achievement of the uniform thickness throughout the section is possible.

4.6.10 Lamination

Lamination is the ability to laminate together several layers of green tape to form a structure that sinters together into a monolithic solid ceramic. The thin green tape is peeled from the carrier and cut into the pieces and with or without calendering these peels are staked together with the help of a binder[71].

Lamination is controlled by applying pressure and mild temperature, whereas the applied temperature and pressure are decided by type of binder, solvent and Tg of plasticizer and other organic additives. Usually, the pressure applied is in the range from 1.4 to 138 MPa. And this pressure is held for 3 to 4 minutes.

Problems associated with conventional lamination are:

Uneven thickness- Problem of uneven thickness can be overcome by 90° rotation of tapes

Uneven shrinkage in x & y direction- again rotation can mitigate this problem too.

4.6.11 Isostatic Lamination

This type of lamination is performed to avoid the defects of uneven pressing. This is carried out by fixing layers on the fixing plate and then this is sealed in the vacuum bag. The bag is put in hot chamber having arrangement of fluid and pressing mechanism. Mostly, the pressures applied are between 34.5 and 68.9 MPa. This is carried out at 70~90°C within 3 to 10 minutes[64].

4.6.12 Shaping

Tape-cast materials are punch to produce the desired shapes. Production facilities use punch-and-die sets in either a hydraulic or a mechanical press. The shaping process is carried out in two stages, these are blanking and hole or via generation.

Blanking, is performed to make the outside shape of the desired object. Hole or via generation helps creating junctions of blanks to make the useful components.

4.7 Calendering

Tape like shapes are produced by the application of high pressure to spherical spray-dried powder material by passing it through the pair of rollers that revolve against each other. This process is known as an alternative process to tape casting. The resulting tape is very sound, it is flat, smooth, and flexible and can be punched into shapes and also can be rolled by the processing equipment.

4.8 Pressure Casting

Slip casting in routine is marred by the excessive shrinkage of the component during and after drying. To avoid the density stratification and obtain better green density during forming pressure is applied on the casting slip and up to 5MPa of pressure can give considerably thickness in relatively short time,

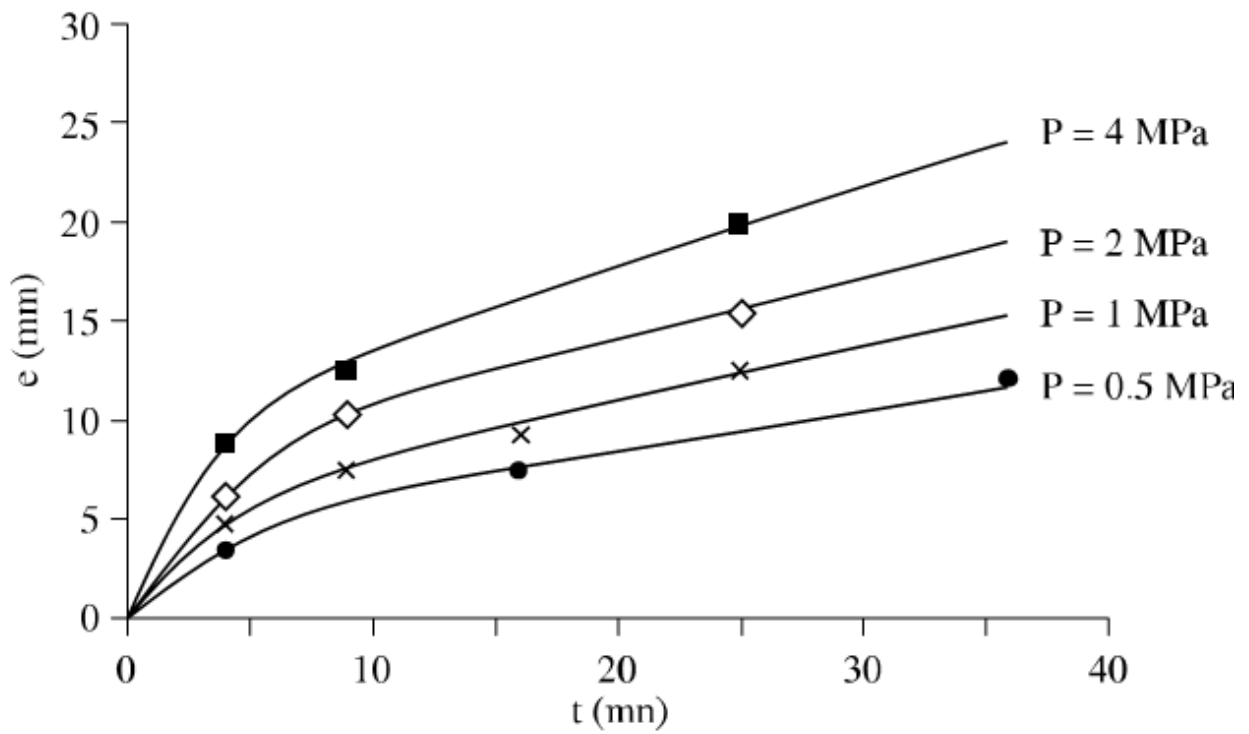


Figure 4-6 Casting kinetics for various applied pressures [GRÜ 72]

[72]GRU et al performed pressure casting of Si_3N_4 using porous mold, as shown in the figure3.7

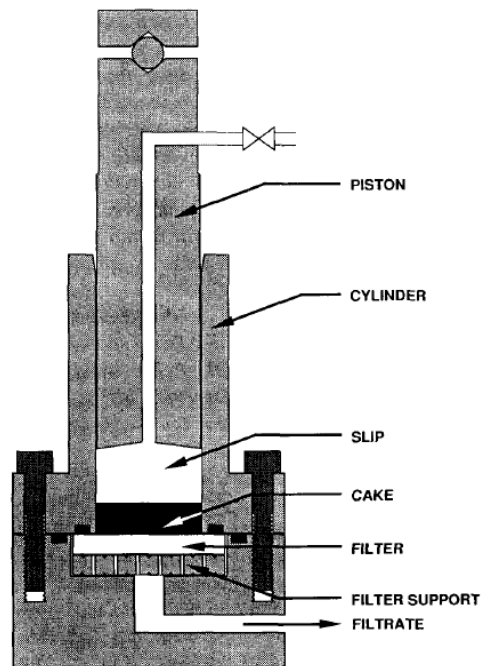


Figure 4-7 A pressure casting using porous mold

Other methods where pressure on the slip can be applied is in centrifugal casting where centrifugal force provided by the rotation acts as pressure. Vacuum casting is an alternate of pressure casting where applied vacuum draws out the solvent.

4.9 Extrusion-injection Molding

To avoid excessive moisture content and associated problem of high shrinkage thick slurries which could retain shape and be deformed when a force is applied are prepared for molding[.]. Slurries containing high solid load, more than 60% solid load can exhibit conditions suitable for molding, this type of system is studied by Aksay and co-workers, [17]

Granules or paste is prepared after mixing the necessary ingredients for extrusion or molding, there ingredients, binders, plasticizers and dispersant for aqueous or non-aqueous system are mixed using different types of mixers as shown in the figure 3.8. The third type of mixer is mainly used for extrusion. The parameters which are important in controlling the mixing are the sequence and type of additives and mixing variables, like, temperature, time, and vacuum etc.

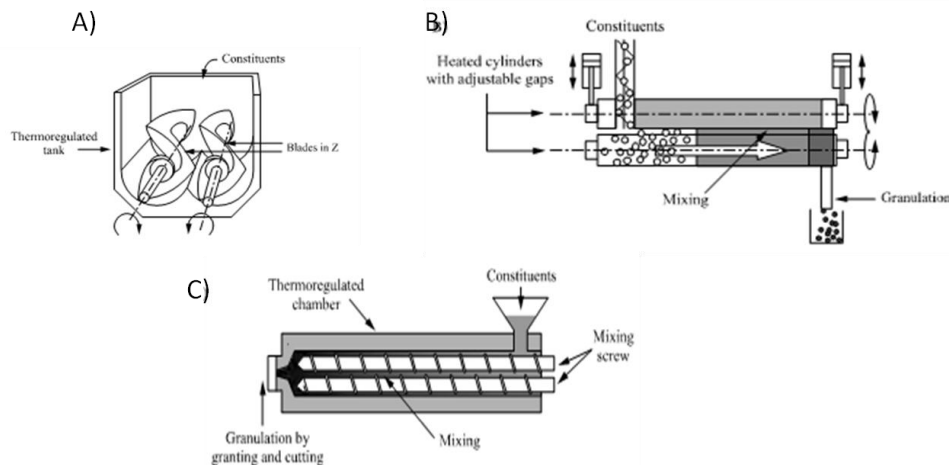


Figure 4-8 A) Z-blade mixer, B) roller mixer, C) double screw mixer[63]

Materials are mixed to gain the plastic flow through the extrusion die to obtain the desired form. Mixture should be able to flow through the injection orifice of low cross-section and on the other hand, ensure the filling of the injection mold. For extrusion too the rheological behavior must

also confer sufficient mechanical strength on the extruded part to avoid its deformation. In general paste should have following characteristics:

1. It must possess enough viscosity during mixing stage, and must demonstrate good dispersion under the effect of high shear forces.
2. It should be fluid during the extrusion and injection stage (high shear rate) to satisfactorily flow and fill the mold.
3. Shape retention- high viscosity after shaping (zero shear rate).

Typical desired rheocharacter of pastes for extrusion and molding are given in the figures 3.9a and 3.9b, respectively.

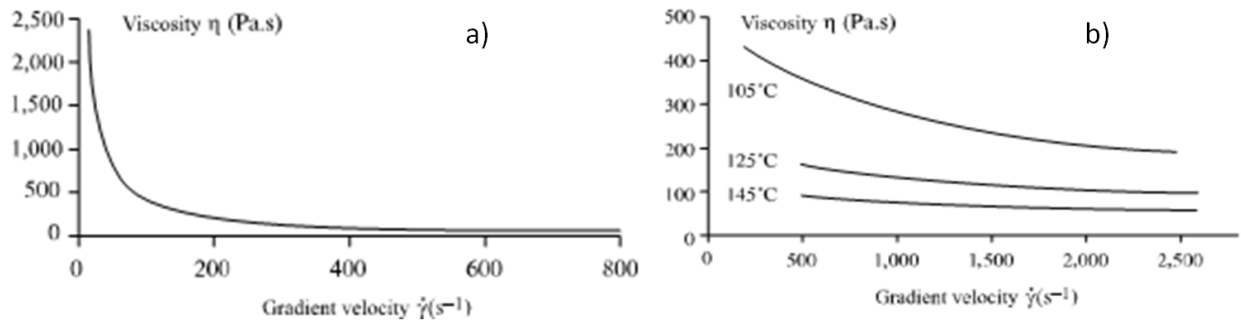


Figure 4-9 Rheogram of an extrusion paste, a and b is the typical rheogram for injection molding machine[63]

4.10 Extrusion-Shaping

Plasticized paste is pushed through the die of the given geometric dimensions using a piston or a screw. Piston extruder's work in batch mode, the paste is placed into the chamber, which is then closed again, a piston extruder is shown in the figure 3.10A Piston type extruders are limited to the lab scale. Whereas, screw extruders shown in the figure 3.10 B. are used for production scale.

Extrusion for the aqueous pastes is carried out at room temperature, whereas, the mixtures containing wax are shaped in the machines equipped with hot chambers. Additionally, hollow shapes can be extruded using special dies with two or more bridges

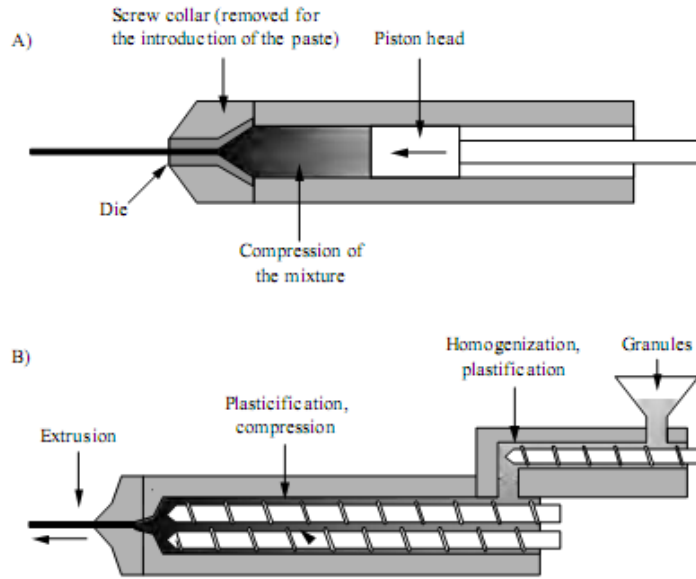


Figure 4-10 Piston extruder, A) and screw extruder B)[63]

4.11 Injection Molding

In this process a mold whose shape is that of the piece to be prepared is filled with a plastic material by applying pressure on the mixture, called feedstock. Feedstock is well mixed using different type of mixtures as explained above. Usually, the mixture is heated and then forced through a small diameter tube into the mold. After solidification, the piece is ejected from the mold.

There are two types of injection molding: high pressure and low pressure injection molding.

High pressure injection molding process uses pressure in the range of 50~300MPa and a screw piston system is used to apply the pressure, one such machine is shown in the figure 3.11, [73].

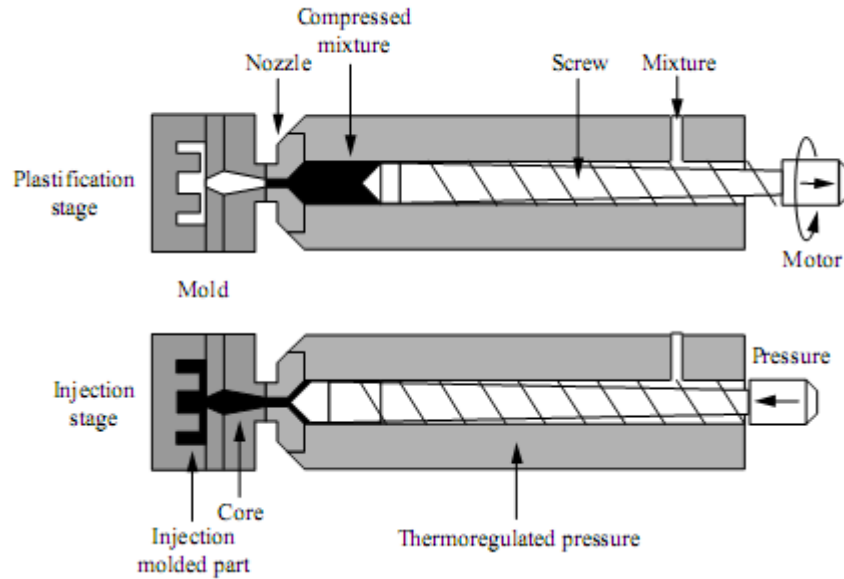


Figure 4-11 High pressure injection molding machine[63]

In order to avoid the degradation strict control of the pressure and temperature is achieved during the processing. Additionally, to avoid the contamination of the ceramic powders with injection molding should be minimized by using the coatings and other stuff on the surface of machines.

Low and medium pressure injection molding utilizes the binders with lower melting points as compared to the ones used in the high pressure molding.

In the injection molding machines for medium pressure, applied pressure ranges from 1 to 5 MPa. Whereas, in low pressure molding, pressure applied is from 0.6 to 0.8 MPa. And this low pressure is mostly applied by the compressed air, Figure shows medium and low pressure injection molding.

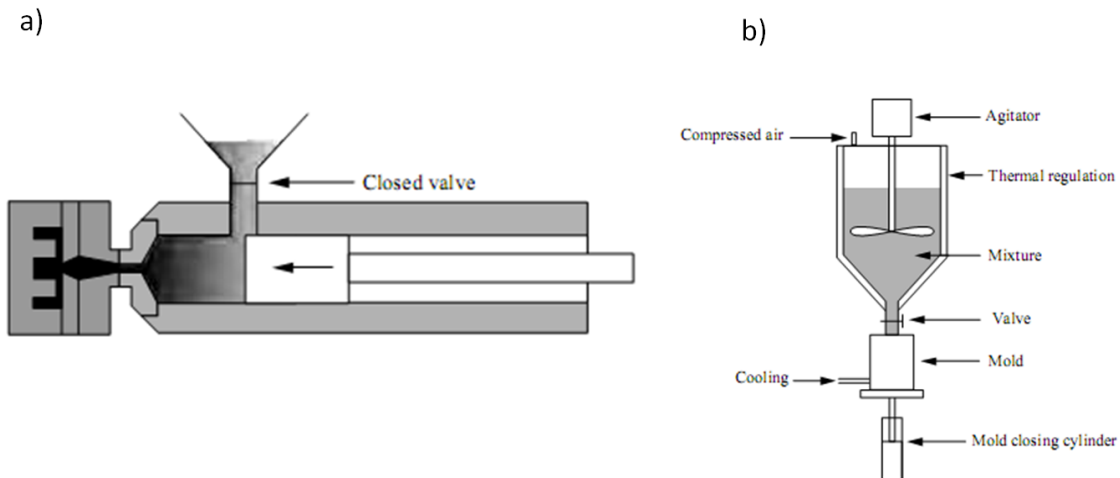


Figure 4-12 injection molding machines, a) Medium pressure and b) low pressure injection molding machine[63]

The material used in this process is much less expensive than the material used in high pressure injection molding as the temperature and pressure required are low. But the chief disadvantage is its capacity to develop materials with low viscosity.

4.12 Rapid Prototyping (RP)

This process is a layer by layer manufacturing of ceramics where a CAD file from a computer is accessed to design and form the component without using molds[74].

This process is further classed as: Stereolithography (SLA) and Fused Deposition Modeling (FDM)

Stereolithography component containing resin is laid layer by layer and cured with ultra violet (UV) laser beam, process is shown in the figure 3.13.

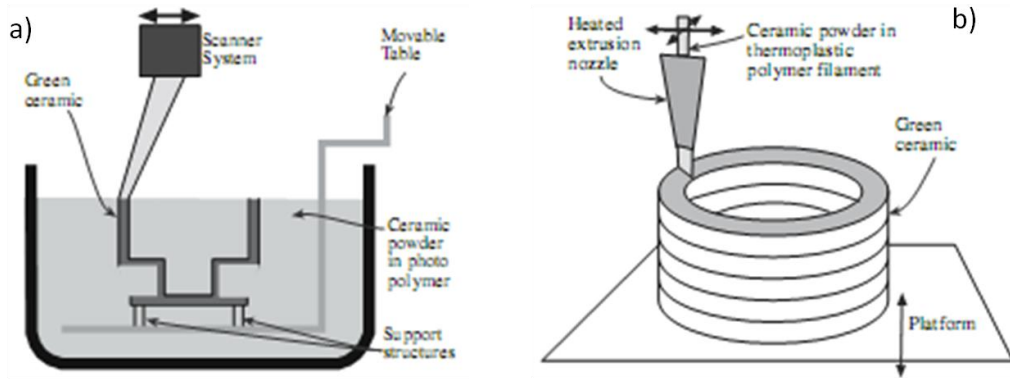


Figure 4-13 Schematic of Processes, Stereolithography (SLA) and b), Fused Deposition Modeling(FDM)[75].

In FDM thermoplastic polymer mixed with ceramic powder is heated and extruded to form a green ceramic mold as shown in figure 3.13b. In this technique too product is formed in layer by-layer manner. Product development, x - y position of the filament and the deposition rate are controlled by a computer. After completion of the deposition binder is removed and the part is sintered. The premix in the extrusion chamber can be loaded with up to 60 vol% ceramic powders. Mostly it is applied for making components out of Al_2O_3 , SiO_2 , and PZT.

4.13 Pressing

Pressing is a compression of a powder or granules using a die rigid (uniaxial pressing) a flexible mold (isostatic pressing). Pressing gives high productivity thus it is the most widely used method for shaping of ceramic pieces like; tiles, plates, cutting tools, as well as various magnetic and dielectric pieces.

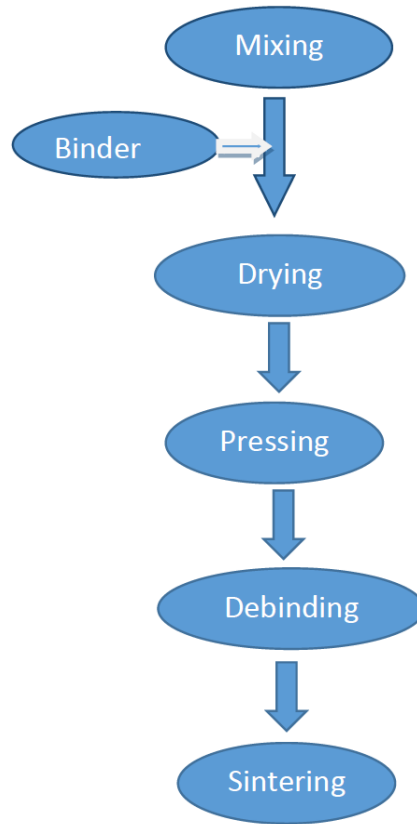


Figure 4-14 Flow diagram of powder pressing process

Conventional pressing can be performed on the spray dried, mechanically mixed and oven dried powders as illustrated in the flow chart, figure 3.14. It consists of three basic steps, filling of die, pressing and ejection of the compact, as shown schematically in the figure 3.15.

Pressing is classified as uniaxial, isostatic and semi-isostatic pressing

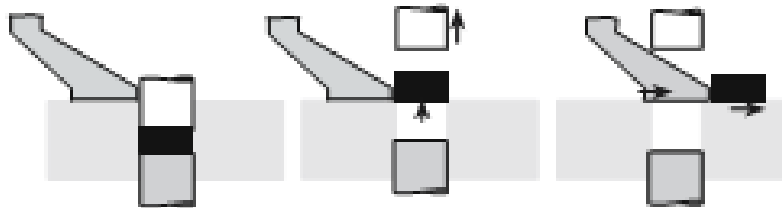


Figure 4-15 Pressing Stages, uniaxial pressing[63].

4.13.1 Uniaxial Pressing

This type of pressing can be performed with one piston (single effect) or two pistons double effect, material is pressed usually in the metallic mold (die) and this process is suitable for components in thickness greater than .5mm.

For pressing good flow able powder is achieved by the: extrusion-extrusion granules, agitation or evaporation granules and spray drying. These granules must be strong enough to maintain the shape and soft to fill the die completely by flowing under pressure. These granules must be in the size range, 50-500 μ m.

Materials undergo pressing in the order; as, rearrangement of particles (spheres), breakage of the particles to fill the spaces between the particles and finally micro porosity is filled.

4.13.1.1 Flaws in Uniaxial Pressing

Pressure distribution is not uniform during pressing pressure at the points mentioned in the diagram is higher, shown in the figure 3.16.

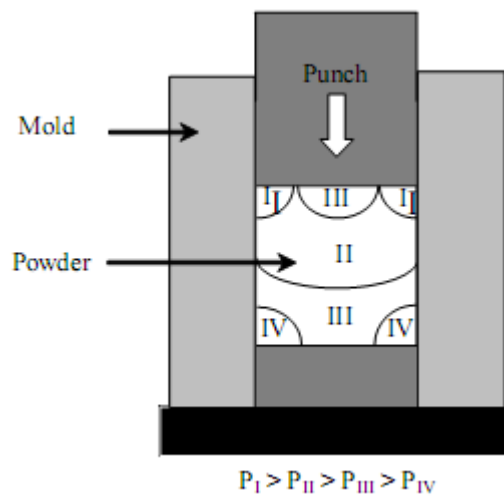


Figure 4-16 Pressure distribution in the powder during uniaxial pressing[63]

4.13.1.1.1 Spring Back

Spring back is the expansion in the pressed part which is caused by the elastic energy stored in the green part during compression. As the part is ejected the phenomenon of spring back happens. The addition of plasticizers can minimize this defect[63]

4.14 Iso-static Pressing

This process consists of pressing a mass in a rubber bag from all-around, force is distributed evenly throughout the cross section. A plastic mold (silicone, polyurethane), with the shape of the part to be produced, is filled with the granules. The pressure in the range of 150-200 MPa is applied on the rubber envelope via a fluid, generally oil.

Process can be called a Semi-isostatic process when a rubber mold in combination with metallic mold

This process is used for the production of pieces that are difficult to shape by conventional pressing, and also require high and uniform green density; tubular-elongated pieces; objects with complex shapes; and cast metal refractory tubes[63].

The granules are similar to those prepared for uniaxial pressing, but are generally more ductile.

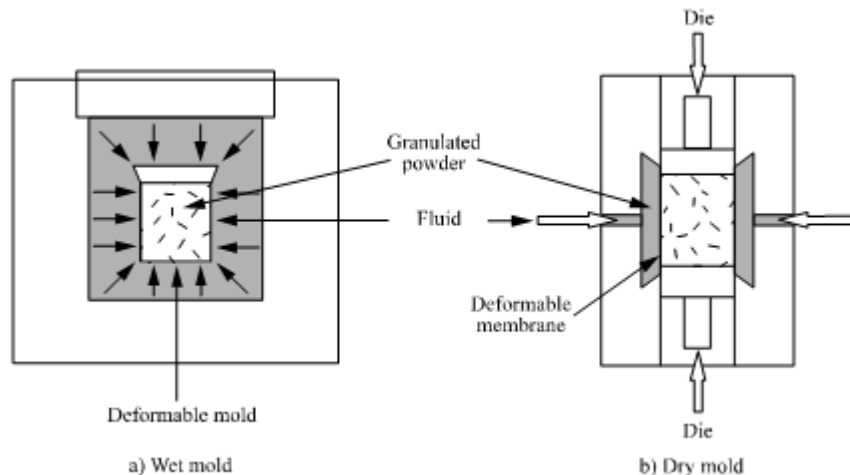


Figure 4-17 Principle of iso-static pressing a) wet mold and b) dry mold[63]

4.15 Spark Plasma Sintering (SPS)

Spark plasma sintering (SPS) is an electric current activated sintering (ECAS) processes [76, 77].

It is applied to consolidate powders of very different natures. SPS applies pressure assisted direct current sintering technique; schematic of the process is shown in the figure 3.18. SPS uses much faster heating rates and shorter sintering times as compared to pressureless sintering (PS), hot pressing and hot isostatic pressing (HIP). Additionally, SPS applies lower sintering temperatures as compared to the other techniques. This technique is very useful to enhance the sinterability and enhance chances of developing new advance materials and tailoring their properties. Most of the SPS use is related to developing new or complex materials as well gaining SPS process insight.

SPS offers the advantage of controlling dissociation of the starting materials, like nitrides and making the phases (materials) which were never achievable by other techniques

Densification of the Si_3N_4 ceramics was first studied by Nishimura et al [78]. The materials which are mixed are commonly $\alpha\text{-Si}_3\text{N}_4$ plus rare earth oxides additives, and are sintered at high temperature 1700-1800°C. Rare earth additives promote the sintering by developing liquid phase (LP). This liquid phase sinters (LPS) results particle rearrangements, solution precipitation and Ostwald ripening grain growth. In the conventional sintering techniques α to β phase transformation and grain growth occurs jointly. Application of SPS technique enhance the sinterability without grain growth and cutting short the use of additives. –

There are several hypothesis about the exact principle of SPS although it is still doubted. About the sintering of Si_3N_4 ceramics, first hypothesis was the generation of plasma between particles applying current, causing surface cleaning and improving the mass transport of the particles surface. Contrary to this the hypothesis of the rapid joule heating and the intrinsic electric field effects is considered more plausible. Whereas, Nygren's group proposed ripening mechanism to explain very fast formations of tough interlocking microstructures by SPS [79]. Due to electric field and rapid heating the motion of charged species was enhanced effecting diffusion and homogenization in liquid phase.

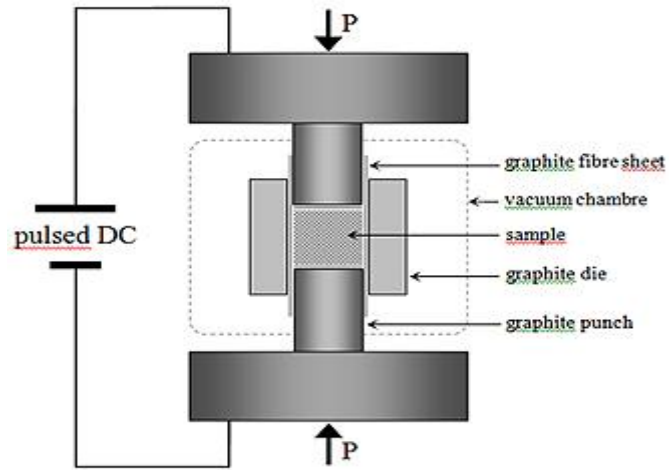


Figure 4-18 Schematic of spark plasma sintering[80]

SPS is a rapid consolidation technique which gives maximum densification in just few minutes.

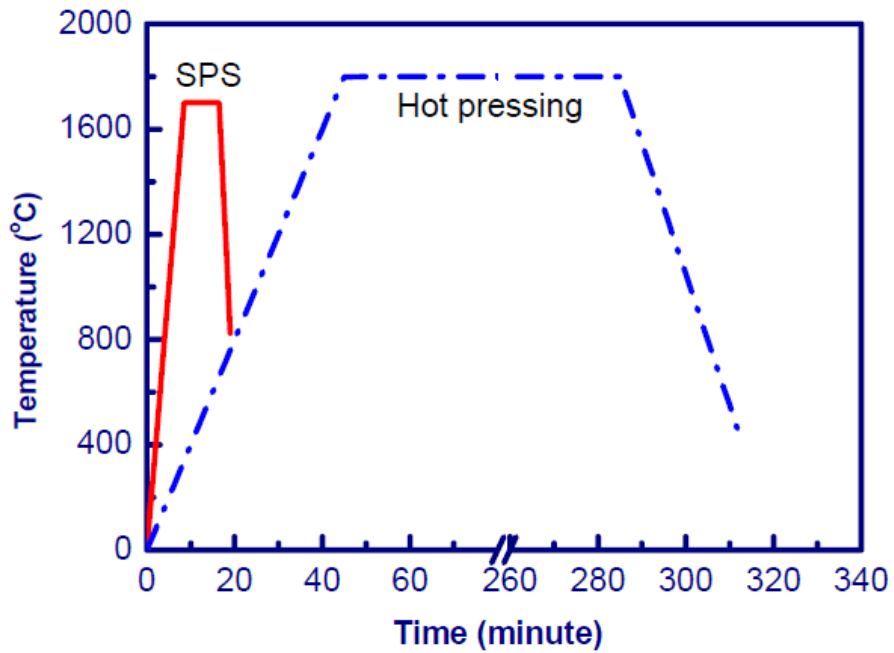


Figure 4-19 Sintering time difference in SPS and hot pressing [81]

5 Experimental

5.1 Colloidal Processing By Controlled Rheology (Compatibility of Colloidal Processing)

It was proposed that if we could have best mixing and the conditions suitable to give maximum green density we might synthesize these materials (Sialons) into serviceable components.

Achievement of good green density by improving Rheology (solid contents in slip) as mentioned in the literature[82] and sintering with fine sized powder processing were the factors considered in this route.

In this set of experiments additive(rheology modifier), a polymer was studied for the slip casting system to check the green density with reference to powder pressing(green density) and tape casting(green density). Methods giving similar green density have the tendency to yield similar products during consolidation.

This processing technique was applied to α -Sialon, β -Sialon, $\text{Si}_3\text{N}_4/\text{SiC}$ system.

These materials were processed in colloidal state; in the form of tapes, pressed pellets and cast using centrifugal casting. Their green densities were noted and samples were sintered using pressureless sintering technique in the N_2 atmosphere to check the nature (extent of dissociation) of the materials which were being processed by tape casting.

5.1.1 Tape Casting

Tape casting consist of slip making, degassing the slip, casting using doctor blade, detaching the tapes from mylar and laminating together to make a sample as shown in figure 4.1. Prepared specimens undergo debinding and sintering.

Ceramic powder materials was mixed in a ball mill. It was alumina jar containing alumina balls inside whereas a solution of Ethanol and butanol was used as solvent and carrier to lay these materials on the mylar in the form of tape.

Additionally slip was heavily modified with binders to impart the flexible rubber type characteristics to the tape. After making the slip slurry was degassed to release the gasses imparted by the additives and

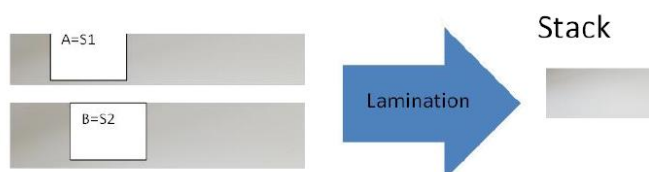
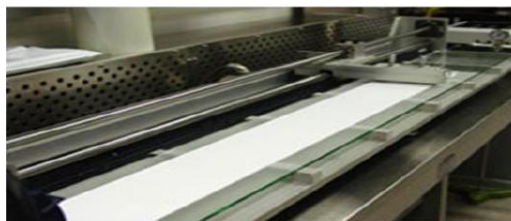


Figure 5-1 Tape casting and Lamination to form Stack (sample).

Binders and then it was cast with doctor blade on a polythene mylar (carrier) Cast tape was peeled of and stacked together to form a stack as shown in the figure 4.1.

5.1.2 Centrifugal/slip Casting

Centrifugal casting gives the direct shape and we can avoid a huge amount of binder (a source of carbon in the final object) and green density close that of pressing could be achieved for chosen materials green density has the impact on sintering.

Slip was made just with .3% of hypermer and cast in porous ceramic mold using centrifugal casting machine at 2300rpm. High evaporation rate of organics causes drying cracks, either the mold should be covered with some material to avoid the drying or other slow drying techniques can prevent cracking

5.1.3 Pressing (Quasi colloidal processing)

Well mixed system was slow dried using hot plate facilitated with magnetic stirring as shown in the figure 4.4 and pressed pellets containing the binder was slow dried to burn off the binder the

5.1.4 Debinding

Debinding was carried out in the controlled atmosphere at a very slow heating rate to get rid of the binders as shown in the figure 4.2. Debinded samples could give the density values satisfactory as compared to the mentioned in the literature [82].

5.1.4.1 Sintering

Of the samples was carried out under the N₂ gas atmosphere following a schedule as shown in the figure 4.2

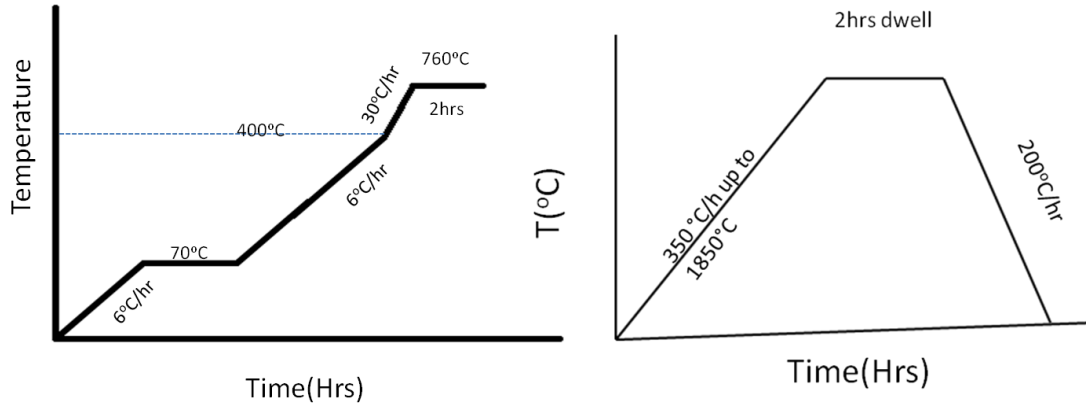


Figure 5-2 Debinding curve (left) and sintering curve (right).

, average density of the samples in green state by three techniques is given in the table 4.1

Table 5-1: Relative Density of differently processed green samples

Process	Binder %	Relative Green Density (%)
Tape Casting	15~17	47
Centrifugal/slip Casting	.3	54~56
Pressing	.03	59

With the little difference in green density between the pressed and slip cast samples in the green condition it is assumed that both can be used for the successive densification of the colloiddally processed and shaped/formed materials. Further improvement in the debinded/green densities can be achieved by applying the pressure forming methods like, injection molding, extrusion and pressure casting using porous mold

5.2 Production of $\alpha\beta$ -Sialon (Quasi- Colloidal Processing)

$\alpha\beta$ -Sialon a hard and tough composite material which is having limited use because of difficulties in the production. It is mostly produced by hot pressing (HP) or spark plasma sintering (SPS). In this research the same was tried to be produced by colloidal processing (pressing) and consolidating (sintering) in the conventional way which is applicable to all the ceramics shaped/formed by colloidal processing.

In this experimentation aluminosilicates (kaolinite and muscovite) were added to the two compositions from sialon region (Janeck Prism) as shown in the figure 4.3. Aluminosilicate can form β -Sialon [19, 20] and also has the tendency to react with sialon precursor materials which can help colloidal processing leading to the sintering. Aluminosilicates ability to react with Y_2O_3 to promote liquid phase sintering by liquid formation(eutectic melting at 1350°C), explained in the α -Sialon synthesis (section number,2.3.2.1) and its role to react with nitrogen and form β -Sialon (explained in the section 2.3.1.3, Synthesis of β -Sialon) is considered important in this scheme.

Point compositions were chosen on in the diagram, by adding the kaolinite, muscovite and alumina compositions are shifted in the direction of higher alumina (Al_2O_3) and SiO_2 on the diagram kaolinite contains more Al_2O_3 and, starting compositions are shown in the table 4.2

Table 5-2 Starting Sialon Compositions, whereas $Me_xSi_{12-(m+n)}Al_{m+n}O_nN_{16-n}$ and $Si_{6-z}Al_zO_zN_{8-z}$ are the general formulae of α and β sialon, respectively.

Molar Formulae		<u>Y2O3(Wt%)</u>	<u>Si3N4(Wt%)</u>	<u>Al2O3(Wt%)</u>	<u>AlN(Wt%)</u>
$Me_{0.67}Si_{8.5}Al_{3.5}O_{1.5}N_{14.5}$ (S215)	m=2,n=1.5	12.16	64.22	2.75	20.97
$Me_{0.4}Si_{9.6}Al_{2.4}O_{1.2}N_{14.8}$ (S1212)	m=1.2,n=1.2	7.58	75.33	3.42	13.76
Pless (z=2 for pless)	Pressureless	3.50	63.88	23.31	9.31

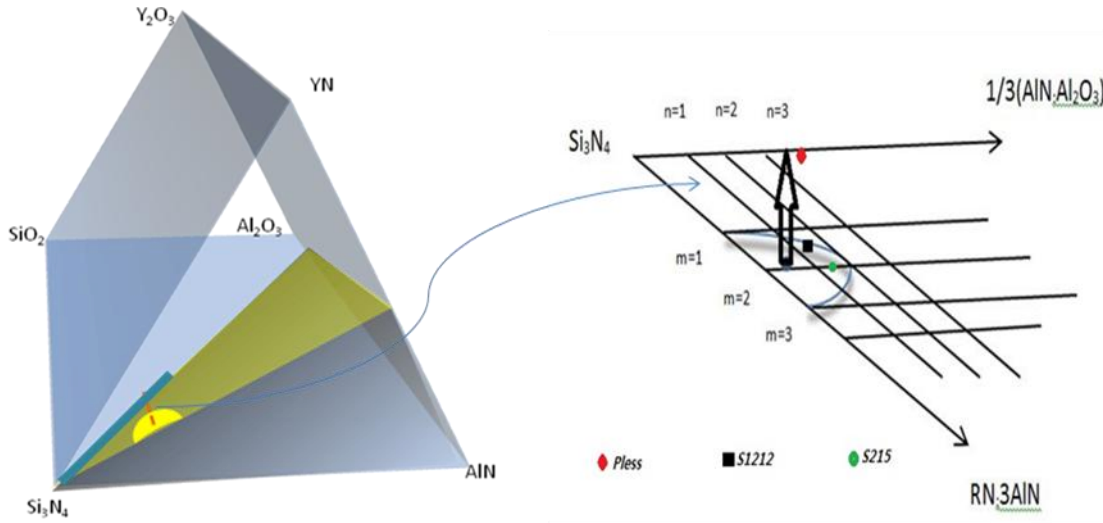


Figure 5-3 A typical sialon composition diagram along with magnified triangle of compositions (Janeck Prism).

On the Janeck-Prism both compositions run closely as shown in the figure 4.3 (Janeck Prism).

5.2.1 Sialon Composition with Aluminosilicates

Starting compositions were chosen with:

$m=2$ and $n=1.5$, this is called as **S215**

$m=1.2$, $n=1.2$, named as **S1212**

Pressureless sinterable material, **Pless**, and these material systems are shown on the diagram (Janeck Prism –magnified area) as green, black and red dots respectively, as shown in the figure 4.3.

5.2.2 Colloidal Processing

Raw materials were mixed in the mixture of ethanol and butanol for 72 hours in plastic bottles containing alumina balls inside.

Processing

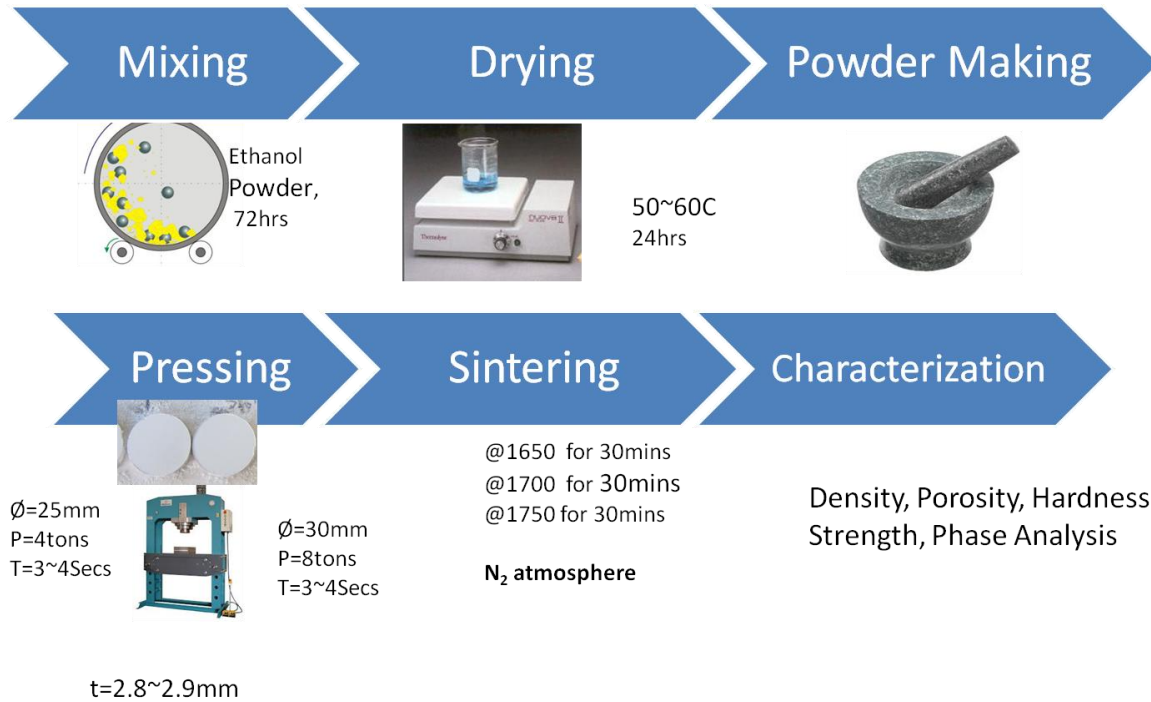


Figure 5-4 Colloidal processing stages of $\alpha\beta$ -Sialon materials

After mixing the slurry was dried on a hot plate for 24 hours at the temperature of 50-60 °C. Dried material was ground again in an agate mortar and pestle and pressed in the form of 25 mm pellets, applying a pressure of 4 tons for 3-4 seconds.

Debinding was applied to the samples which contained binder. Finally pellets were sintered in a furnace under 600-800 mbar of N_2 ; samples were heated at 5 °C/min to 1650°C and 1700°C, and cooled inside the furnace to room temperature. Whereas, the samples to be sintered at 1750°C were mixed with 3% of binder (PVA, PVB and PEG). These samples were pressed to 30mm pellets by cold pressing technique. These pellets were made by applying 8ton of pressure and then debinded in N_2 gas atmosphere at 760°, debinding and sintering cycles are shown in the figure 4.2.

Sintering was started from low temperature (1650°C) and then it is was performed at high temperature (1750°C). Initially, temperature was low to avoid the risk of softening/melting, as

the presence of silicates (kaolinite and muscovite can reduce the softening point. Finally, sintering at higher temperatures was devised to achieve densification (theoretical density).

5.3 Characterization

Sintered samples were characterized for bulk density, image porosity, Vicker's hardness, fracture toughness, and bend test was only performed for the samples sintered at 1750°C. XRD analysis was performed for the phase analysis. Bulk density and hardness testing was carried out to evaluate the densification. Bulk density of sintered samples was measured by Archimedes' principle using ethanol as a medium, and values are given in table 5.1 along with Vicker's hardness

5.3.1 X-ray diffraction

Phase analysis was performed on the powder material by X-ray diffraction. Powder was made using the tungsten carbide ball and pan for grinding the hard materials and materials were ground for 1-2 hrs.

Crystalline structure of a material can be studied by XRD[83]. The X-rays are scattered by the atoms inside the material and this brings information about the distribution of these atoms in the material, peaks are the fingerprints(cards) of the material and are matched with the reference data using software.

5.3.2 Bulk Density Measurement

Bulk density was measured in the ethanol medium and samples were soaked for the 12Hrs to remove all the entrapped air. Weight of the sample in the air (W_{air}), ethanol (W_{fl}) and in saturated condition was determined

d_{fl} = density of the liquid

W_{air} = weight of body in the air

W_{fl} = weight of body in liquid

W_s = saturated weight

$$d_{bulk} = \frac{W_{air} d_{fl}}{W_s - W_f}$$

5.3.3 Relative Density

Relative density was calculated by dividing the bulk density to the theoretical density, whereas the theoretical density was calculated by combining the oxide densities of the starting materials

$$Relative\ Density(RD) = \frac{Bulk\ Density(BD)}{Theoretical\ Density(TD)}$$

5.3.4 Vicker's Hardness

Vicker's hardness was measured by using the equation given below, in this test (ASTM E92-72) was used.

The test consists of penetrating a surface under investigation by an indenter, in this case a diamond pyramid with square-base that forms an angle of 136° with the opposite sides as shown in the figure 4.5.

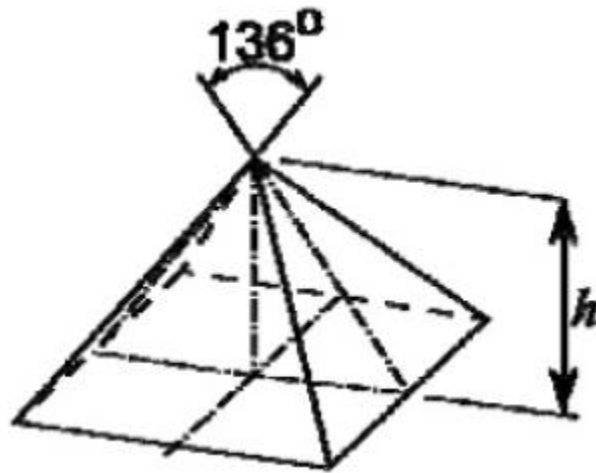


Figure 5-5 Diamond indenter with included angle 136°.

The force applied is known and the diagonals are recorded and values are put in the formula given below to calculate the hardness.

$$H = \frac{1.864P}{L^2}$$

5.3.5 Fracture Toughness

Toughness was measured using the Antis relationship for indentation test. Crack length c (from the center to tip of crack, shown in the figure 4.6) is recorded along with the load (P) and hardness number (H) and E (young's modulus) in the equation below to calculate the fracture toughness. This method is not precise (absolute) but for the sake of comparison between the results it can be used.

$$K_{Ic} = 0.016 \left(\frac{E}{H} \right)^{\frac{1}{2}} (P/c^{3/2})$$

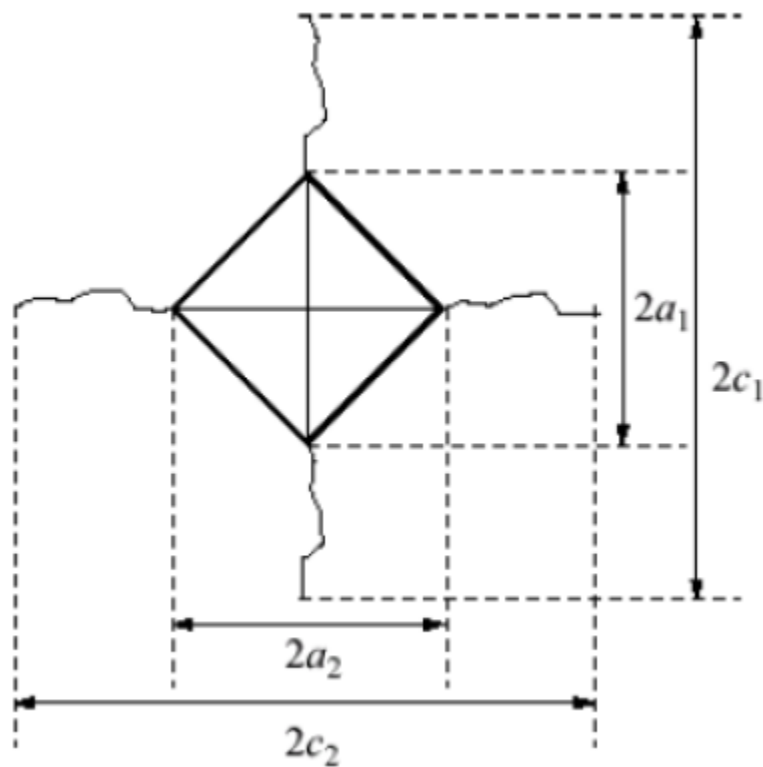


Figure 5-6 Illustration of Vicker's impression with typical brittle fracture

5.3.6 Bending Strength (Flexural Strength)

Bending strength was determined by using three point bending machine and using rectangle shaped samples,

$$\sigma_f = \frac{3PL}{4bd^2}$$

σ_f = Flexural strength, P = Load, L = span length, b = width of sample, and

d = thickness of specimen

6 Results

Starting compositions, S215, S1212 and Pless sintered at three temperatures, 1650°C, 1700 °C and 1750 °C and their physical properties are given in the table5.1.

Table 6-1 Compositions chosen for colloidal processing and physical properties after sintering

Sample		Sintered at 1650°C					Sintered at 1700 °C					Sintered at 1750 °C					
		Sample, 5% increment	BD(g/cc)	Porosity	Hv(GPa)	Toughnes(MPa)	phase	BD(g/cc)	Porosity	Hv(GPa)	Toughnes(MPa)	phase	BD(g/cc)	Porosity	Hv(GPa)	Toughnes(MPa)	phase
S215(13)	Kaolinite	13	68	30	11			52	22	17			68	37	9		
		27(5%)	96	9	13	3.18		76	12	18			89	7	18	3.7	
		22(10%)	94	8	14	3.19		96	7	20			99	2	18	3.9	
		21(15%)	97	6	20	2.8		98	6	20			100	5	18	3.5	
		20(20%)	95	3	20	2.93		97	5	19			99	2	17	3.0	
	muscovite	01(5%)	86	20	19	2.9		79	21	21	nil		85	11.0	nil	nil	
		04(10%)	91	17	21	3.9		91	13	17	nil		89	14.3	nil	nil	
		2(15%)	94	33	23	4.0		92	13	18	nil		92	12.4	nil	nil	
		3(20%)	97	21	21	5.2		87	21	20	nil		54	27.0	nil	nil	
	Kaolinite+Al	47(5%)	86	8.8	20	xxx		92	2.0	19.5	ok		93	2.6	21.2	2.6	
		43(10%)	98	3.0	18	2.6		97	2.8	18.2	ok		100	1.9	17.5	2.7	
		41(15%)	100	2.5	18	2.9		100	3.0	18.7	ok		100	3.4	19.7	2.6	
		45(20%)	100	2.8	18	3.3		93	3.0	17.5	ok		99	2.2	18.8	2.9	

ST212(11)	Kaolinite	17(5%)	80	8.3	18	3		87	8	18.3	3.1		67	4.8	17.5	3.8		
		23(10%)	98	8.0	18	3		94	10	18.7	3.5		95	6.0	17.9	3.3		
		19(15%)	93	9.0	17	4		98	4	16.6	3.9		93	4.0	17.9	3.7		
		18(20%)	93	1.4	18	3		93	3	15.2	3.3		99	7.0	16.6	4.7		
	muscovite	9(5%)	89	10	nil	nil		89	12	15.3	nil		75	27.0	nil	nil		
		5(10%)	91	11	nil	nil		88	09	16.5	nil		81	6.0	nil	nil		
		6(15%)	90	11	nil	nil		88	22	15.4	nil		90	7.0	nil	nil		
		14(20%)	89	18	nil	nil		87	12	13.3	nil		84		nil	nil		
	Kaolinite+Al	30(5%)	99	2.0	17.6	2.9		97	4	17.3	ok		96	3.6	17.9	3.6		
		46(10%)	98	2.0	18.0	3.3		100	3	14.9	ok		98	2.6	16.5	3.1		
		51(15%)	100	0.6	16.1	8.2		97	4	12.8	ok		100	2.6	16.9	3.3		
		49(20%)	97	2.0	15.2	3.9		85	1	15.5	ok		98	2.8	16.5	4.3		
	Kaolinite	26(5%)	89	3.5		3.7		89	9	15.5	3.3		91	4.0	16.2	3.4		
		25(10%)	93	6.0		3.2		87	7	15.4	2.9		91	6.0	15.8	3.1		
		24(15%)	95	4.0		3.2		92	3	15.7	3.2		92	2.0	16.2	2.9		
		16(20%)	90	11.0		3.4		96	2	15.2	3.3		91	4.0	13.9	3.5		
Pless(12)	Muscovite																	
		08(5%)	86	13				83					88	10				
		07(10%)	85	13				84					85	11				
		15(15%)	87	18				72					79	30				
		10(20%)	77	20				64					68	15				

6.1 Production of S215 (Composite Sialon) with Kaolinite

Visuals of The Samples All the samples were observed for the type of scale and defects occurred during the final stage (sintering) of the production, as shown in the figure 5.1. Visuals combined with the optical microscopy and density reveals the how successful this route has been to produce Sialon (S215). Visible of the sample combined with the optical microscope images at low magnification showed that all the samples with muscovite at 1750°C were very porous and fractured (small embedded images).

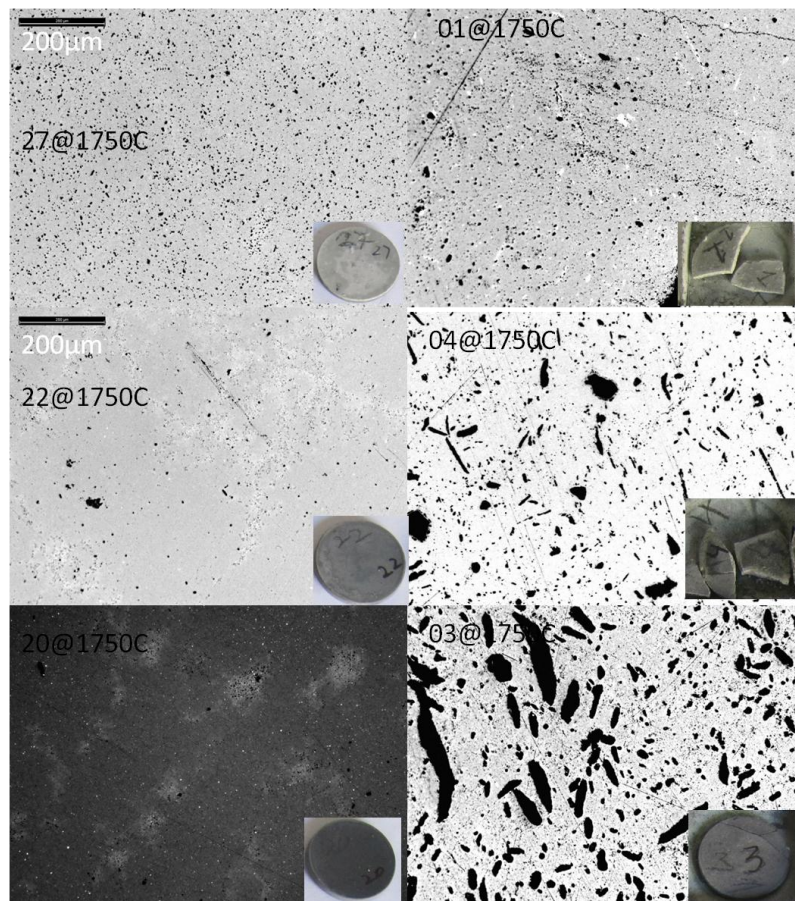


Figure 6-1 Kaolinite containing S215, samples embedded in microstructure of the same sample (left in the picture), whereas on the right muscovite containing samples are displays

Relative Density: At 1650°C, as shown in figure 5.2, kaolinite-modified samples showed a roughly linear increase in the density as the silicate addition passed from 5 to 20%. Samples with kaolinite contents greater than 10% reached maximum density at this temperature. Although, theoretical density based on oxides may not be the close enough to actual density for such intergranular and multiphase materials [25, 84] as it is indicated by the values of image porosity

that there is not much change in porosity hence increase in density is due to the higher contents of aluminosilicate and its tendency to form more liquid and prevent the dissociation of Si_3N_4 . Reference(starting) sample(S215) manifested low density and concurrent porosity which could be the result of no sintering and dissociation of Si_3N_4 as explained in the section (Dissociation of Si_3N_4 ,2.2) [30]. Whereas, samples containing 5% kaolinite, K-5, showed densification with increasing temperature, at temperature 1650°C was densified up to the 80% of the theoretical value.

Samples in this composition range could be sintered to 90% of theoretical density at 1750°C .

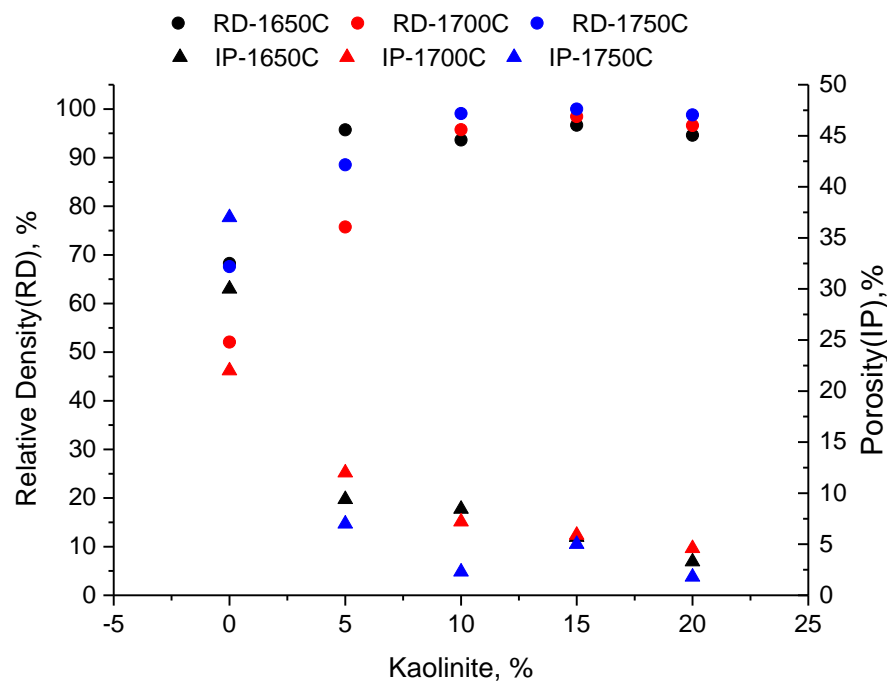


Figure 6-2 Porosity (IP) and Relative density (RD) of S215, samples containing kaolinite and sintered at 1600°C , 1700°C and 1750°C are shown.

Increasing the temperature density kept on increasing, higher kaolinite provided more flux and samples could be sintered as early as at 1650°C , as shown for the 15% flux(kaolinite).

Samples with high flux might have developed a liquid phase (black point), which might have been considered as a pore this could be the reason for high porosity

Densification of the compositions with kaolinite above 10% at low temperature might be due to the arrest of nitride dissociation in the presence of kaolinite and this kaolinite might have

transformed to β -sialon this situation of no escape of nitrogen and other components was corroborated by no or minimal scale presence on the samples containing higher aluminosilicate contents as shown in the figure 5.1.

Hardness is measured by Vicker's method as mentioned in the article (characterization).

Hardness values indicate that samples containing 5-10% or no kaolinite could not be sintered at 1650°C. Original sample was difficult to be sinter at all the temperatures tested so the hardness and toughness values could not be calculated. And samples with 5% kaolinite additions showed excellent hardness values at 1750°C.

Hardness values became stable as we moved from the heating temperature of 1650°C to 1750°C, this phenomenon is concluded from the decrease in the standard deviation values as shown in the figure 5.3. Kaolinite contents greater than 15% resulted in the loss of hardness it might be due to soft phase/glass development.

S215 with Kaolinite

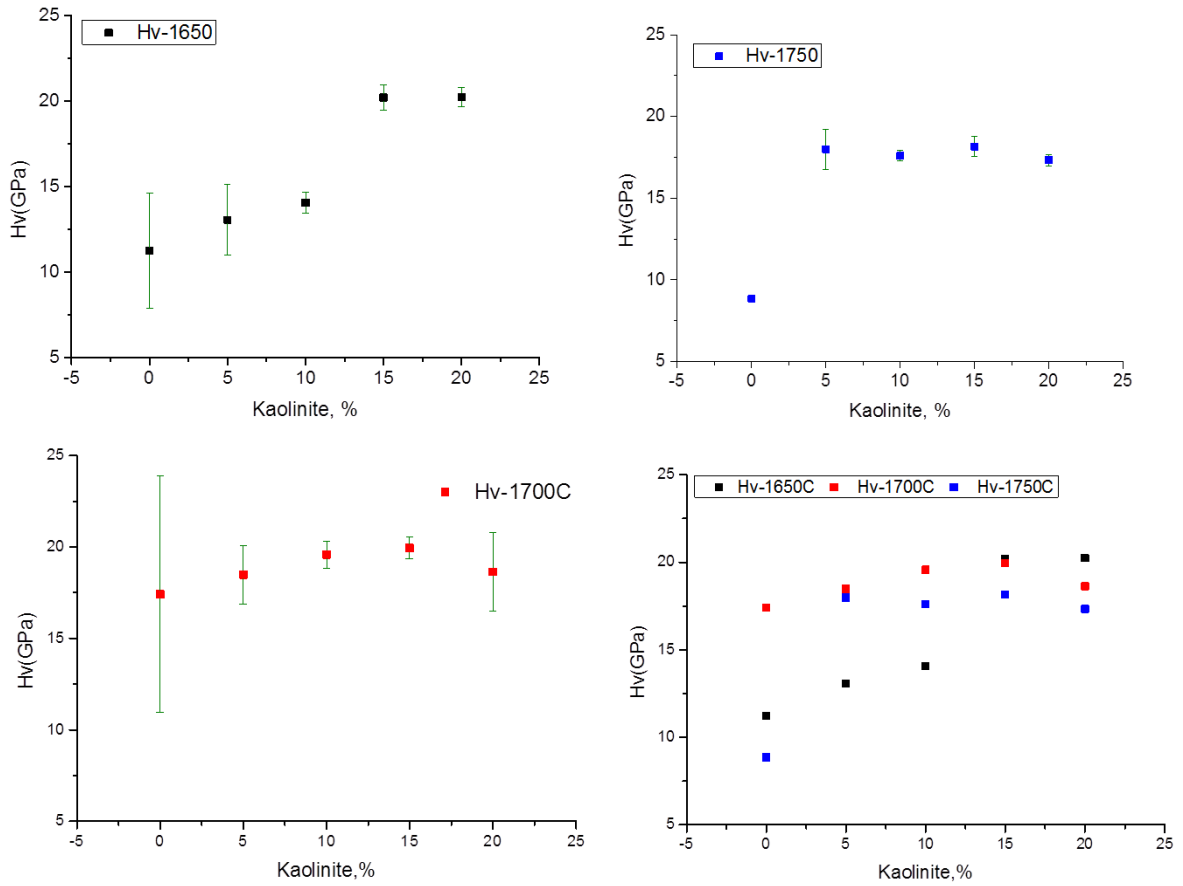


Figure 6-3 Hardness variation as a functions of temperature and additive quantity in S215

Variation in the hardness values was minimized for the samples containing kaolinite more than 5% as we increased the sintering temperature from 1650°C to 1750°C.

Fracture Toughness Anstis relation as mentioned in the characterization chapter was used to measure the toughness[85].

Samples at 1650°C showed least hardness for all the compositions, in contrast to the hardness values of the other samples. Whereas the samples with higher kaolinite (>10%) showed decrease in the toughness and hardness at highest sintering temperature, 1750°C.

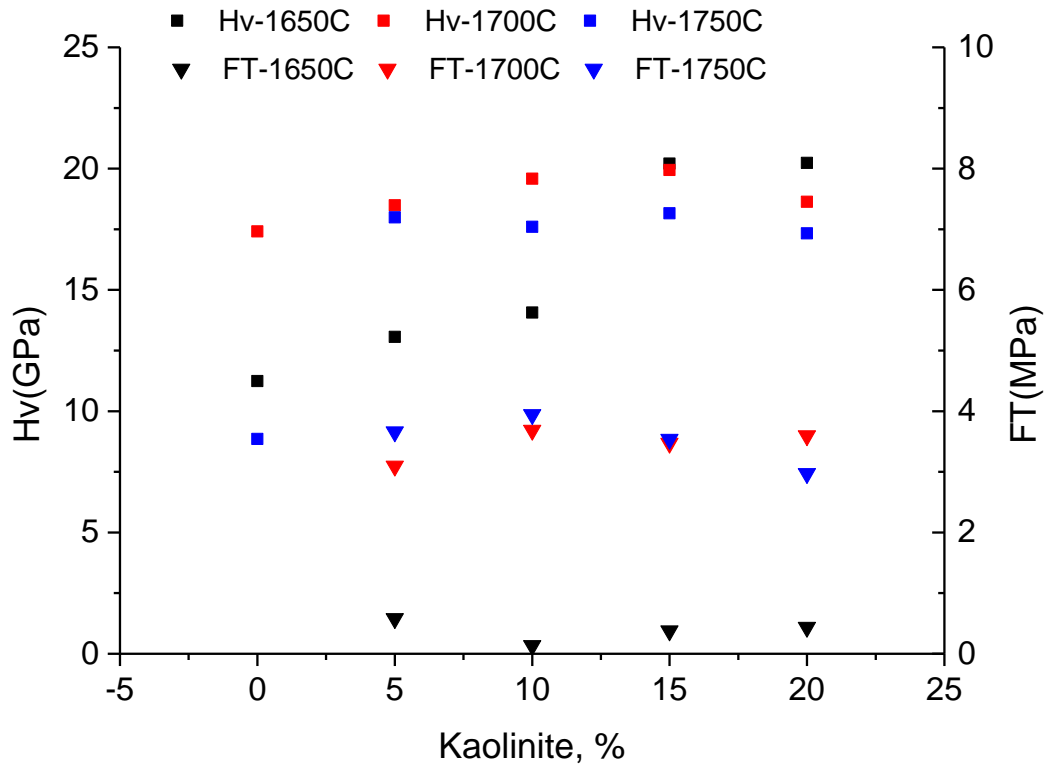


Figure 6-4 Hardness and fracture toughness of S215 with kaolinite

Hardness and toughness values were good up to 15% addition of the kaolinite and after that both the hardness and fracture toughness decreased.

XRD Analysis: XRD analysis was performed on the powder samples, for 5, 10 and 15% kaolinite samples sintered at 1750°C. Samples sintered at 1750°C could show α -Sialon, β -Sialon and YAG as shown in the figure 5.5. Compositions greater than 10% could not develop the α -Sialon.

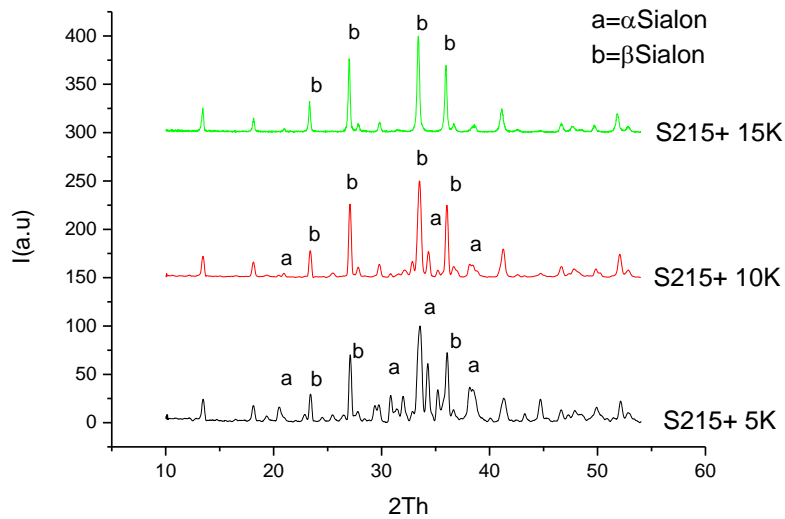


Figure 6-5 XRD analysis of S215 samples with 5, 10 and 15% Kaolinite sintered at 1750°C.

Excellent gain in the results: densification up to 90% with excellent hardness, suitable value of toughness and development of proposed phases was achieved but there were some discrepancies.

Higher porosity values contrary to the densification trend, as shown in the figure 5.2. Low hardness and low toughness despite having good density values and development of tough phase (β -Sialon). These contradictory values might have been resulted by segregated local melting resulting in the small precipitates (black dots in microscopic image) that could have caused low hardness and low toughness in this material system.

Looking at the anomalies it was realized that mixing should be done in efficient way the results with efficient mixing are mentioned in the section of ‘S215 with free alumina’

6.2 Production of S215 (Composite Sialon) modified with Muscovite

Samples modified with 5-20% muscovite sintered good at 1650°C and as the sintering temperature was increased to 1700°C samples containing up to only 10% muscovite showed densification up to 90% of the theoretical value. As the temperature was further increased density decreased for all the samples and samples were crumbled as shown in the figure 5.1.

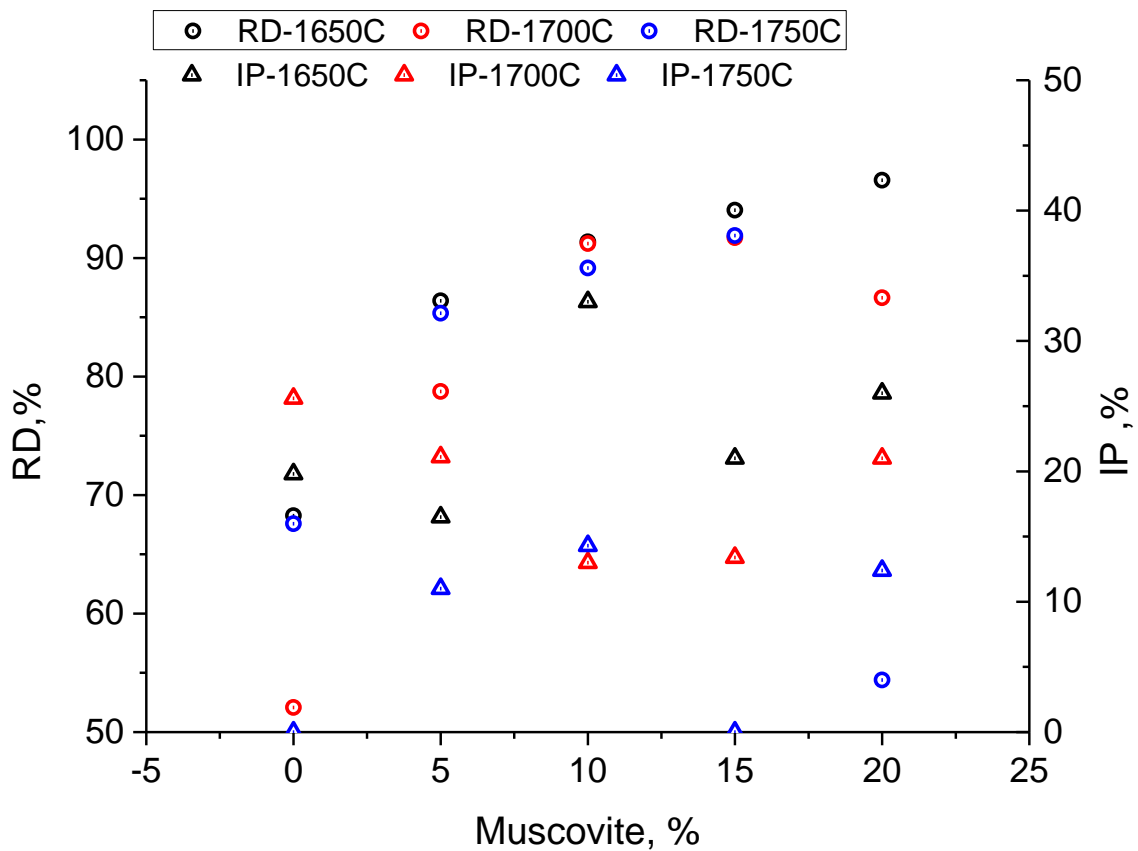


Figure 6-6 Densification and porosity in the S215 modified with muscovite

Samples modified with muscovite as aluminosilicate additive showed that the effect of increasing the densifications temperature seems to be a reduction of the overall density of the samples, in particular for the sample with the 20% muscovite, but also for the other samples.

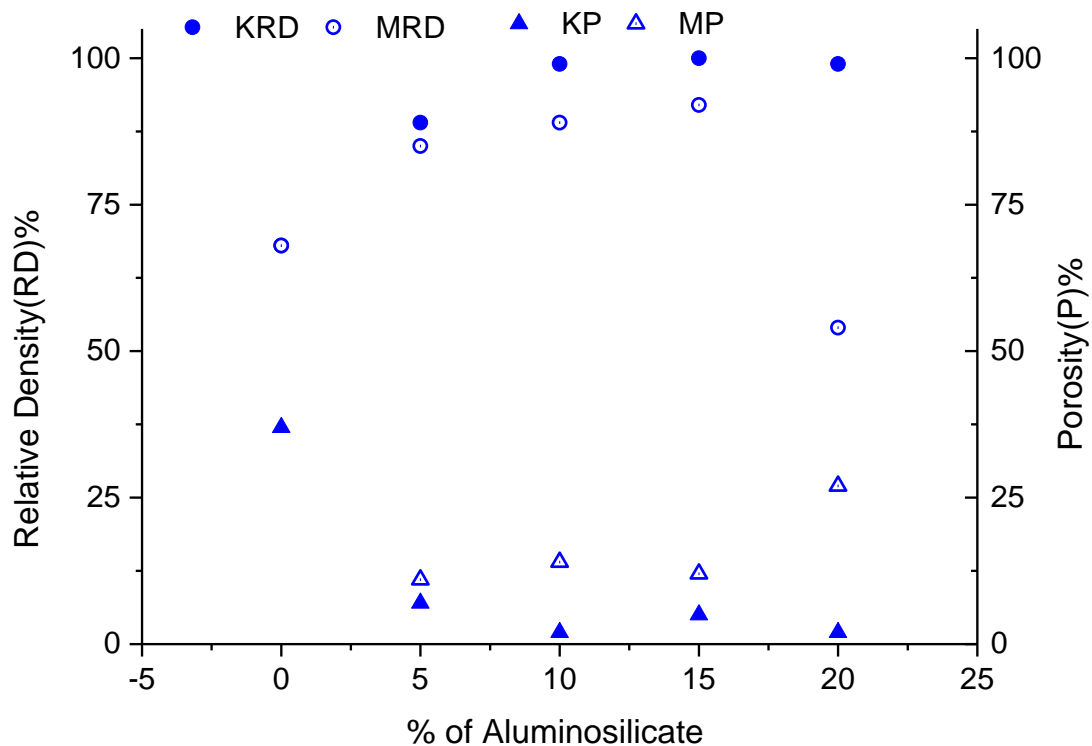


Figure 6-7 Relative density and porosity of S215 samples sintered at 1750°C with kaolinite and muscovite, where KRD= =Relative density with kaolinite, KP=porosity in the kaolinite containing samples and MRD=Relative density with muscovite and MP= porosity in the muscovite containing samples

At higher temperature, kaolinite addition is better than muscovite. This is also confirmed by the hardness values that are often well correlated with the density.

6.3 Production of S1212 (Composite Sialon) with Kaolinite.

Relative Density: S1212 showed densification trend similar to S215 with the exception to the S1212 with 20% kaolinite as compared to the one S215 with 20% kaolinite.

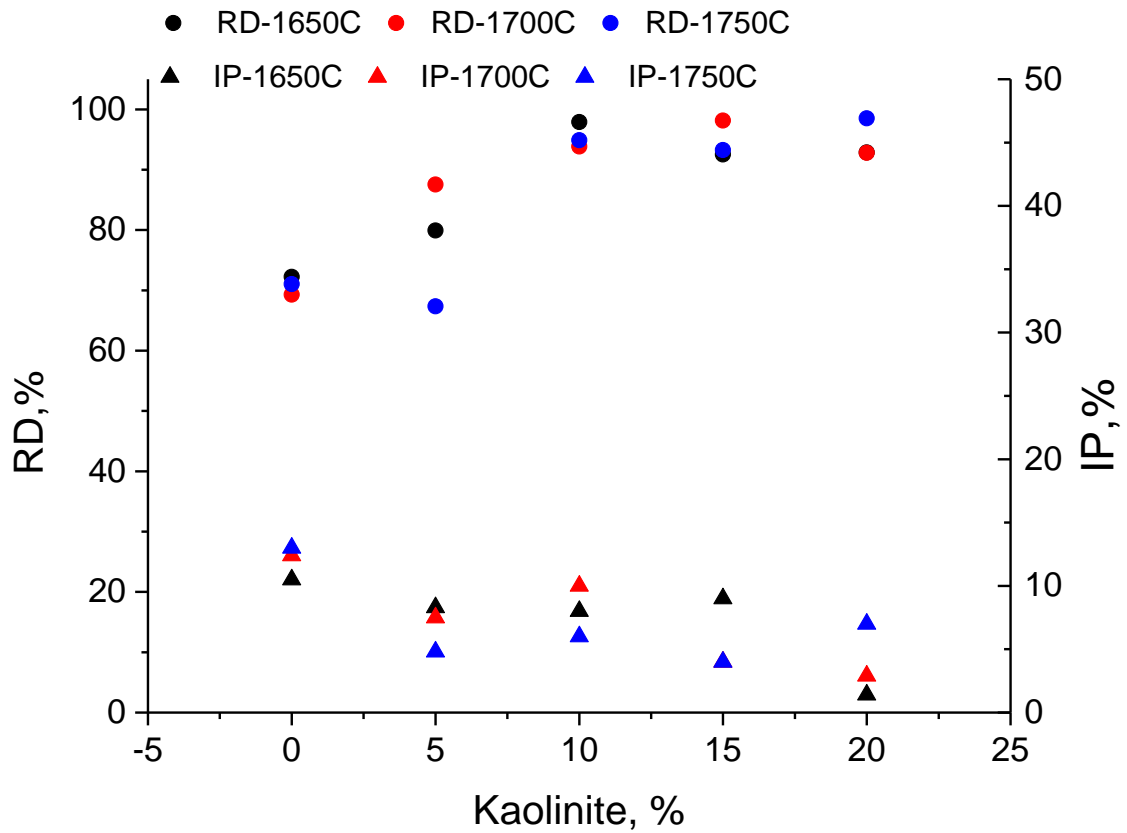


Figure 6-8 Relative density (RD) and Image porosity (IP) of S1212 sintered at 1650°C, 1700°C, 1750°C.

XRD Results for the S1212K indicated that S1212 could give composite Sialon, where α -Sialon was a trace phase, only up to 10% kaolinite modifications

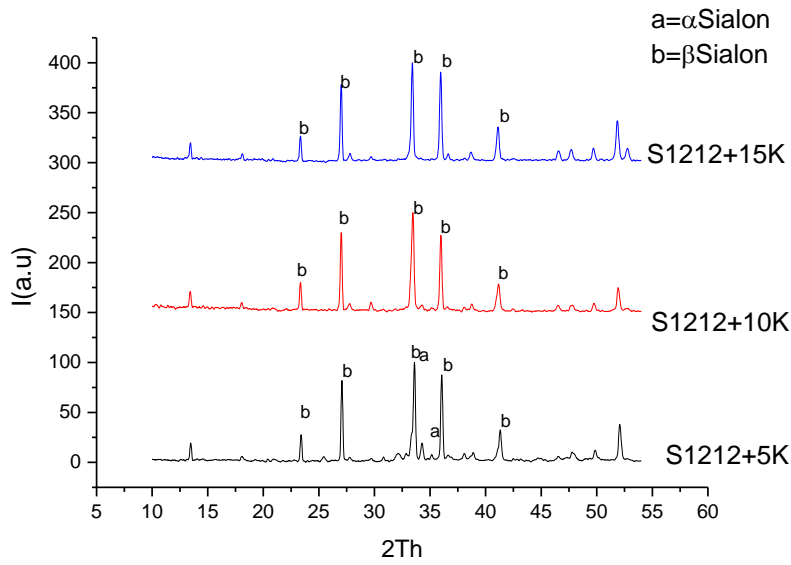


Figure 6-9 XRD patterns of S1212 modified with 5, 10 and 15% kaolinite and sintered at 1750°C.

Despite the lack of dual phase development S1212 compositions were considered reasonable for the further experiments as the hardness values of S1212 alloyed with kaolinite was better than the S215 contemporaries as shown in the table 5.1.

6.4 Production of S1212 (Composite Sialon) with Muscovite

Muscovite containing samples even in the S1212 system showed less densification and higher porosity as it was observed for the muscovite containing samples in S215, with the exception that samples did not crumble.

Samples with muscovite never reached 100% of the theoretical density and the overall density values were lower than the contemporary kaolinite containing samples as shown in the figure 5.10.

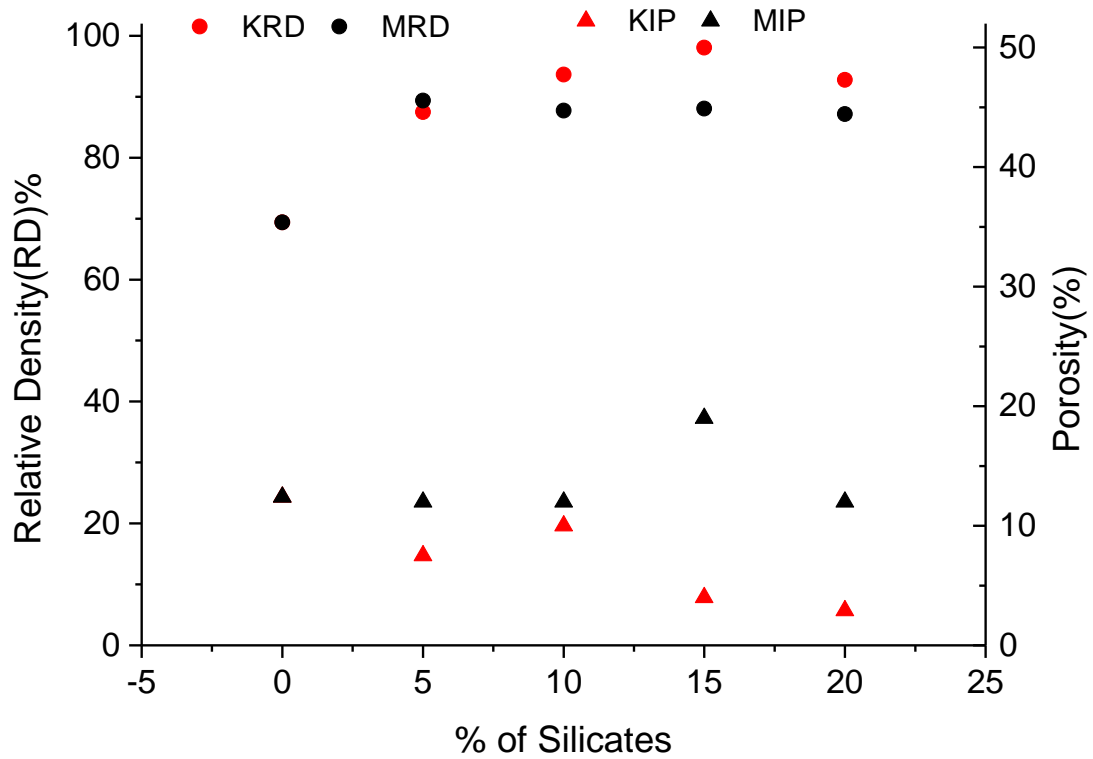


Figure 6-10 Relative density (KRD, MRD for kaolinite and muscovite samples, respectively) and porosity (KIP, MIP for kaolinite and muscovite samples, respectively) for S1212 samples modified with silicates (kaolinite and muscovite) at 1700°C.

Hardness values of S1212 with muscovite were lower and with high standard deviation supporting the presence of porosity, glass phase and other structural in homogeneities. Trend in the hardness increase and decrease was similar for both groups (with kaolinite and with muscovite, shown in the figures 5.11 and 5.12).

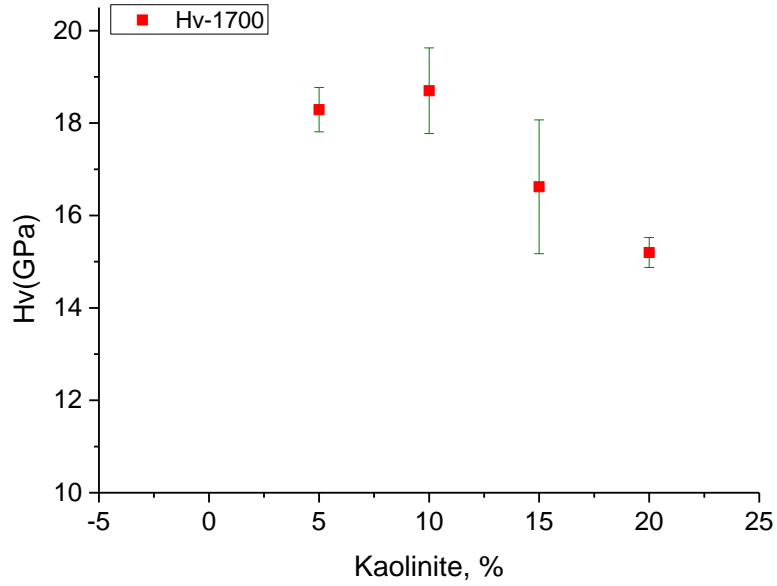


Figure 6-11 Hardness values of S1212 modified with kaolinite and sintered at 1700°C.

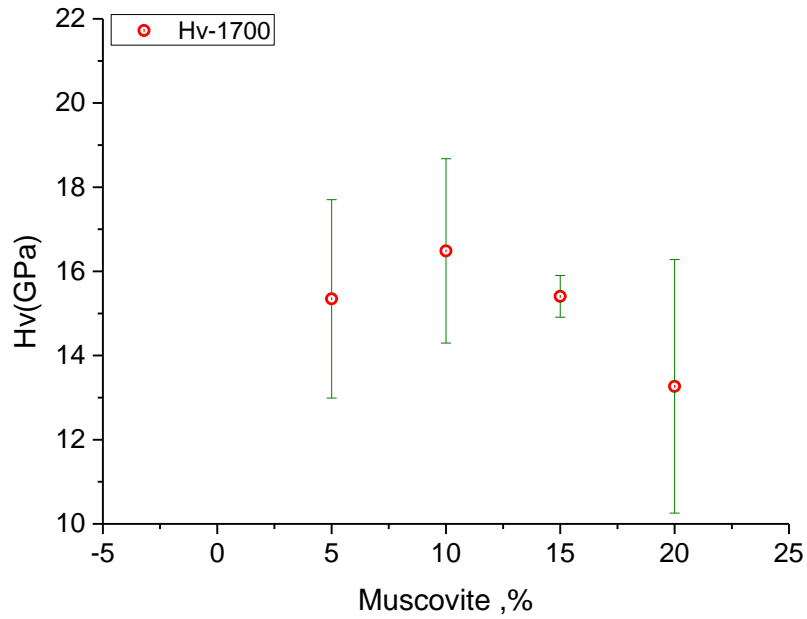


Figure 6-12 Hardness of S1212 samples modified with muscovite

Compositions with muscovite were not considered fit for the development of Sialon system may be the reason is K (potassium) ion as it can form more liquid because of its alkali nature and

additionally, it is not able to be dissolved and form α -Sialon solid solution like Y, Mg and other RE ions[20].

6.5 Production of Pless (Pressureless sinterable) Sialon

Composition outside the single phase zone as shown in figure 4.3 (in the materials section) and marked 3 was modified with aluminosilicates (kaolinite and muscovite). The aluminosilicates added were up to 20% of the original composition. Samples were prepared by giving the similar treatment as mentioned above. Sintered samples were characterized for the density, porosity, microstructure hardness and bending strength.

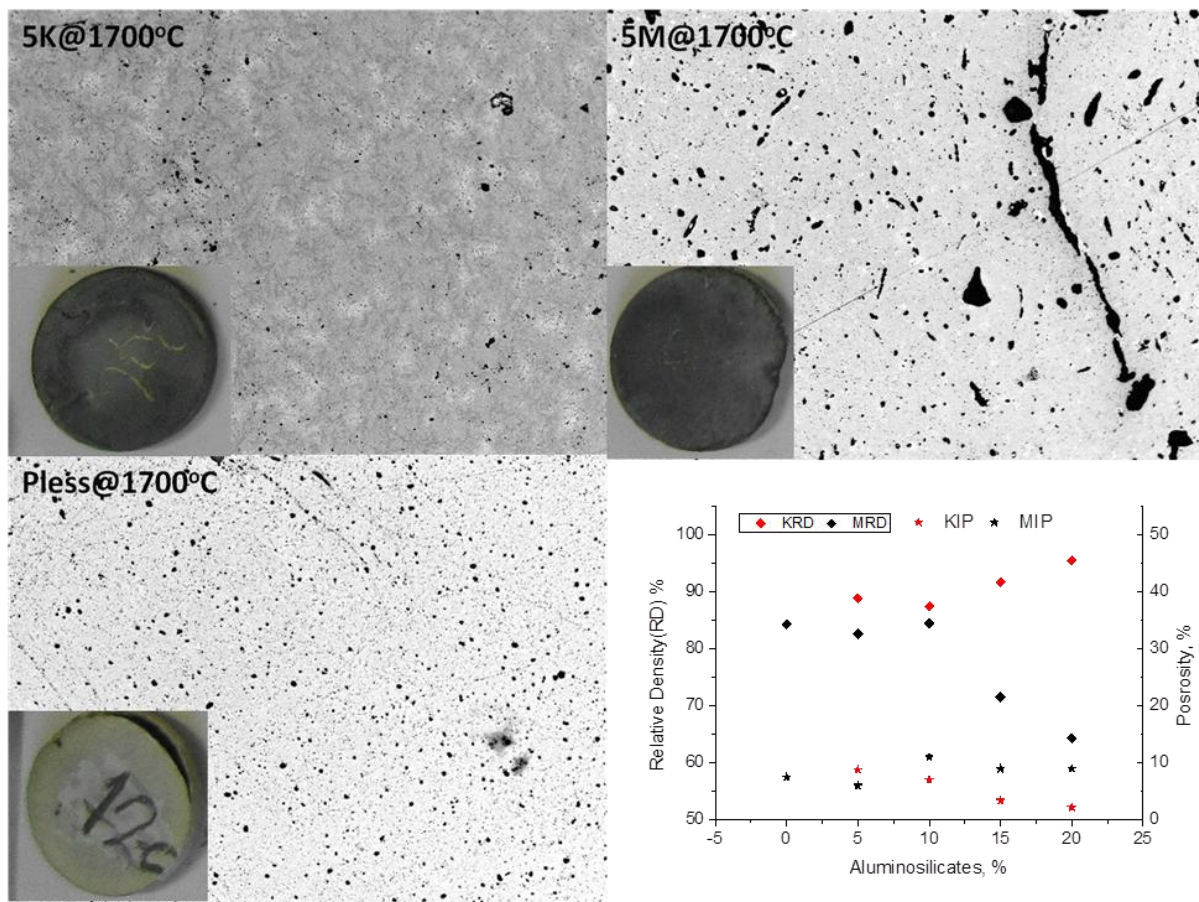


Figure 6-13 Low magnification images with embedded original samples of pless batch with 5% kaolinite and muscovite represented as 5K and 5M, respectively. Whereas, the graph in the corner indicates the density and porosity, KRD, MRD; KIP, MIP stand for relative densities and porosities of the samples containing kaolinite and muscovite, respectively.

Visible of samples (Pless) as shown in the figure 5.13 indicate that Pless composition without additive showed tearing of sample, it might be a pressing defect but might be exaggerated by the lack of liquid phase during the sintering

Samples with the muscovite was light, porous, torn from one side and associated low magnification microstructure give the indication of precipitate/pores(black points)

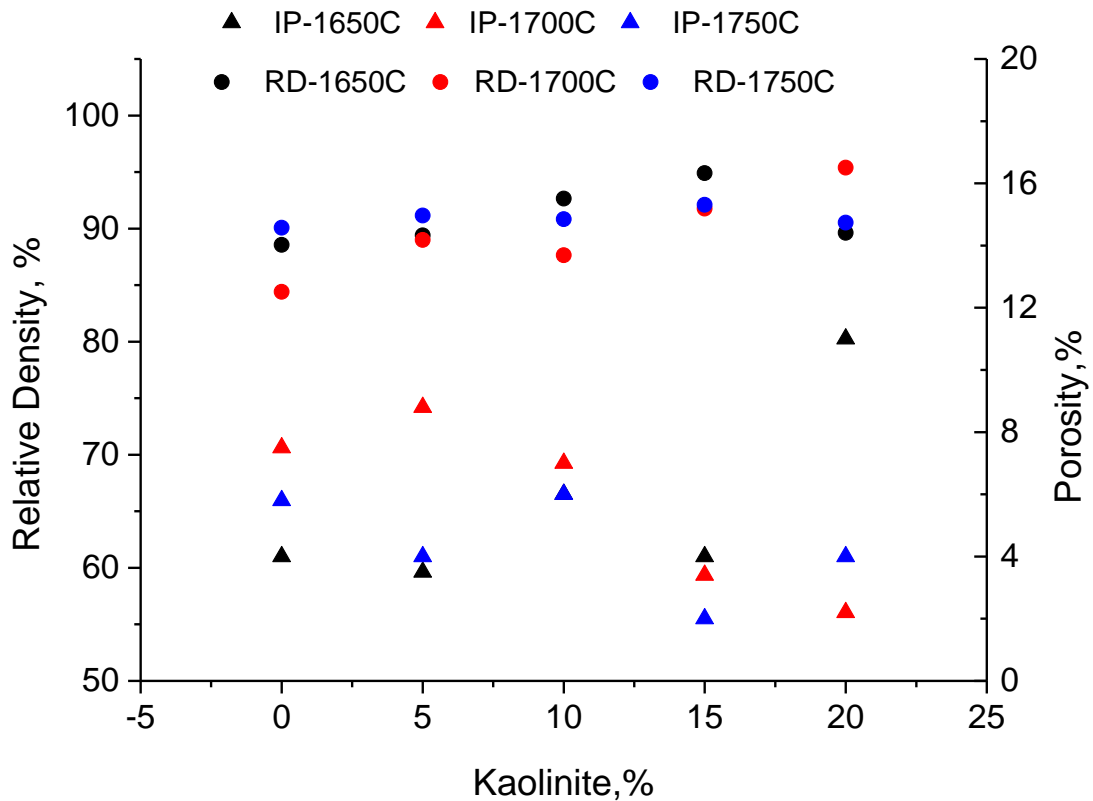


Figure 6-14 Relative density (RD) and porosity(IP) of the samples sintered at 1650°C (black),1700 °C(red) and 1750°C(blue)

Relative density increased as the temperature value and the quantity of the additive is increased except the sample containing 20% kaolinite which might have developed liquid and evaporated during the course of heating

Hardness values measured gave the indication that 1650°C is low to gain the mature product as standard deviation is high enough. Hardness is optimum at 1700°C, whereas the higher

temperature has developed softening probably because of glass development or coarse grained β -Sialon.

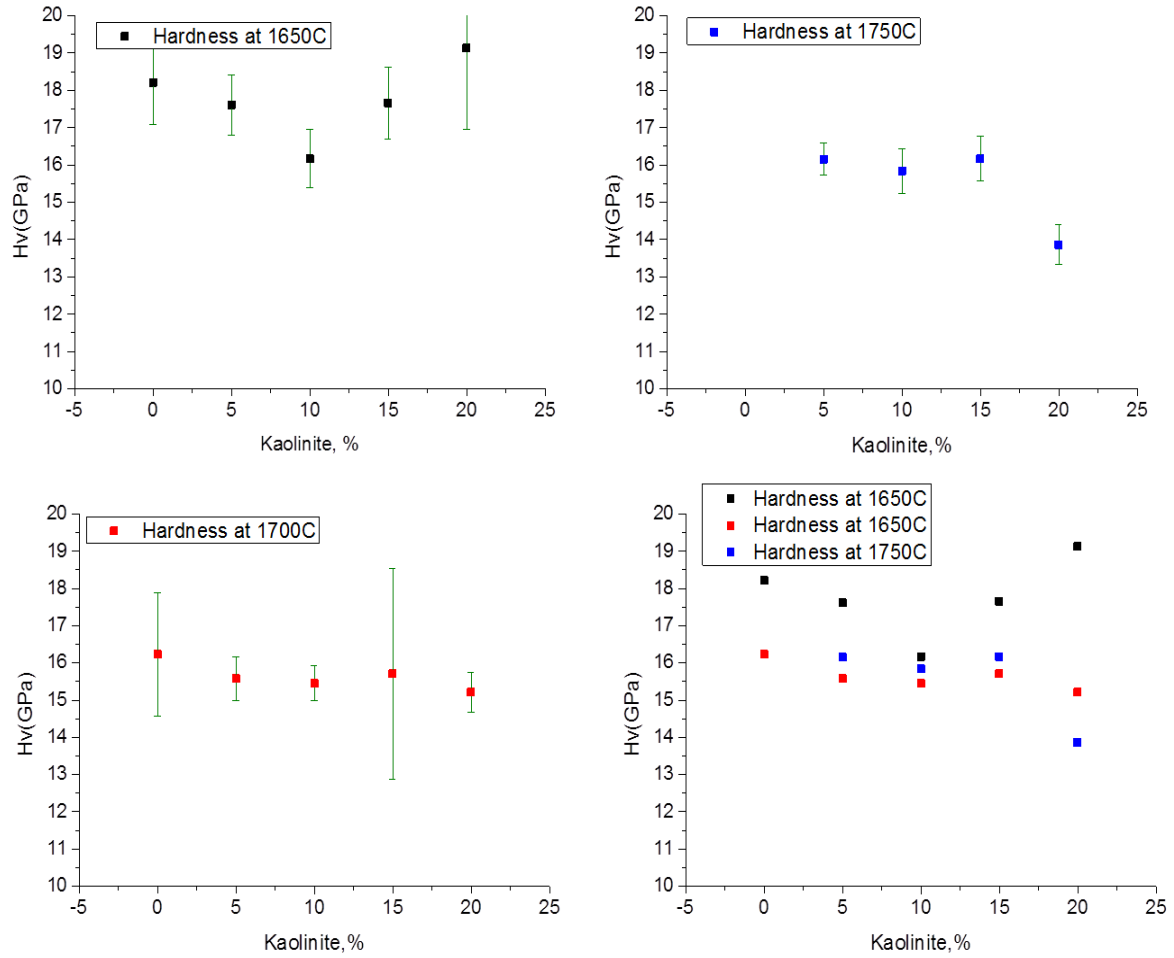


Figure 6-15 Hardness of Pless sintered with 5, 10, 15 and 20 % of Kaolinite sintered from 1650°C to 1750°C

XRD of the samples indicated only β -Sialon, as shown in the figure 5.16. Presence of β -Sialon (a soft phase) is the reason that Pless samples has low hardness as compared to the samples with S1212 and S215.

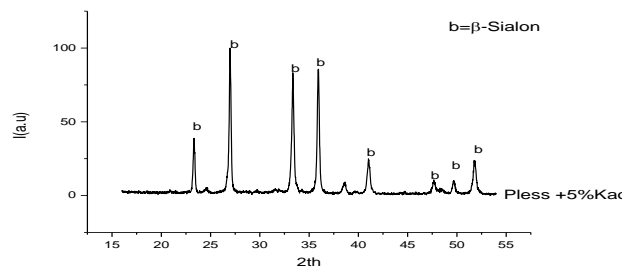


Figure 6-16 XRD pattern of pless composition with 5% kaolinite

6.6 Production of S215 (Composite Sialon) with Free Alumina

Samples of the material system S215 were reprocessed to gain the efficient mixing of the materials in the big alumina jar containing alumina balls inside as the grinding media. The alumina contamination from the system is termed as free alumina. Exactly, similar compositions, S215 and S1212 alloyed with kaolinite, as discussed in the start were sintered at 1650°C, 1700°C and 1750°C

Contrary to the toughness measured based on the hardness test values the maximum stress obtained from bend test results showed the maximum value for the samples containing only 5% kaolinite and then other values showed an increasing trend of stress after a jag in stress value at K-10, whereas the overall value of the stress was lower than the K-5 sample.

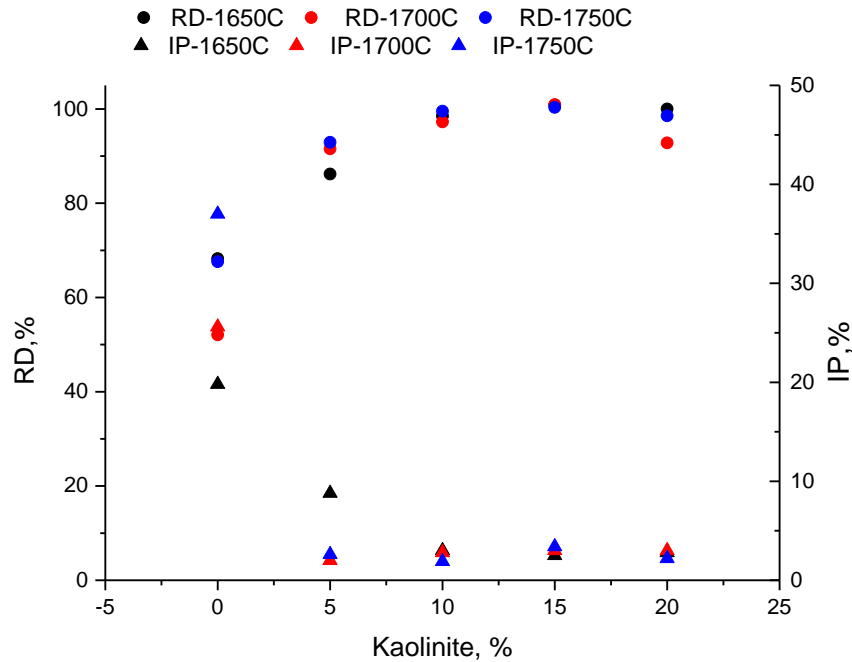


Figure 6-17 Relative density(RD) and porosity(IP) of the samples sintered at 1650 °C(black),1700 °C(red) and 1750°C(blue)

At 1650°C, as shown in Fig. 17, kaolinite-modified samples showed a roughly linear increase in density as the silicate addition passed from 5 to 20%. Samples with kaolinite contents greater than 10% reached maximum density at this temperature. Although, theoretical density based on oxides may not be the close enough to actual density for such intergranular materials[25]. As it is indicated by the values of image porosity that there is not much change in porosity hence increase in density is due to higher contents of aluminosilicate and its tendency to form more liquid and prevent the dissociation of Si_3N_4 , later phenomenon is supported by low oxide contents on the surface of such samples and a low shrinkage value is indicative of less dissociation as highlighted in the figure 5.18. Reference sample manifested low density and concurrent porosity which could be the result of no sintering and dissociation of Si_3N_4 as encountered by Soderlund et al[86]. Whereas, samples containing 5% kaolinite showed densification with increasing temperature, K-5 at temperature 1650°C was densified up to the 80% of the theoretical density only. Samples in this composition range could be sintered to 95% of theoretical density at 1750°C, this composition showed shrinkage increase from 1650°C to 1700°C and very little shrinkage for the samples sintered at 1750°C. Porosity for this

composition decreased drastically as we moved from 1650 to 1700°C as is indicated by the porosity graph. It is indicated that most of the densification took at 1700°C.

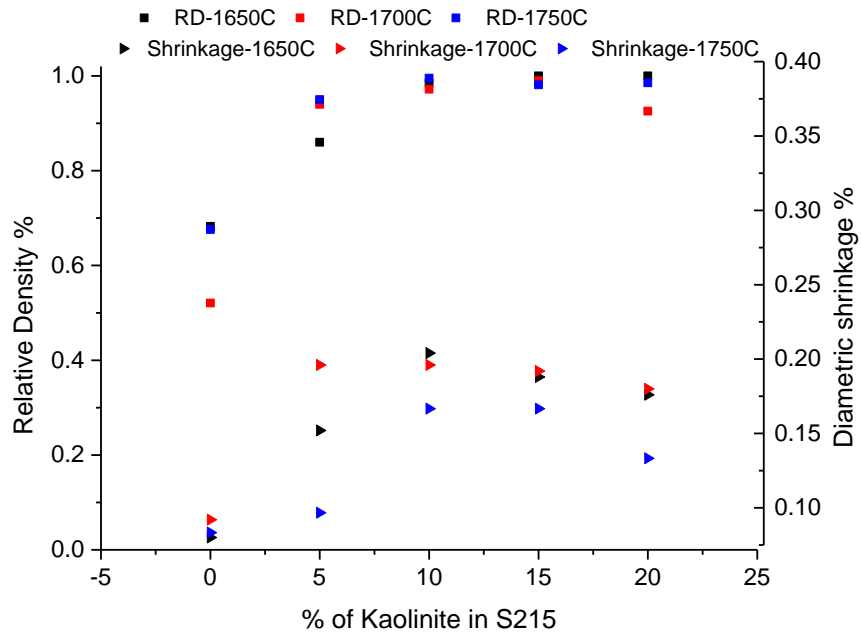


Figure 6-18 Relative density and shrinkage of S215 samples containing kaolinite

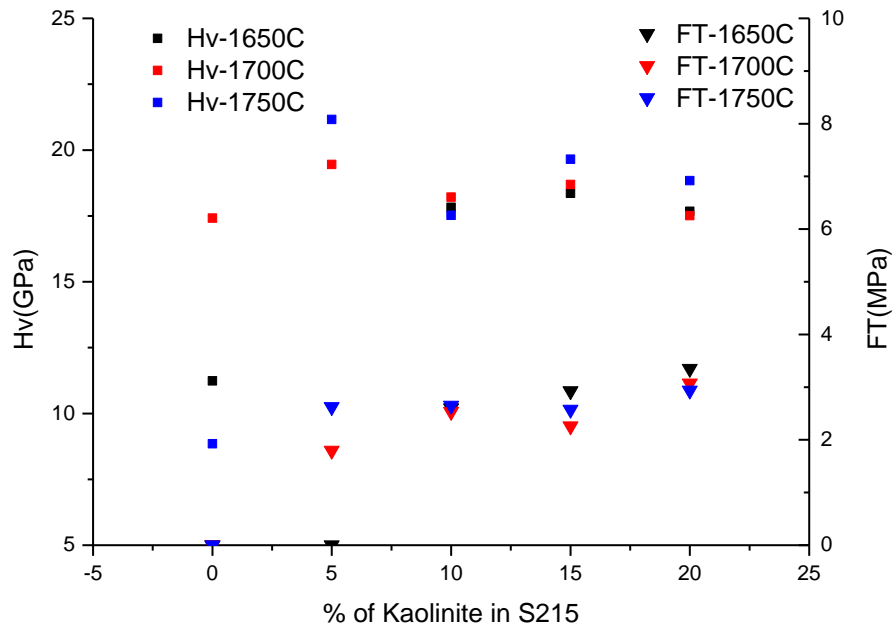


Figure 6-19 Hardness (Hv) and toughness (FT) of S215 sintered at 1650 °C, 1700 °C and 1750 °C

Hardness values indicate samples containing 5% or no kaolinite could not be sintered at 1650°C. Original sample was difficult to be sintered at all the temperatures tested so the hardness and toughness values could not be calculated. And samples with 5% kaolinite additions showed excellent hardness values at 1700°C and 1750°C. Samples with the kaolinite addition 10% and greater than 10% showed a decreasing trend in the hardness values which reached minimum hardness values for maximum kaolinite addition, as shown in the figure 5.19.

This decrease in hardness is accompanied by the continuous gain in the toughness values as shown by the same graph. This decrease in hardness and increase in the toughness values indicates the formation of some tough phase as indicated in the XRD patterns of these samples, XRD patterns are shown in figure 5.20.

XRD results supported the observations had from the hardness, toughness and stress values. As the samples with 5% kaolinite addition showed considerable presence of α -Sialon along with β -sialon, YAG, traces of AlN and silicates, at temperatures 1700°C and 1750°C whereas this composition could not be sintered well at 1650°C and the XRD results showed lot of silicates along with α/β -Sialon peaks. Samples with 10% kaolinite showed very strong development of

beta phase. K-10 at 1650°C showed less β -Sialon and YAG, whereas, the amount of β -Sialon increased at the intermediate and higher sintering temperatures.

Samples with 15% kaolinite, K-15 showed considerable β -Sialon at all the sintering temperatures whereas the β -Sialon development was maximum at 1700°C, traces of α -Sialon could also be found.

K-20 at all the temperatures showed strong presence of β -Sialon; YAG and traces of AlN and α -Sialon is also present.

The variation of hardness observed does not follow exactly the same trend than the density. This could be explained by the formation, in particular for high aluminosilicate contents, of softer glassy phases, that reduce the hardness even if the density is further increasing.

XRD results as discussed above showed that kaolinite presence might have given a softer phase, β -sialon rather than the formation of a glass as the either of the stress and fracture toughness values showed an increasing trend.

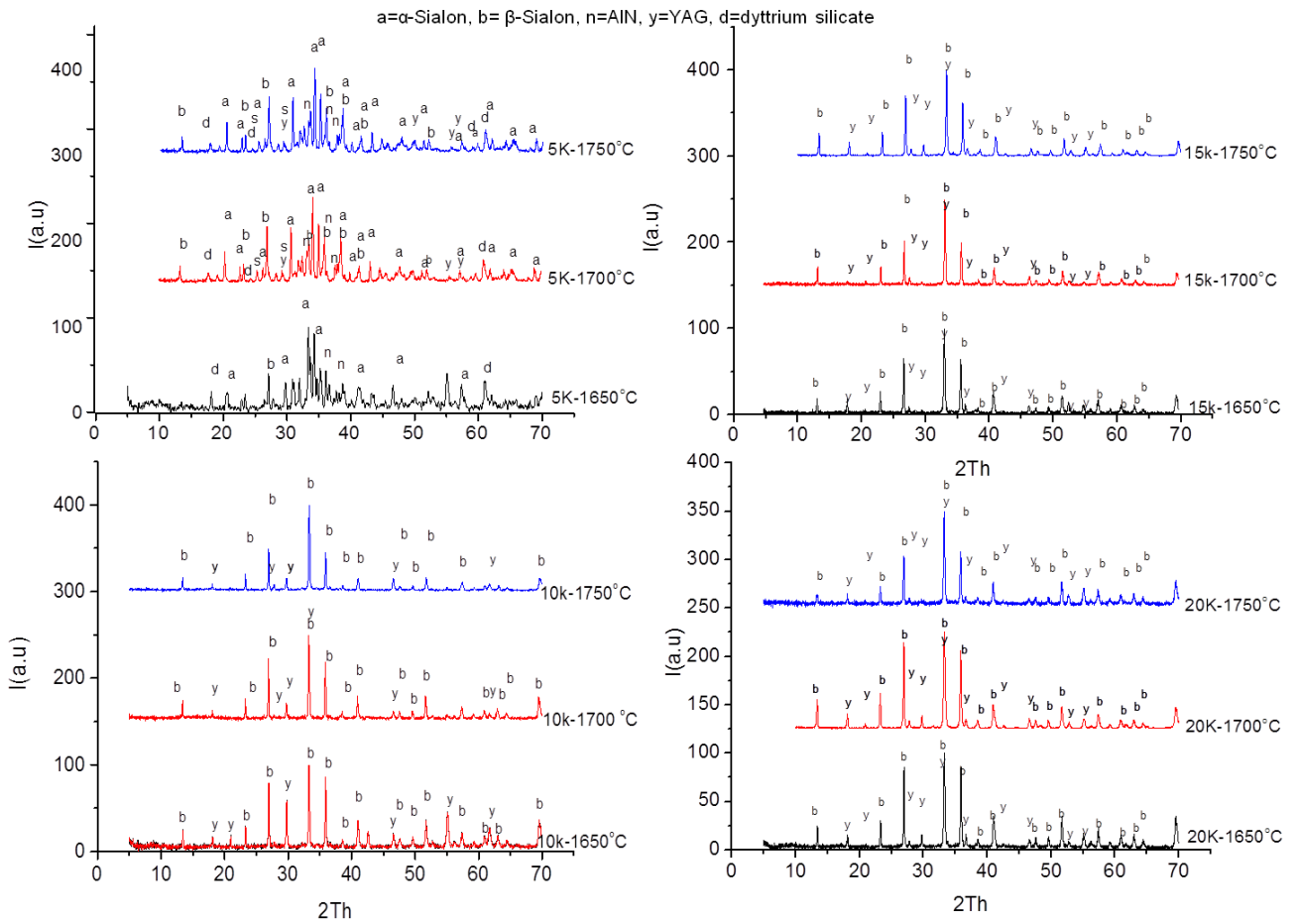


Figure 6-20 XRD patterns of S215 with free alumina sintered at 1650°C, 1700°C and 1750°C.

Contrary to the toughness measured based on the hardness test values the maximum stress obtained from bend test results showed the maximum value for the samples containing only 5% kaolinite and then other values showed an increasing trend of stress after a jag in stress value at K-10, whereas the overall value of the stress was lower than the K-5 sample

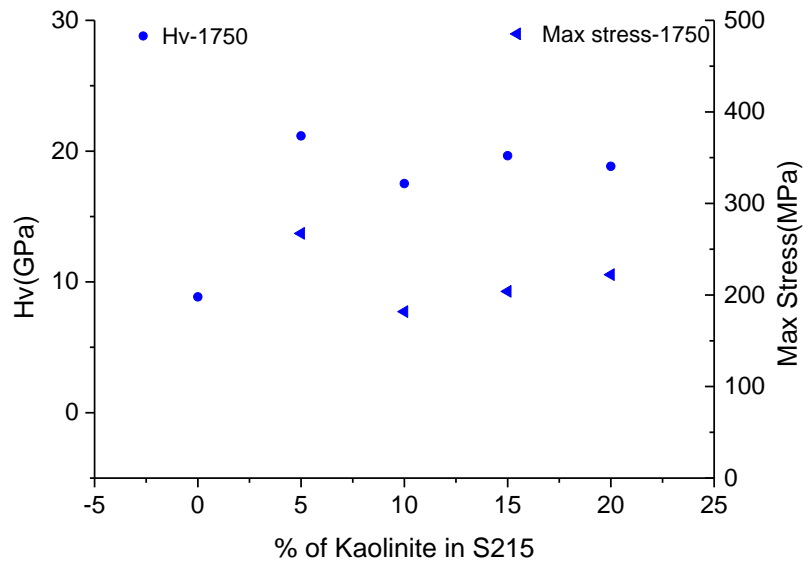


Figure 6-21 Hardness and bending strength of S215 samples sintered at 1750°C.

6.7 Production of S1212 (Composite Sialon) with Free Alumina

S1212 showed hardness values less, good relative density and at the same time gave the indication of porosity. There hardness values are less than the S215 with free alumina samples but more than the pressureless (Pless) sintered samples

Table 6-2 Bending Strength of S215 and S1212 samples

	S1212	S215
Kaolinite Additions	Max Stress(Mpa)	Max Stress(Mpa)
0		
5	181.61	267.21
10	228.83	181.88
15	299.50	203.91
20	440.89	222.17

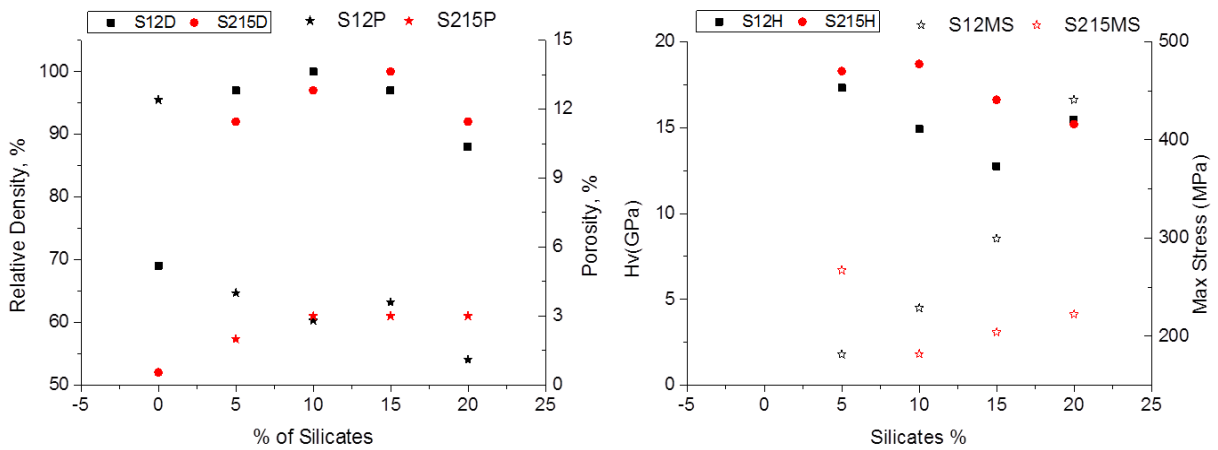


Figure 6-22 Comparison of S1212 and S215 after colloidal processing, where S12D, S12P, S12H and S12M are relative density, porosity, hardness and flexural strength, respectively, for S1212 batch. Similarly, S215D, S215P, S215H and S215MS represent relative density, porosity, hardness and flexural strength of, S215 sintered at 1750°C

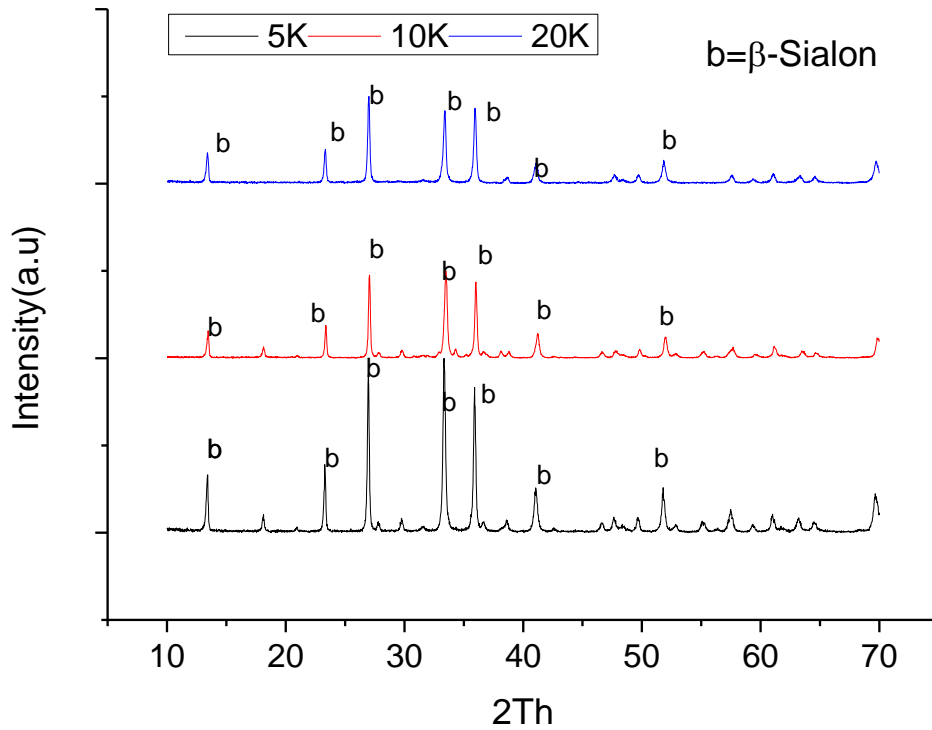


Figure 6-23 Patterns of the S1212 with free alumina, batches sintered at 1700C and alloyed with 5, 10 and 20 percent kaolinite respectively.

XRD patterns of S1212 with free alumina indicated that the materials which gave composite Sialon after the addition of free alumina and good mixing these systems turned out only β -Sialon as is obvious by comparing the XRD patterns of S1212 without free alumina (figure 5.11) with the one containing free alumina, well mixed system (figure 5.23).

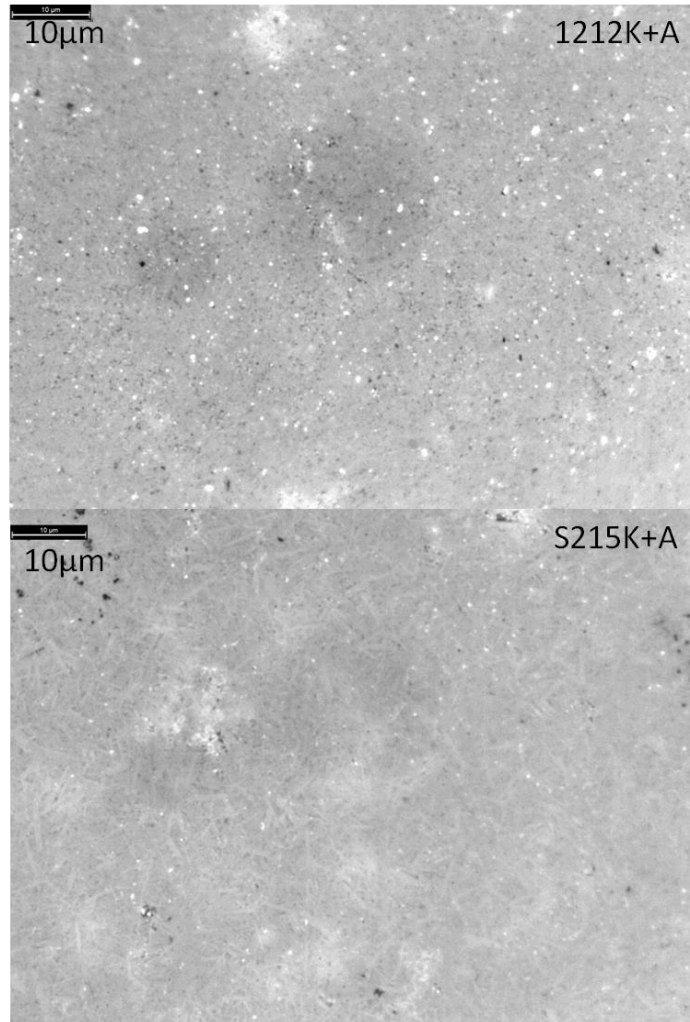


Figure 6-24 Optical micrograph of β -Sialon (S1212+A) and α -Sialon (S215+A)

Samples with 5% kaolinite in addition to free alumina in S215 showed fine optical micrograph with needle like structure and showed moderate values of toughness, bending strength and very good hardness as compared to the rest of materials produced moderate.

S1212 samples with free alumina and efficiently mixed gave good fracture toughness, bending strength as compared to the rest of samples, whereas the hardness values were inferior to that of S215 material system.

S215 with 5% kaolinite is considered the best composition and it was targeted for the further modifications

6.8 MgO-Y₂O₃ and Spinel-Y₂O₃based Sialons (S215)

MgO and Spinel (MgAl₂O₄) were added in the starting material as a filler to replace the costly yttria ions from the structure of the material and additionally introduce the effect of multication, i.e. introduction of another ion at the place of yttria can introduce the stresses and different thermal characteristics of the two ions can prevent the transformation of α -Sialon to β -Sialon. Spinel could modify the process positively as compared to the MgO. MgO has effect in densification very little as compared to nano sized Spinel (MgAl₂O₄), which helped densification to some extent these samples were only possible to be sintered at high temperatures only as shown in the figure 5.25 .

But the samples with Spinel gave good flexural strength; these results are shown in the bending strength diagram. Whereas, the relative density in none of the samples tested was above 90%.

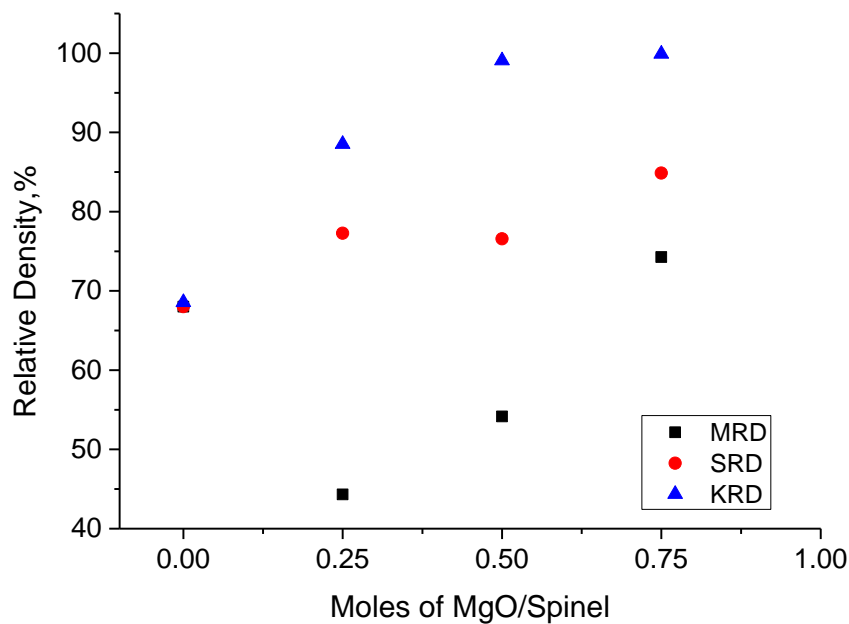


Figure 6-25 Relative density of S215 samples as the mole fraction of yttria is replaced with mole % of MgO and Spinel (MgAl₂O₄)

6.9 Effect of Free Alumina and Kaolinite on Sialon (S215)

Kaolinite alone could help sintering the samples with good control of phases and produced negligible glass, but there was porosity as indicated in figure 5.17. Contrary to this the samples with alumina showed glass formation as was observed with microscope in the low magnification images. Only the samples containing very small percentage of alumina in combination with kaolinite resulted in the combination of good phase and sound density, as shown in the figure 5.26.

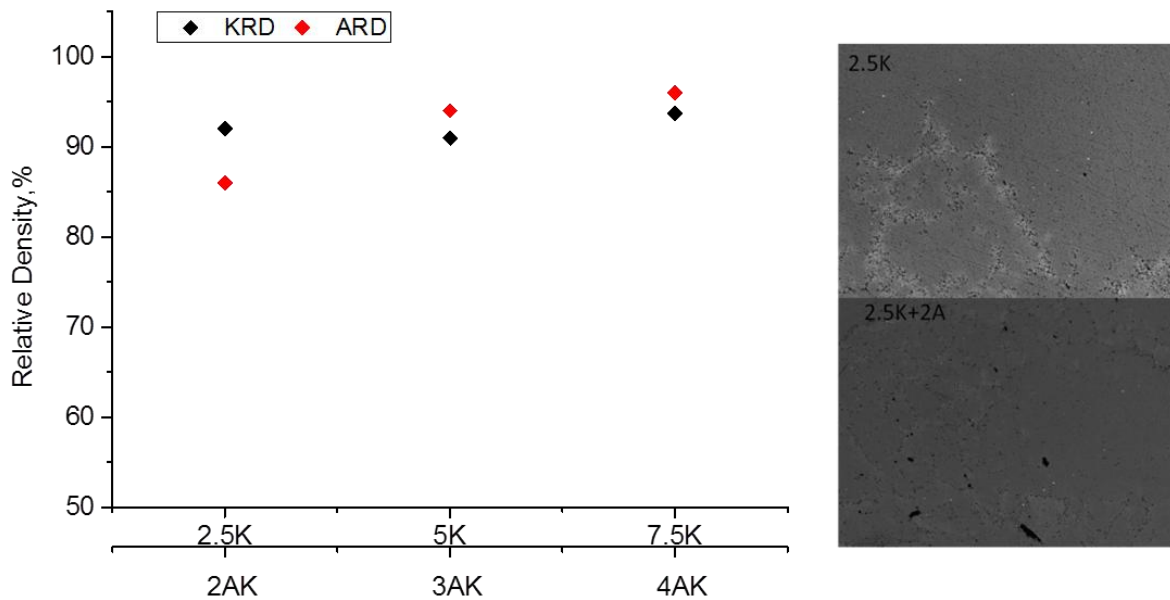


Figure 6-26 S215 processed with kaolinite (2.5% to 7.5%) and with free alumina (2-4%) in S215 on the left, whereas on the right is the low magnification image of the samples with free alumina and without it for 2.5K

6.10 Effect of MgO on S215K

MgO could replace yttria in small amount changing large amount is the present system is still as difficult as mentioned for non-kaolinitic systems. Large quantity of MgO replacing the Y_2O_3 shifted the composite Sialon to only β -Sialon predominately, as shown in the figure 5.28

6.11 Effect of Ce_2O_3 on S215K

Ceria and lanthanum oxide are used to replace the yttria from the system in order to increase the high temperature oxidation resistance and reduce cost. But for the Sialon systems without kaolinite it is reported that La/Ce reduce the stability of α -Sialon. In the current study, S215k, a

Sialon system with kaolinite has shown that Ce_2O_3 could replace up to 25 mole percent of yttria without impairing the relative density and phase stability as shown in the figure 5.28.

6.12 Graphene-S215K

Production of carbon nanotube (CNT), SWNT, based composites has demonstrated 100% increase in the fracture toughness of ceramics. Graphene imparts similar characteristics to the ceramics but it is easy to disperse in the materials during processing[45]

To have the similar effect we tried to include the graphene into our composite sialon produced by pressureless sintering technique. Graphene hindered the processing may be because of the same reason as presence of C in the material might have promoted carbothermal nitridation [21]. Minute quantities of the graphene up to 1% only decreased the response towards densification drastically.

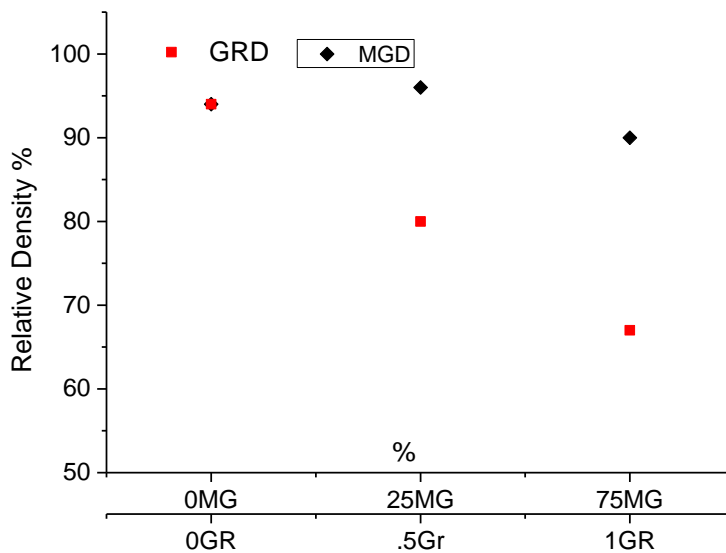


Figure 6-27 Processing of MgO and Graphene modified S215K, MgO replaces mole percent of Y_2O_3

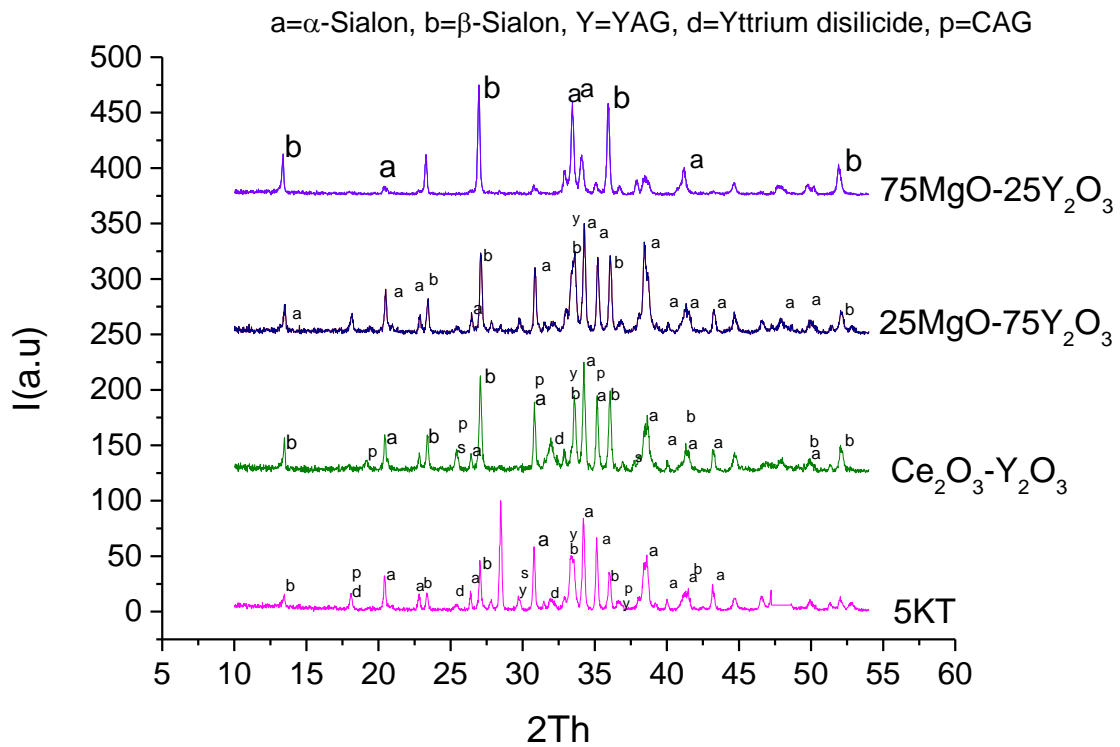


Figure 6-28 XRD patterns of samples with MgO and Ce₂O₃ replacing yttria in S215, samples were sintered at 1700°C

6.13 Colloidal Processing of Si₃N₄/SiC

SiC containing samples could be processed well as the relative density values were higher than 90% as shown in figure 5.29. SiC containing Si₃N₄ was made a system similar to Sialon S215 by modifying with extra AlN and Y₂O₃ and SiC was considered as an additive in the Sialon S215, again kaolinite was used as an additive to facilitate the processing

Even the sample without kaolinite showed much better densification as compared to the original sample. This effect might be due to the presence of SiO₂ on the surface of SiC.

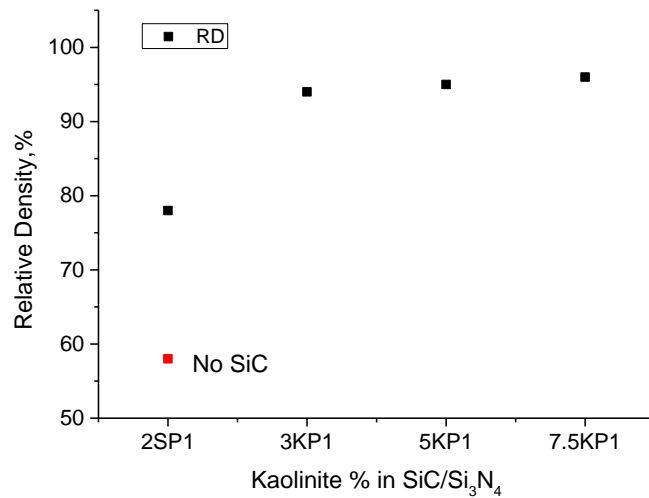


Figure 6-29 Sialon (S215) processed with SiC and kaolinite

6.14 Thermal Analysis

6.14.1 Hot Chamber XRD of Colloidal Processed β -Sialon

Colloidal processed and pressureless sintered S215 with 20% kaolinite (sample named 45C) consisted of β -Sialon and YG, whereas S215 with 5% kaolinite just could be processed to 95% of the theoretical density giving composite Sialon structure. To check the phase stability two samples were heat treated in the hot chamber XRD. During heat treatment some new peaks appeared or the broad peaks split into two peaks, position of such peaks is highlighted in the figure 5.30 (blue marks) and position of such peaks is given in the table 5.3

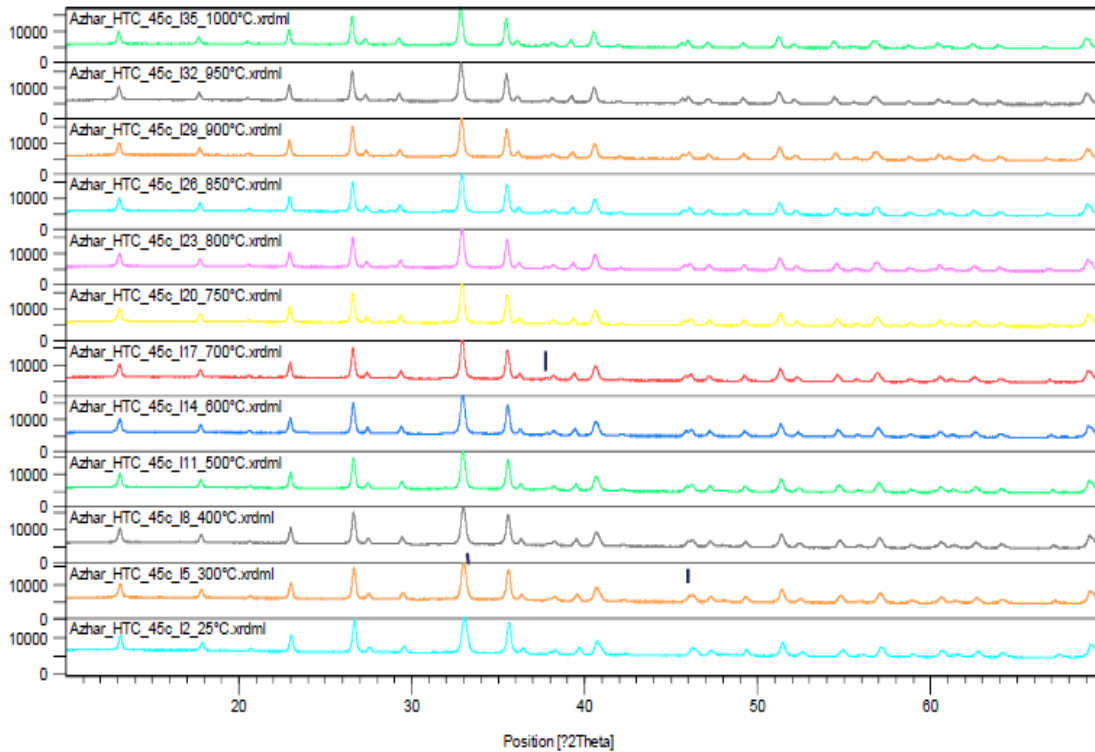


Figure 6-30 Thermal oxidation and phase stability analysis of colloidal processed Sialon215 with 20% kaolinite, β -Sialon.

Table 6-3 Peaks status as a function of temperature during and after heat treatment

Temp	New Peak	Splitting	Diminishing	Comments
300	33.06	46.26,69.41		
400				
700	37.76			
750		56.79		
After HT				
25		46.16		Split peaks again disappeared

Peaks for the beta sialon remained unmodified during heating and after heat treatment as shown in Figures 24 and 25. However pattern shifted towards left during heating and after cooling towards right slightly whereas it showed less oxidation and low thermal activity as compared to α -Sialon, shown in the figure 5.31.

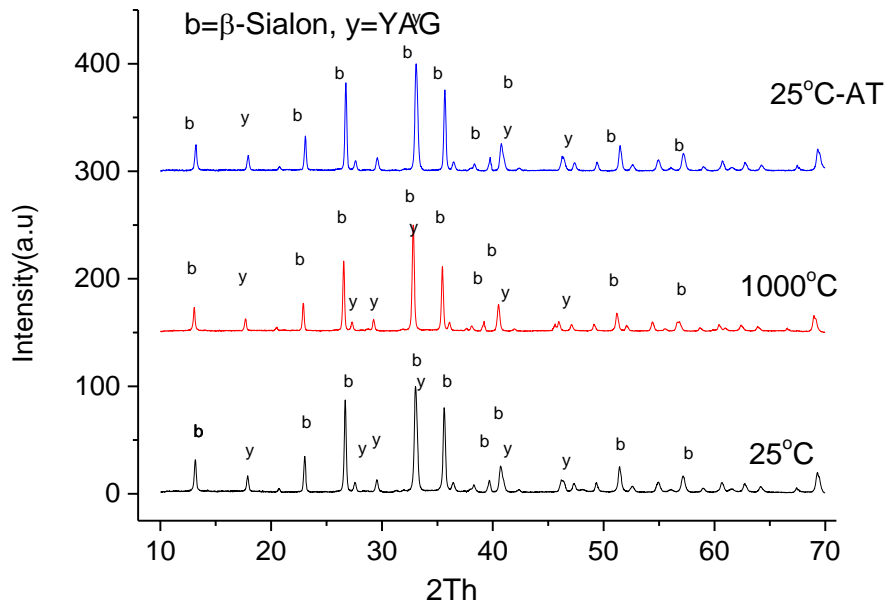


Figure 6-31 XRD patterns of beta Sialon tested up to 1000°C

6.14.2 Hot Chamber XRD of $\alpha\beta$ -Sialon

$\alpha\beta$ - Sialon was treated up to 1700°C and it showed some peak changes during heat treatment as shown in the table 5.4. Although there was no major change during all the heat treatment process but one peak, at room temperature, which might be an unreacted Y_2SiO_5 , represented as d in the pattern, in figure 5.32, vanished during heat treatment. Peaks are identified during and after heat treatment as shown in figure 5.33

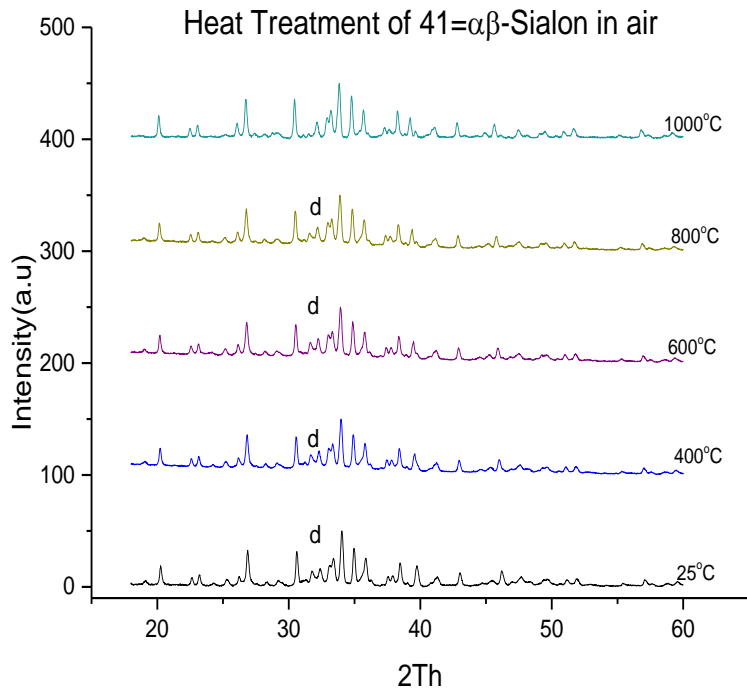


Figure 6-32 XRD patterns during and after heat treatment of αβ-Sialon

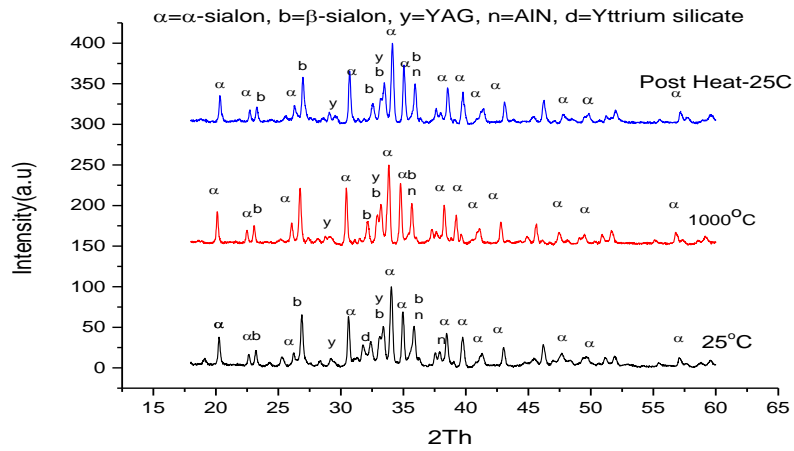


Figure 6-33 XRD patterns during and after heat treatment of αβ-Sialon

Table 6-4 Peak alterations during the heat treatment

Temperature (°C)	New Peak position 2th	Split position 2th	Diminishing Position 2th	Comments
300	24.2633			
400	44.61,65.38			
600	34.004,57.52, 67.677			
700	69.6475	65.24	58.6	
800		34.88,49.21		63.7 big shift
850		39.69		
Post Heat Treatment				
25			28.33, 31.77, 58.81	

6.15 Thermal Gravimetry

Small samples of known dimensions were prepared for thermogravimetric analysis (Mettler Toledo AG – TGA/STDA851e). The main purpose of this test was to check the effect of heat treatment in the air whether the samples melt or not. Samples were heated in the air at 10°C/mints. up to 1000°C and differential mass gain and heat signals were recorded

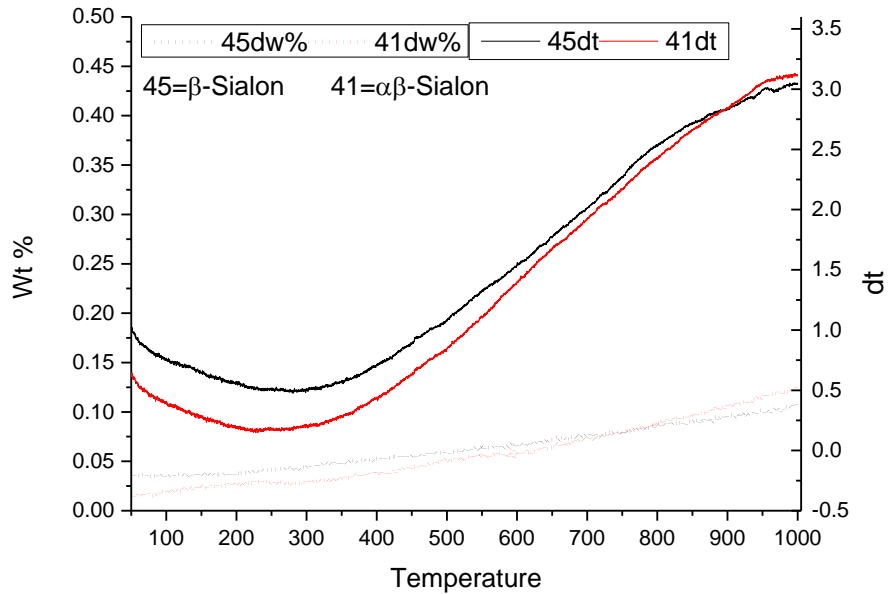


Figure 6-34 Thermogravimetric analysis of colloidal processed Sialons

Mass variation (oxidation) noted in the table 5.5 is so small almost touching the least count of the instrument

Table 6-5 Thermal Character of Sialon materials up to 1000°C.

Material	Oxidation (mg/mm²)	Phase Stability
β-Sialon	0.00056	stable
αβ-Sialon	0.001274	stable

Thermal gravimetric results combined with hot chamber XRD indicate that the composite material, αβ-Sialon, was relatively unstable as compared the single phase, β-Sialon, material. It might be due the relatively less density of this material.

6.16 Results Comparison

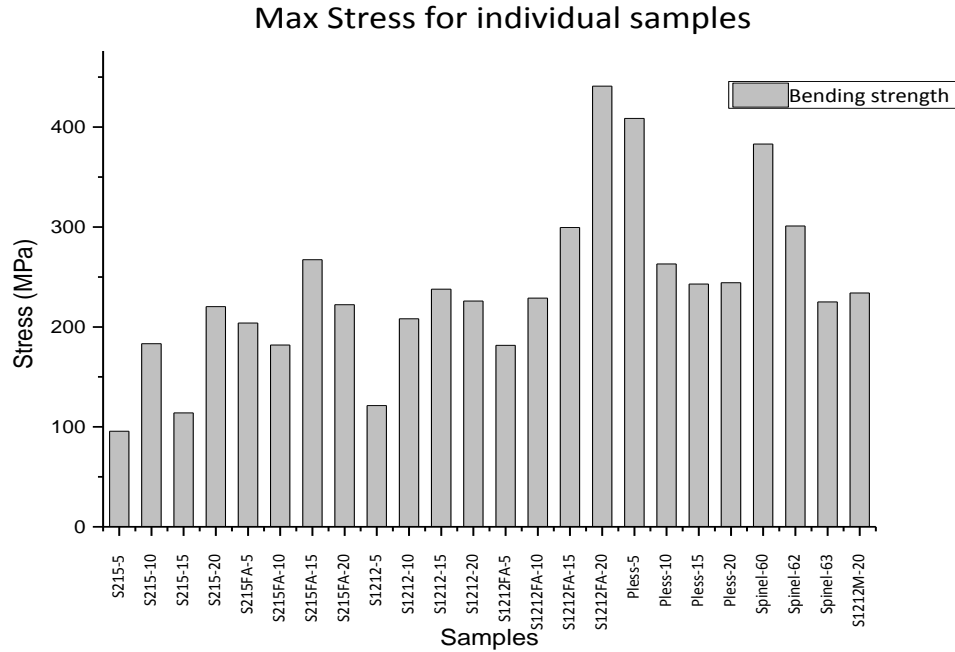


Figure 6-35 Flexural strength of samples sintered at 1750°C.

Samples, Pless-5 and S1212FA-20 which showed highest bending strength, these materials contain β -Sialon as the most dominant phase, whereas the samples with S2155FA is the sample with the good hardness and dual phase structure. Spinel containing sample is the third in this race but these samples were nearly 80% dense as compared to the theoretical density and were not produced further.

6.17 Comparison between colloidal processed pressureless sintered and other systems

Table 6-6 Comparison of results with SPS and HIP results

Sample ID	Sialon Type	Processing	Fracture Toughness	Hardness	Reference
			(Mpa)	Hv(Gpa)	
Y-5	β	GPS	6.4	14.2	[56]
	β	SPS	5.7	15	[56]
	$\alpha\beta$	HIP	6.5	19.3	[87]
	β	Col./Pless		15	[86]
S215-5K	$\alpha\beta$	Col/Pless	2.62	21.6	New
S215-20K	β	Col/Pless	2.98	18.88	New
S1212-20K	β	Col/Pless	4.34	16.53	New

Note: Col/Pless= is colloidal processed and pressureless sintered material

Composite $\alpha\beta$ -Sialon demonstrated very good hardness comparable to the counterparts produced by HIP. β -Sialon starting from **S215** showed a Sialon with very good hardness again the toughness was low. Whereas the β -Sialon form **S1212** was best in the lot with respect to hardness again and toughness was close to the ones processed with HIP and SPS.

7 Conclusions.

Colloidal processing and pressureless sintering was successfully applied to synthesize $\alpha\beta$ -Sialon, β -Sialon and SiC/Si₃N₄ based SiC-Sialon composites.

New processing technique yielded the Sialons competitive to the developed by spark plasma sintering (SPS) and hot isostatic pressing (HIP).

MgO in kaolinitic Sialon system with colloidal processing and pressureless sintering could replace Yttria in S215 to less than half quantity by moles.

Colloidal processing was efficient in retaining α -Sialon proportion in $\alpha\beta$ -Sialon synthesized with Ce₂O₃ replacing a portion of Yttria.

Processing was successful with small quantity of free alumina in addition to kaolinite.

8 Future Works

1. Application of colloidal processing and pressureless sintering technique to study all the additives modifiers which are studied for SPS and HIP.
2. Application to develop SiC/ β -Sialom-Si₃N₄ system
3. Colloidal processing to develop long fiber reinforced composite as there is no risk of damaging fibers in slip casting and pressureless system.
4. Study of the similar compositions with focus on improving packing by controlling particle size and shapes to control the amount of fluxes and to improve toughness.
5. Application as rotor and vanes in the compressor and lower temperature end of turbine to replace TiAl and other vane blades

6. Reference List

1. Rolls-Royce, *The Jet Engine*, T.P. Department, Editor. 1996, Rolls-Royce Plc: Derby.
2. El-Sayed, A.F., *Aircraft Propulsion and Gas Turbine Engines*. 2008: Taylor & Francis.
3. Hünecke, K., *Jet Engines: Fundamentals of Theory, Design, and Operation*. 1997: Motorbooks International.
4. Boyce, M.P., *Gas Turbine Engineering Handbook (4th Edition)*.
5. *Turboshaft Engines*. Available from:
http://www.quazoo.com/q/Turboshaft_engines.
6. Mattingly, J.D., *Elements of Gas Turbine Propulsion*. 1996: McGraw-Hill.
7. Campbell, F.C., *Chapter 6 - Superalloys*, in *Manufacturing Technology for Aerospace Structural Materials*, F.C. Campbell, Editor. 2006, Elsevier Science: Oxford. p. 211-272.
8. Giampaolo, T., *The gas turbine handbook: Principles and practices*. 2003: The Fairmont Press, Inc.
9. Institution of Mechanical, E., *Proceedings of the Institution of Mechanical Engineers*. Proceedings of the Institution of Mechanical Engineers., 1989.
10. Muktinutalapati, N.R., *Materials for Gas Turbines–An Overview*. Advances in Gas Turbine Technology VIT University India, 2011.
11. Campo, E. and V. Lupinc, *High temperature structural materials for gas turbines*. Metallurgical Science and Tecnology, 2013. **11**(1).
12. Angus, J.P. and R.-R. Ltd, *Aero Engine Ceramics - the Vision, the Reality and the Progress*. 1992: Rolls-Royce plc.
13. Gogia, A., *High-temperature titanium alloys*. Defence Science Journal, 2005. **55**(2): p. 149-173.
14. Dressler, W. and R. Riedel, *Progress in silicon-based non-oxide structural ceramics*. International Journal of Refractory Metals and Hard Materials, 1997. **15**(1): p. 13-47.
15. Jack, K.H., *Sialons and related nitrogen ceramics*. Journal of Materials Science, 1976. **11**(6): p. 1135-1158.
16. Izhevskiy, V.A., et al., *Progress in SiAlON ceramics*. Journal of the European Ceramic Society, 2000. **20**(13): p. 2275-2295.
17. Lange, F.F., *Powder Processing Science and Technology for Increased Reliability*. Journal of the American Ceramic Society, 1989. **72**(1): p. 3-15.
18. Ulrich, K.T., *Product design and development*. 2003: Tata McGraw-Hill Education.

19. Harper, C., *HANDBOOK OF CERAMICS, GLASSES, AND DIAMONDS*. 2001: McGraw-Hill Professional. 848.
20. Jansen, M., *High Performance Non-Oxide Ceramics II*, Springer.
21. Priest, H.F., G.L. Priest, and G.E. Gazza, *Sintering of Si₃N₄ Under High Nitrogen Pressure*. Journal of the American Ceramic Society, 1977. **60**(1-2): p. 81-81.
22. Mitomo, M., *Pressure sintering of Si₃N₄*. Journal of Materials Science, 1976. **11**(6): p. 4.
23. Greskovich, C.D., S. Prochazka, and J.H. Rosolowski, *Basic Research on Technology Development for Sintered Ceramics*. 1976, DTIC Document.
24. Katz, R.N., *Nitrogen Ceramics 1976-1981*, in *Progress in Nitrogen Ceramics*, F.L. Riley, Editor. 1983, Springer Netherlands. p. 3-20.
25. Ekström, T., et al., *Dense single-phase β -sialon ceramics by glass-encapsulated hot isostatic pressing*. Journal of Materials Science, 1989. **24**(5): p. 1853-1861.
26. Ekström, T., et al., *Formation of an Y/Ce-doped α -sialon phase*. Journal of the European Ceramic Society, 1991. **8**(1): p. 3-9.
27. Olsson, P.-O. and T. Ekström, *HIP-sintered β - and mixed α - β sialons densified with Y₂O₃ and La₂O₃ additions*. Journal of Materials Science, 1990. **25**(3): p. 1824-1832.
28. Ekström, T. and P.-O. Olsson, *β -Sialon Ceramics Prepared at 1700°C by Hot Isostatic Pressing*. Journal of the American Ceramic Society, 1989. **72**(9): p. 1722-1724.
29. Tajima, Y., *Development of High Performance Silicon Nitride Ceramics and their Applications*. MRS Online Proceedings Library, 1992. **287**: p. null-null.
30. Yokoyama, K. and S. Wada, *SOLID-GAS REACTION DURING SINTERING OF Si₃N₄ CERAMICS. PT. 1. STABILITY OF SiO₂, Y₂O₃ AND Al₂O₃ AT HIGH TEMPERATURE*. Journal of the Ceramic Society of Japan, 2000. **108**(1): p. 6-9.
31. Petzow, G. and M. Herrmann, *Silicon nitride ceramics*, in *High performance non-oxide ceramics II*. 2002, Springer. p. 47-167.
32. Gauckler, L. and G. Petzow, *Representation of multicomponent silicon nitride based systems*. Nitrogen Ceramics, Noordhooft, 1977: p. 118-121.
33. Moya, C.J.S., et al., *A method for the production of beta'-sialon based ceramic powders*. 1988, Google Patents.
34. Panneerselvam, M. and K. Rao, *A microwave method for the preparation and sintering of β' -SiAlON*. Materials Research Bulletin, 2003. **38**(4): p. 663-674.

35. Hwang, S.-L. and I.W. Chen, *Reaction Hot Pressing of α' - and β' - SiAlON Ceramics*. Journal of the American Ceramic Society, 1994. **77**(1): p. 165-171.
36. Kolitsch, U., et al., *Phase equilibria and crystal chemistry in the Y2O3–Al2O3–SiO2 system*. Journal of Materials Research, 1999. **14**(02): p. 447-455.
37. Sun, W.Y., P.A. Walls, and D.P. Thompson, *Reaction Sequences in the Preparation of Sialon Ceramics*, in *Non-Oxide Technical and Engineering Ceramics*, S. Hampshire, Editor. 1986, Springer Netherlands. p. 105-117.
38. Sun, W.Y., P.A. Walls, and D.P. Thompson, *Reaction Sequences in the Preparation of Sialon Ceramics*, in *Non-Oxide Technical and Engineering Ceramics*, S. Hampshire, Editor. 1987, Springer Netherlands. p. 105-117.
39. Menon, M. and I.W. Chen, *Reaction Densification of α' -SiAlON: 1, Wetting Behavior and Acid-Base Reactions*. Journal of the American Ceramic Society, 1995. **78**(3): p. 545-552.
40. Pearson, R.G., *Absolute electronegativity and hardness: application to inorganic chemistry*. Inorganic Chemistry, 1988. **27**(4): p. 734-740.
41. Sun, W.-Y., T.-Y. Tien, and T.-S. Yen, *Subsolidus Phase Relationships in Part of the System Si,Al,Y/N,O: The System Si3N4—AlN—YN—Al2O3—Y2O3*. Journal of the American Ceramic Society, 1991. **74**(11): p. 2753-2758.
42. *<Subsolidus phase relationships in the System Dy2O3-Si3N4-AlN-Al2O3.pdf>*.
43. Thompson, D.P. *New grain-boundary phases for nitrogen ceramics*. in *MRS Proceedings*. 1992: Cambridge Univ Press.
44. Mandal, H., D.P. Thompson, and K. Jack, *$\alpha = \beta$ Phase Transformations in Silicon Nitride and Sialons*. Key Engineering Materials, 1998. **159**: p. 1-10.
45. Porwal, H., S. Grasso, and M. Reece, *Review of graphene-ceramic matrix composites*. Advances in Applied Ceramics, 2013. **112**(8): p. 443-454.
46. Kasuga, T., et al., *Formation of titanium oxide nanotube*. Langmuir, 1998. **14**(12): p. 3160-3163.
47. Niihara, K., K. Izaki, and T. Kawakami, *Hot-pressed Si3N4-32% SiC nanocomposite from amorphous Si-CN powder with improved strength above 1200 C*. Journal of Materials Science Letters, 1991. **10**(2): p. 112-114.
48. Sternitzke, M., *Structural ceramic nanocomposites*. Journal of the European Ceramic Society, 1997. **17**(9): p. 1061-1082.

49. Rouxel, T., F. Wakai, and K. Izaki, *Tensile ductility of superplastic Al₂O₃-Y₂O₃-Si₃N₄/SiC composites*. Journal of the American Ceramic Society, 1992. **75**(9): p. 2363-2372.
50. Rendtel, A., et al., *Silicon nitride/silicon carbide nanocomposite materials: II, hot strength, creep, and oxidation resistance*. Journal of the American Ceramic Society, 1998. **81**(5): p. 1109-1120.
51. Herrmann, M., et al., *Silicon Nitride/Silicon Carbide Nanocomposite Materials: I, Fabrication and Mechanical Properties at Room Temperature*. Journal of the American Ceramic Society, 1998. **81**(5): p. 1095-1108.
52. Herrmann, M. and O. Goeb, *Colour of gas-pressure-sintered silicon nitride ceramics Part I. Experimental data*. Journal of the European Ceramic Society, 2001. **21**(3): p. 303-314.
53. Schleicher, H.M., *Form for slip-casting ceramics and method of making the same*. 1942, US Patent 2,303,303.
54. Lewis, M.H. and R.J. Lumby, *Nitrogen Ceramics: Liquid Phase Sintering*. Powder Metallurgy, 1983. **26**(2): p. 73-81.
55. Kingery, W., *Densification during sintering in the presence of a liquid phase. I. Theory*. Journal of Applied Physics, 1959. **30**(3): p. 301-306.
56. Eser, O. and S. Kurama, *A comparison of sintering techniques using different particle sized β -SiAlON powders*. Journal of the European Ceramic Society, 2012. **32**(7): p. 1343-1347.
57. Ring, T.A., *Fundamentals of ceramic powder processing and synthesis*. 1996: Academic Press.
58. Waku, Y., *A new ceramic eutectic composite with high strength at 1873 K*. Advanced Materials, 1998. **10**(8): p. 615-617.
59. Shelby, J.E., *Introduction to glass science and technology*. 2005: Royal Society of Chemistry.
60. Rhodes, W.H., *Agglomerate and Particle Size Effects on Sintering Yttria-Stabilized Zirconia*. Journal of the American Ceramic Society, 1981. **64**(1): p. 19-22.
61. Everett, D. and J. Goodwin, *The rheology of dispersions*. 2007.
62. Onoda Jr, G.Y. and L.L. Hench, *The Science of Ceramic Processing Before Firing*. 1977, DTIC Document.
63. Boch, P. and J.-C. Niepce, *Ceramic Materials: Processes, Properties, and Applications*. Vol. 98. 2010: John Wiley & Sons.
64. Mistler, R.E. and E.R. Twiname, *Tape casting: theory and practice*. 2000: American ceramic society Westerville, OH.
65. Mistler, R.E. and D.J. Shanefield, *Washing ceramic powders to remove sodium salts*. American Ceramic Society Bulletin, 1978. **57**(7): p. 689.

66. Rives, J. and B.I. Lee, *The effect of water on the dispersion of alumina in nonaqueous media*. Colloids and surfaces, 1991. **56**: p. 45-58.
67. Lindqvist, K., et al., *Organic silanes and titanates as processing additives for injection molding of ceramics*. Journal of the American Ceramic Society, 1989. **72**(1): p. 99-103.
68. Groat, E., *Aqueous processing of AlN powders*. Ceramic Industry, 1993. **140**(3): p. 34-38.
69. Mikeska, K.R. and W. Cannon, *Non-aqueous dispersion properties of pure barium titanate for tape casting*. Colloids and surfaces, 1988. **29**(3): p. 305-321.
70. Cannon, W.R., J. Morris, and K. Mikeska, *Dispersants for nonaqueous tape casting*. Adv. Ceram., 19 pp., 1986. **161**.
71. Gyurk, W.J., *Methods for manufacturing multilayered monolithic ceramic bodies*. 1965, Google Patents.
72. Kotte, J., J. Denissen, and R. Metselaar, *Pressure casting of silicon nitride*. Journal of the European Ceramic Society, 1991. **7**(5): p. 307-314.
73. German, R.M., *Powder Injection Molding*. 1990: Metal Powder Industries Federation.
74. Yan, X. and P. Gu, *A review of rapid prototyping technologies and systems*. Computer-Aided Design, 1996. **28**(4): p. 307-318.
75. Callister, W.D. and D.G. Rethwisch, *Materials science and engineering: an introduction*. Vol. 7. 2007: Wiley New York.
76. Belmonte, M., et al., *Spark plasma sintering: A powerful tool to develop new silicon nitride-based materials*. Journal of the European Ceramic Society, 2010. **30**(14): p. 2937-2946.
77. Orrù, R., et al., *Consolidation/synthesis of materials by electric current activated/assisted sintering*. Materials Science and Engineering: R: Reports, 2009. **63**(4-6): p. 127-287.
78. Nishimura, T., et al., *Fabrication of silicon nitride nano-ceramics by spark plasma sintering*. Journal of Materials Science Letters, 1995. **14**(15): p. 1046-1047.
79. Shen, Z., H. Peng, and M. Nygren, *Rapid Densification and Deformation of Li-Doped Sialon Ceramics*. Journal of the American Ceramic Society, 2004. **87**(4): p. 727-729.
80. *Transparent Technology*. 27/11/2013; Available from: <http://ltp.epfl.ch/page-35605-en.html>.
81. Peng, H., *Spark Plasma Sintering of Si₃N₄-based Ceramics*. 2004, Stockholm University: Stockholm.

82. XinXu, M., et al., *Effect of dispersant on the rheological properties and slip casting of concentrated sialon precursor suspensions*. European Ceramic Society, 2003: p. 1525-1530.
83. Cullity, B., *Elements of X-ray Diffraction*, 1978. **2**.
84. Wang, M. and N. Pan, *Predictions of effective physical properties of complex multiphase materials*. Materials Science and Engineering: R: Reports, 2008. **63**(1): p. 1-30.
85. Anstis, G., et al., *A critical evaluation of indentation techniques for measuring fracture toughness: I, direct crack measurements*. Journal of the American Ceramic Society, 1981. **64**(9): p. 533-538.
86. Söderlund, E. and T. Ekström, *Pressureless sintering of Y2O3-CeO2-doped sialons*. Journal of Materials Science, 1990. **25**(11): p. 4815-4821.
87. Yeckley, R.L., *Alpha-beta SiAlON ballistic armor ceramic and method for making the same*. 2012, Google Patents.